Aspects of Permian Paleowind Directions in the Unayzah-A Reservoir, Subsurface Eastern Central Saudi Arabia, Utilizing Integrated Core and Image Log Data

BY

Mohammed Ali Al-Masrahy

A Thesis Presented to the
DEANSHIP OF GRADUATE STUDIES

KING FAHD UNIVERSITY OF PETROLEUM & MINERALS

DHAHRAN, SAUDI ARABIA

In Partial Fulfillment of the
Requirements for the Degree of

MASTER OF SCIENCE

In

GEOLOGY

JANUARY 2011

KING FAHD UNIVERSITY OF PETROLEUM & MINERALS

DHAHRAN 31261, SAUDI ARABIA

DEANSHIP OF GRADUATE STUDIES

This thesis, written by **Mohammed Ali Al-Masrahy** under the direction of his thesis advisor and approved by his thesis committee, has been presented to and accepted by the Dean of Graduate Studies, in partial fulfillment of the requirements of the degree of MASTER OF SCIENCE IN GELOGY.

Thesis Committee

Dr. Osman Abdullatif (Thesis Advisor)

Dr. Mohammed H. Makkawi (Member)

Dr. Abdulaziz Al-Shaibani
Department Chairman

Dr. John Melvin (Member)

Dr. Salam Adel Zummo
Dean of Graduate Stuies

عمادة الدراسات العليا
DEANSHIP OF GRADUATE STUDIES

Date 21/5/11

DEDICATION

This thesis is dedicated to my family, for their encouragement, support, and patience throughout the work of this thesis

ACKNOWLEDGMENTS

I am very grateful to my thesis committee; Dr. Osman Abdullatif thesis advisor, Dr. Mohammed Makkawi committee member, from King Fahd University of Petroleum and Minerals (KFUPM) and Dr. John Melvin Geological Consultant, committee member from Saudi Aramco for their support, ideas, guidance, and constructive comments. Special thanks go to the faculty of the Earth Sciences Department, represented by Dr. Abdulaziz Al-Shaibani, Chairman of the department, for their continual support and dedication throughout my study at KFUPM.

My acknowledgement and thanks go to Mr. Abdullah A. Naim, Vice President of Exploration for Saudi Aramco, for his support and permission to publish the results of this study. Special thanks to Aus Al-Tawil, Manager of Saudi Aramco's Reservoir Characterization Department, and to Mr. Matter Al-Shammary, current Chief geologist of the Gas Reservoir Characterization Division and to Mr. Jamil Hajhog former Chief geologist of the Gas Reservoir Characterization Division for their support during my study.

I would like to express my gratitude to Rono, Jose D, and Sinan, Hassan M from UiC and Hadi Al-Uraij, Saidi Hassani, Ghazi Al-Eid, Osama Musharfi, Ron Sprague , Mark Prudden, , Nigel Machin, Nazih Najjar and Gurhan Aktas for their continual support and help during this work.

TABLE OF CONTENTS

LIST OF TABLES & CHARTS

LIST OF FIGURES

THESIS ABSTRACT (ENGLISH)

Name: Mohammed Ali Al-Masrahy
Title: Aspects of Permian Paleowind Directions in the Unayzah-A Reservoir, Subsurface Eastern Central Saudi Arabia, Utilizing Integrated Core and Image Log Data

Major Field: Geology
Date: January 2011

The Lower Permian Unayzah A reservoir unit in the subsurface of eastern central Saudi Arabia displays widespread evidence of deposition under arid to semi-arid conditions, very commonly in a wind-dominated, aeolian setting. A number of distinctive aeolian depositional facies are recognized from core and image logs including: dunes, interdunes, sand sheet, and playa lakes. They occur with a high degree of repeatability throughout the Unayzah A reservoirs. The study investigated the distribution of azimuthal variability in Permian paleowind data across the Kingdom. The data were derived from image log patterns throughout the aeolian dune facies identified in the subsurface Unayzah A reservoir unit from within four fields selected for this study. The study involved sedimentological description of 1160 feet of core data from six wells and analysis of 4000 feet of image log data from twenty one wells, which spanned the area from central to eastern Saudi Arabia. A hierarchical approach was employed to investigate the paleo-wind directions as follows: Paleowind azimuth data were i) recorded appropriately for each identifiable bed; ii) averaged over each bedset within each well; iii) averaged over each well; iv) averaged over each field; v) and finally averaged over the four studied fields. This rigorous approach resulted in the identification of a dominant paleowind direction toward east-northeast direction (present day), with a window ranges between 40 and 100 degrees and a mean vector of 72 degrees. Identifying the dominant paleo-wind direction provides an understanding of dune distribution and shape throughout the reservoir. It also facilitates hydrocarbon development program optimum exploitation of porosity and permeability distribution.

Master of Science Degree
King Fahd University of Petroleum and Minerals
Dhahran, Saudi Arabia
January 2011

ملخص الرسالة

الاسم: محمد علي المسرحي
عنوان الرسالة: اتجاهات الرياح القديمه في العصر البرمي في خزان العنيزة أ، وسط و شرق المملكة العربية السعودية، وذلك باستخدام عيانات اللب الصخري وبيانات الآبار التصويريه.
التخصص: الجيولوجيا
تاريخ التخرج: يناير 2011 م

مكمن العنيزه أ من العصر البرمي السفلى تحت سطح الأرض في شرق ووسط المملكة العربية السعودية يعرض أدلة على نطاق واسع من الترسب في إطار ظروف صحراويه إلى شبه صحراويه ،والتي تتميز بعوامل الترسيب الهوائيه التي تهيمن عليها الرياح. من خلال دراسة العينات الصخريه وبيانات الآبار التصويريه لطبقات العنيزه أ ثبت وجود البيئه الترسيبيه الهوائيه ممثلة في وجود السحنات الهوائيه مثل الكثبان الرمليه ,الروابي الرمليه و الرواسب الطينيه بين الكثبان. أثبتت الدراسه ايضاً حدوثها على درجة عاليه من التكرار في مكمن العنيزة أ. دراسة توزيع اتجاهات الرياح في العصر البرمي والتي استمدت من بيانات الآبار التصويريه للكثبان الرمليه المحددة في مكمن العنيزة أ في أربعة من الحقول المحددة لهذه الدراسة. وشملت الدراسة 1160 قدم من عينات اللب الصخري من 6 آبار و4000 قدم من البيانات التصويريه من 21 بئراً التي امتدت من المنطقة الوسطى إلى شرق المملكة العربية السعودية. أُجريت الدراسه على نهج هرمي على النحو التالي : (1) بيانات اتجاهات الرياح التي سجلت بشكل مناسب لكل طبقه يمكن تحديدها ؛ (2) إيجاد متوسطها لكل مجموعه من الطبقات, (3) إيجاد متوسطها لكل بئر ؛(4) إيجاد متوسطها لكل حقل ؛ وأخيراً ، إيجاد متوسها للأربعة حقول التي أُجريت عليها الدراسه. وأسفر هذا النهج في تحديد الاتجاه السائد للرياح القديمه في العصر البرمي نحو اتجاه الشرق والشمال الشرقي (اليوم) ، مع متوسط 72 درجة. تحديد اتجاه الرياح السائدة القديمة يتيح فهم توزيع الكثبان الرملية وأشكالها في جميع أنحاء الخزان. وتسهل أيضا برنامج تطوير الاستغلال الأمثل لتوزيع المسامية والنفاذية.

.

درجة الماجستير في العلوم
جامعة الملك فهد للبترول والمعادن
الظهران – المملكة العربية السعودية
2011 يناير

CHAPTER 1

INTRODUCTION

1.1 INTRODUCTION

Since 1989, Saudi Aramco has explored for, discovered and developed a number of oil and gas fields, many of which have been found in the Unayzah Formation of the Permo-Carboniferous siliciclastics sequence in the subsurface of the central and eastern of Saudi Arabia. The Unayzah Formation was deposited following a major tectonic event in the mid-Carboniferous, upon a widespread unconformity generally referred to within Arabia as the 'Hercynian Unconformity'. This is the "pre-Unayzah Unconformity" of Al-Husseini (2004). The Unayzah Formation varies considerably in thickness, and has been subdivided into four stratigraphic members, namely the Unayzah-A (youngest), Unayzah-B, un-named middle Unayzah member and Unayzah-C (oldest) (Ferguson and Chambers 1991; McGillivray and Husseini 1992, Wender et al. (1998); Al-Husseini 2004, and Melvin and Sprague 2006) (Figure1.1). The Unayzah-B and C members have the greatest thickness variations, while the Unayzah-A member has a much more uniform distribution across the area (Melvin et al. 2010a).

The Unayzah-C was deposited directly upon the Hercynian Unconformity. It is considered to be late Carboniferous (Stephanian) in age (Stephenson et al. 2003)

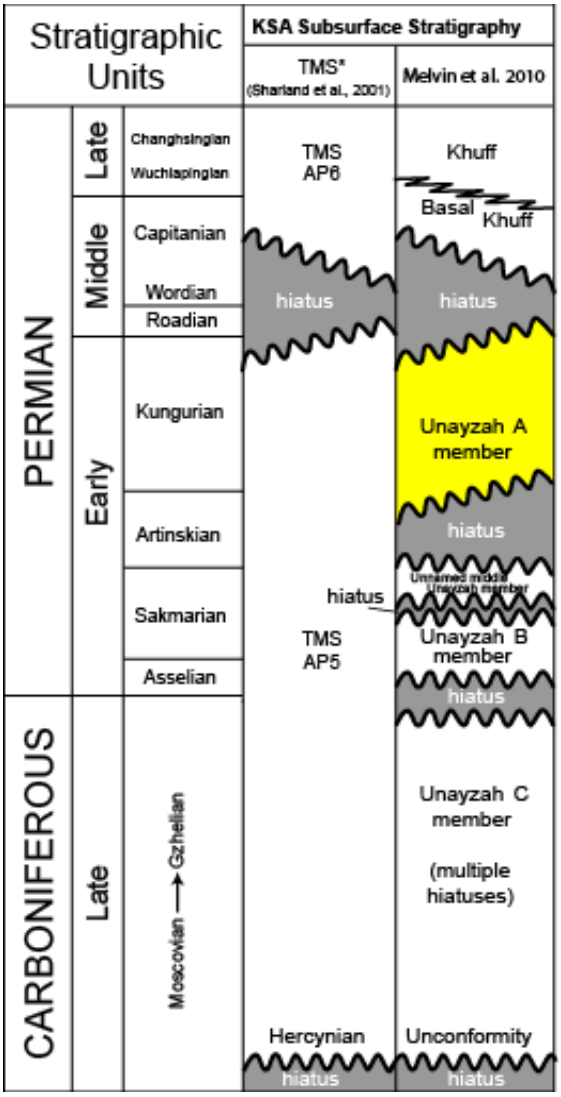

Figure 1.1: The late Carboniferous-Permian stratigraphy of Saudi Arabia (Modified after Melvin et al. 2010a).

and it was laid down very shortly after the initiation of the late Paleozoic ice age in this part of the Gondwanan continent (Al-Husseini 2004). The Unayzah-B is early Permian in age (Asselian to early Sakmarian) (Stephenson and Filatoff 2000 and Stephenson et al. 2003). The un-named middle Unayzah member was recognized by Melvin and Sprague in 2006. It is late Sakmarian in age and occurs between the Unayzah-A and Unayzah-B members with very sharp bounding surfaces (Melvin et al. 2010a). The Unayzah-A is considered to be Artinskian in age (Stephenson et al., 2003), although these rocks are notoriously barren of dateable fossil material (Melvin et al. 2010b). Deposition of the Unayzah-A terminates at the pre-Khuff Unconformity, where it is overlain by a Basal Khuff clastic section which passes up into the widespread Khuff carbonate deposits (Senalp and Duaiji 1995).

The Unayzah-B, Unayzah-C, and the un-named Middle Unayzah member are beyond the scope of this study, which will concentrate on the Unayzah-A member only. The Unayzah-A reservoir unit displays widespread evidence of deposition under arid to semi-arid conditions, very commonly in a wind-dominated, eolian setting (Melvin et al. 2010a). This indicates a significant climatic shift to arid conditions following glacially-dominated deposition during Unayzah-C and B times.

1.2 PROBLEM STATEMENT

Melvin et al. (2010 a, b) have conducted depositional facies analysis of the Unayzah-A throughout the subsurface of Saudi Arabia and concluded that it was laid down in three major eolian depositional sub-settings, namely, (1) eolian dunes, (2)

eolian sand sheets, (3) interdunes, and (4) playa lakes. The eolian facies have a widespread occurrence and include to varying extent of eolian dune cross-bedded sandstone. To date, no specific studies have been carried out that involved detailed analysis of theses dunes deposits with regard to the analysis of paleowind directions.

The current study focuses specifically on analysis relating to the eolian dune facies where they occur in the studied wells. It is important because of the economic importance and complex stratigraphic and sedimentologic nature (3D facies architecture) of the Unayzah succession. Furthermore, it has become essential for reservoir modeling and future exploration and development to accurately identify the continuity and reservoir quality of sandstones of each depositional system.

1.3 OBJECTIVE OF THE STUDY

The objective of this study is to identify and document: i) the distribution and variability (if any) of eolian facies and ii) the paleowind direction in the Unayzah-A in a number of selected areas across Saudi Arabia's subsurface. It will further discuss any variance in data in the context of (1) identifying any variation in eolian dune type, (2) evaluating the paleogeographic significance, and (3) evaluating potential economic significance of the data.

1.4 STUDY METHODS

The project entailed work in four fields, which will be referred to as Field A, field B, Field C, and Field D. The Unayzah-A in those fields was analyzed as follows:

i. For each field one well was selected that was fully cored and the cores were described in detail (Appendix 1). This enabled depositional facies to be identified and interpreted, and hence a depositional model was derived for the Unayzah-A in each cored well.

ii. Each cored well and additional wells from each of the fields (which may or may not have been cored) were further analyzed in terms of their image log data to specifically gather depositional dip-directional data on a hierarchical basis as follows:

iii. The directional data were analyzed statistically with a view to evaluating variance in the data:

   a) Within individual beds in each well
   b) Among bed sets in individual wells
   c) Among wells in each of the fields
   d) Among the fields themselves

iv. Identifying the dominant wind direction within and among bedsets enables the evaluation of dune types, within and between wells and fields, and the consistency (or otherwise) of wind direction.

1.5 LOCATION OF THE STUDY AREAS

This study was conducted using core and borehole imaging data obtained from the Unayzah-A member in four proven oil and gas fields in eastern and central Saudi Arabia. The four related study areas are shown in (Figure 1.2).

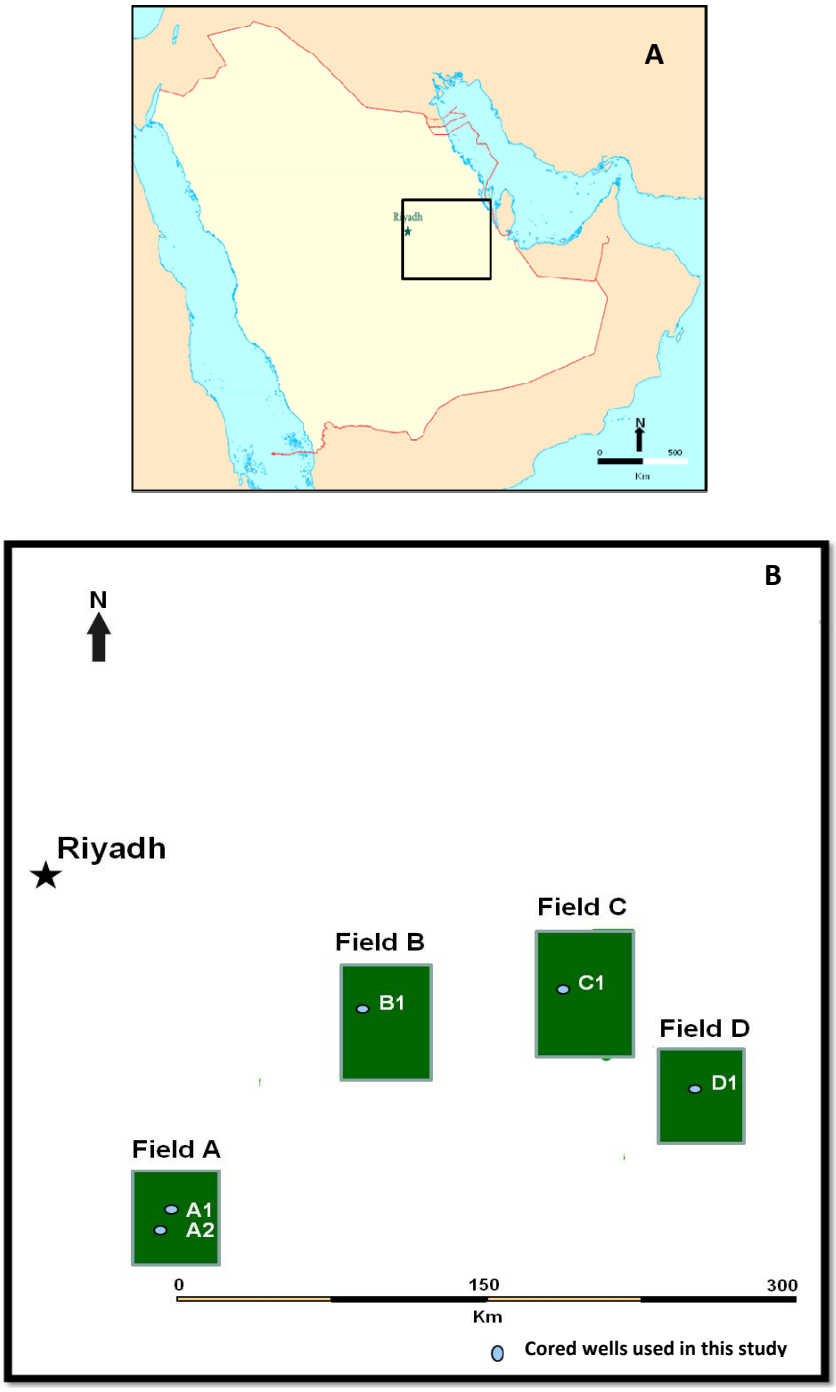

Figure 1.2: Location maps. (A) Map of the Arabian Peninsula showing the general location of the study area. Box highlights position of Figure B. (B) Map of eastern-central Saudi Arabia showing the studied fields (A, B, C, and D), and the selected cored wells used in this study.

1.6 PREVIOUS STUDIES AND LITERATURE REVIEW

Ferguson and Chambers (1991) defined the subsurface Unayzah Formation and recognized a tripartite lithostratigraphic subdivision comprising an uppermost Unayzah-A member that was underlain by the Unayzah-B member and a basal unit that was referred to as the Unayzah-C member. McGillivray and Husseini (1992) reported that, regionally, the Unayzah formation thickens eastward and southward from the central Arabian arch into the Rub' al-Kali basin.

Evans et al. (1997) identified an eolian facies at the top of Unayzah-A member in a well in central Saudi Arabia, and Heine et al. (1998) identified eolian facies generally within the Unayzah-A, based on interpretation of borehole image logs.

Aktas et al. (2000) and Al-Qassab et al. (2001) identified two higher-frequency sequences within the Unayzah-A member in wells in central Saudi Arabia, and correlated them to the Ghawar region and beyond. These sequences comprise at least five regionally correlative vertical cycles composed of varying proportions of lake, ephemeral fluvial, and eolian sediments. The authors interpreted the cycle as allogenic in origin and caused by major climatic fluctuations. They attributed the lake transgression to regional deglaciation during warm wet periods and the deposition of eolian sediments to cold arid periods.

Melvin and Heine (2004) identified a number of eolian facies in the Unayzah-A in a core and image log based study. Heine et al. (2004) extended the conceptual model and applied it to object-based geological modeling of the Unayzah reservoir.

Melvin and Sprague (2006) discussed the stratigraphic development and architecture of the lower Unayzah member in east-central Saudi Arabia. They illustrated the considerable thickness variation of the Permo-Carboniferous Unayzah reservoirs and subdivided them into four stratigraphic units, namely the lowermost Unayzah-C, overlain unconformably by Unayzah-B and overlain by the unnamed Middle Unayzah member and Unayzah-A.

Melvin et al. (2010a) in a detailed geological study based on core data and supported by image logs produced a conceptual reservoir stratigraphic model of the Unayzah-A reservoir in South Haradh. The model is allostratigraphic in concept, being related to identifiable rises in the paleo-water table, some of which are correlatable across the extent of the field. This study also revealed that the Unayzah-A in the study area can be divided into two stratal units (Lower and Upper). The lower part is comprised mainly of thin discontinuous basal eolian sandstone that passes abruptly upward into a silty sandstone unit that was deposited in a widespread playa lake depositional system. The upper unit comprises a number of eolian depositional facies.

Melvin et al. (2010) discussed, through a detailed geological study based on core data, the late Paleozoic Gondwanan glaciation and its aftermath in Saudi Arabia, and provided a view on the depositional systems of the Unayzah Formation’s four members. They noted that the Unayzah-A member is dominated by sediments that are strongly characteristic of terrestrial deposition in a simi-arid to arid environment (including ephemeral lakes and streams as well as eolian deposits).

CHAPTER 2

GEOLOGICAL BACKGROUND

2.1 INTRODUCTION

The subsurface Unayzah Formation was described for the first time by Ferguson and Chamber (1991) who informally divided the Unayzah reservoir into Unayzah-A, Unayzah-B and Unayzah-C members. Subsequently, Melvin and Sprague (2006) investigated the lower Unayzah sandstones of eastern central Saudi Arabia, and confirmed the presence of Unayzah-B and C. They also introduced the new “un-named middle Unayzah member” that overlies the Unayzah-B member. The Unayzah Formation varies considerably in thickness, with the greatest thickness variations occurring in the Unayzah-B and C members, while the Unayzah-A member has a much more uniform distribution across the area.

2.2 STRUCTURAL SETTING

During the Carboniferous, a structural event interpreted as a crustal response to compression uplifted central Arabia and tilted the Arabian Plate eastward (Husseini 1992). As a result, the northeast margin of Gondwana was transformed from a passive to an active compressional margin (Beydoun 1991). This major tectonic event, the Hercynian Orogeny, had a dramatic effect on the geology of the Arabian Peninsula (Pollastro 2003). Changes in basin geometry, regional uplift,

basement-cored uplifts, and the evidence of folding and inversion tectonics suggest that the Arabian Plate underwent multiple phases of compression during the Hercynian Orogeny (Konert et al. 2001).

Following the Hercynian uplift, structural movement's deformational processes were less significant during the Permian, and the Arabian Plate was essentially a passive margin setting (McGillivray 1994).

Unayzah-A sediments were deposited within large intra-cratonic sub-basins. These basins were progressively infilled from both the east and west with sediment onlap of relict Hercynian topography, according to Sharland et al. (2001).

In several places, the uppermost deposits of the Unayzah-A member are characterized by thick paleosols (Aktas & Cocker 1996); Melvin et al 2010b). These represent a prolonged period of minimal to non-deposition, interpreted to be directly related to thermal doming of the Arabian Plate prior to rifting and opening of the Neotethys Ocean (Melvin et al. 2010a&b), and the consequent formation of the pre-Khuff unconformity, which terminated the Unayzah deposition.

2.3 STRATIGRAPHIC SETTING

Sharland et al. (2001) recognized a number of "Tectonostratigraphic Megasequences" (TMS) that provided the foundations of a sequence stratigraphic framework for the subsurface of Saudi Arabia. Specifically, their TMS AP5 megasequence comprises in its entirety the Unayzah Formation. It is bound at its base by the "Hercynian" unconformity (pre-Unayzah unconformity of Al-Husseini, 2004), representing the middle Carboniferous "Hercynian" tectonic event. The upper

boundary of TMS AP5 is the pre-Khuff unconformity of Senalp and Al-Duaiji (1995) (Figure 2.1).

Ferguson and Chambers (1991) defined the Unayzah Formation, recognizing a tripartite lithostratigraphic subdivision comprising an uppermost Unayzah-A member that was underlain by the Unayzah-B member and a basal unit they referred to as the Unayzah-C member. This broad subdivision of the Unayzah found general acceptance among subsequent workers in the field (e.g. McGillivary and Husseini 1992; Senalp and Al-Duaiji 1995; Aktas et al. 2000; Al-Qassab et al. 2001; Al-Husseini 2004). Melvin and Sprague (2006) revisited the lower part of the Unayzah in an extensive core-based study. They confirmed and characterized the presence of the Unayzah-C and Unayzah-B members and also identified a new stratigraphic unit which they referred to as the "un-named middle Unayzah member". This new member can be recognized throughout the subsurface of eastern central Saudi Arabia and occurs stratigraphically between the Unayzah-B member and the Unayzah-A member (Melvin and Sprague 2006). It occurs in a position that occupies a previously will-defined interval in the lower part of the Unayzah-A member, as it was originally described by Ferguson and Chambers (1991). The Unayzah-A member is the highest-occurring stratigraphic unit within the Unayzah Formation and is truncated at its upper boundary by the pre-Khuff unconformity of Senalp and Al-Duaiji (1995) (Melvin et al. 2010 a&b). Melvin and Heine (2004) believe that the base of the Unayzah-A is also an unconformable surface. It appears to be generally true that all four of these component lithostratigraphic members of the Unayzah-A are separated from each other, as well as from overlying and underlying

Formations by significant depositional hiatuses (Melvin et al. 2010b) (Figure 2.1).

Palynology is the primary biostratigraphic tool used for the Unayzah Formation due to the dominant terrestrial depositional setting throughout its time of deposition, as discussed by Stephenson and Filatoff (2000a, b) and Stephenson et al. (2003). Such studies have historically proved challenging as a result of a general lack of preserved material. It has been possible, however, to assign ages to the various members of this reservoir. Thus the Unayzah-C member is considered to be Late Carboniferous (Serpukhovian-Ghzelian) in age and the Unayzah-B is Early Permian (Asselian-early Sakmarian). The unnamed middle Unayzah member is late Sakmarian in age (Melvin et al. 2010a). The Unayzah-A member is considered, based on very poor biostratigraphic data, to be datable as Artinskian to Kungurian (Melvin et al. 2010a).

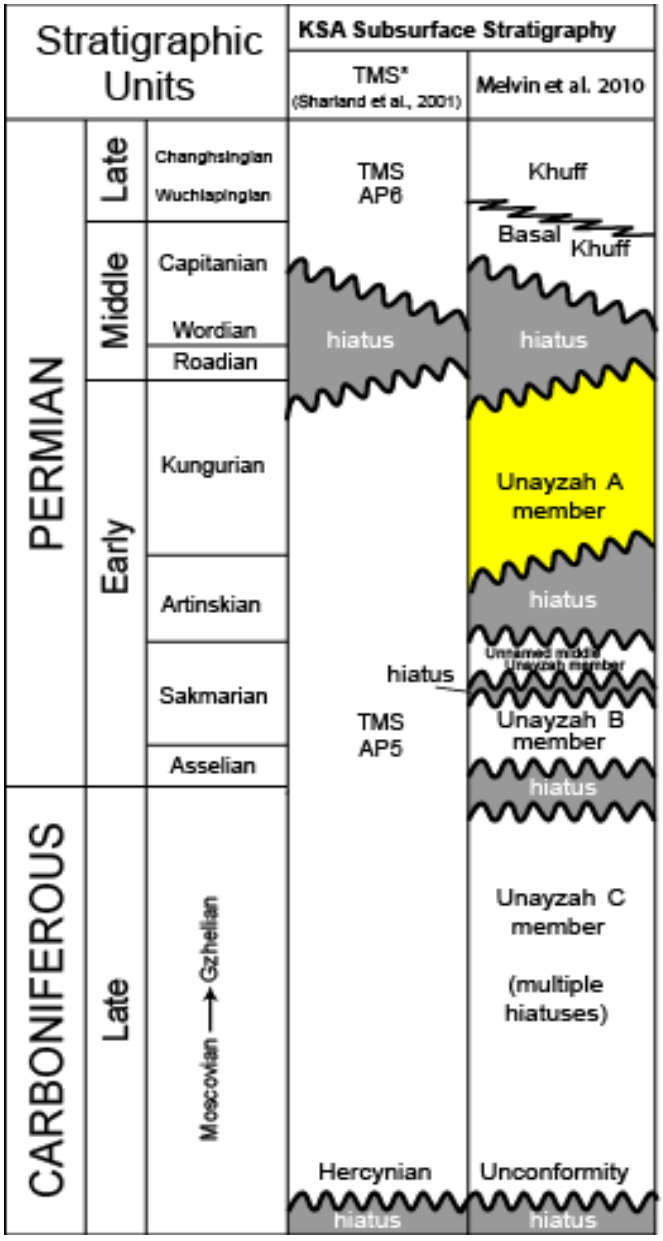

Figure 2.1: Diagram illustrating the late Carboniferous to Late Permian stratigraphy of Saudi Arabia. The Unayzah-A member (the subject of this study) is highlighted in yellow. Note that the TMS AP5 is the Tectonostratigraphic Megasequence of Sharland et al. 2001 (modified after Melvin et al. 2010a).

2.4 DEPOSITIONAL SETTING

The Unayzah-A reservoir unit in the study area displays widespread evidence of deposition under arid to semi-arid conditions, very commonly in a wind-dominated, eolian setting. The Unayzah-A comprises various eolian facies associations (including erg-center and erg-margin), as well as playa lake and ephemeral stream deposits (Melvin et al. 2010a). In South Haradh, a robust layering scheme is identified both within and between these diverse facies, which is based on paleo-water table fluctuations during Unayzah-A times, and thus is considered to have sequence stratigraphic significance (Melvin et al. 2010b). The Unayzah-A is truncated by the Pre-Khuff Unconformity (Senalpn and AL-Duaiji 1995.) This is recognizable throughout the subsurface (Al-Husseni 2004) and is overlain by the Basal Khuff Clastics member of the Khuff Formation.

Evans et al. (1997) identified an eolian facies at the top of the Unayzah-A in a well in central Saudi Arabia and subsequently Heine et al. (1998) identified eolian facies more generally within the Unayzah-A, based on interpretation of borehole image logs.

Aktas et al. (2000) and Al-Qassab et al. (2001) recognized two sequences in the Unayzah-A in the Hawtah field, which they correlated to the Ghawar area and interpreted as comprising varying proportions of lacustrine, ephemeral fluvial, and eolian sediments. Melvin and Heine (2004) described how the Unayzah-A in many places is characterized by sediments of an arid to semi-arid depositional setting. Melvin et al. (2005), in notes for a core-based workshop, elaborated by

demonstrating how in the subsurface across the entire eastern-central part of Saudi Arabia the Unayzah-A comprises a complex mix of facies representing eolian ergs, ephemeral streams, and ephemeral (playa) lakes.

Based on a detailed core and image log study, Melvin et al. (2010a) demonstrated that the Unayzah-A member is dominated by sediments that are strongly characteristic of terrestrial deposition in a semi-arid to arid environment (including ephemeral lakes and streams as well as eolian deposits). Paleomagnetic data suggest paleolatitudes of ~28° S. (Melvin et al. 2010b). The continental eolian clastic deposits of this member in places display cyclicity in their stratal architecture that is related to fluctuations in the paleo–water table. These fluctuations are possibly related to distant marine transgression, which is supported by the occurrence of a distinctive bioturbated sandstone very close to the top of the Unayzah-A member (Melvin et al. 2010b). Elsewhere, along the Hawtah Trend, Aktas et al. (2000) attributed similar cyclic sedimentation to major climatic fluctuations and lacustrine transgression, Melvin et al. (2010a) also demonstrated that the Unayzah-A could be readily subdivided into a lower stratal unit and an upper one. The lower unit comprised a limited number of eolian depositional facies, whereas the upper unit displayed a more varied suite of facies.

CHAPTER 3

CORE STUDIES

3.1 INTRODUCTION

A total of 1096 feet of Unayzah-A core from four fields was described in detail in this study (Figure 3.1) (See (Appendix 1), which includes incorporating the structure and lithology. The studied core displays widespread evidence of deposition under arid to semi-arid conditions, very commonly in a wind-dominated, eolian setting.

A number of distinctive eolian depositional facies were recognized in the studied wells, and these include: dune, sand sheet, and interdune. These various depositional facies occur with a high degree of repeatability throughout the Unayzah-A reservoirs and were recognized in all of the studied wells.

3.2 EOLIAN DEPOSITIONAL ENVIRONMENT

Webster's (2002) dictionary defines eolian as: *born*, deposited, produced, or eroded deposits by the wind. Origin of eolian: Latin Aeolus. First known use: (1622). From Glossary of Geology (Jackson 1997), eolian is defined as: pertaining to the wind; esp. said of such deposits as loess and dune sand, of sedimentary structure such as wind-formed ripple marks, or of erosion and deposition accomplished by the wind.

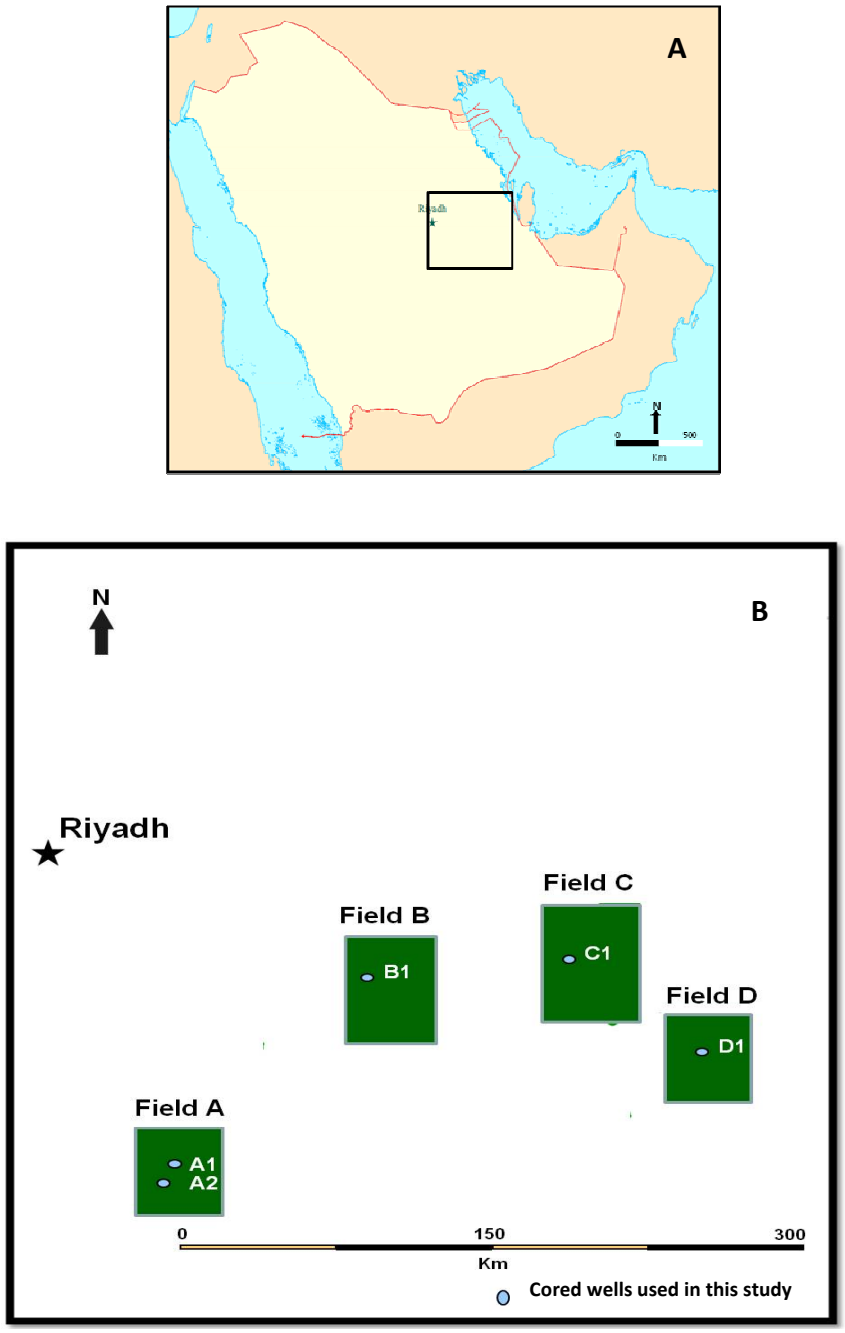

Figure 3.1: Location maps. (A) Map of the Arabian Peninsula showing the general location of the study area. Box highlights position of figure B. (B) Map of eastern-central Saudi Arabia showing the studied fields (A, B, C, and D), and the cored wells used in the current study.

3.2.1 Eolian Sand

Studies have shown that the sand that is generally available for transport by the wind is restricted to an extremely narrow grain sand size range, which is mainly between 10-30 phi (Pye and Tsoar 2009) (Figure 3.2). Very fine particles that can be held in suspension are therefore classified as silt or dust, while heavier particles unaffected by wind are classified as pebbles or gravel (Bagnold 1941; Cooke and Warren 1973) (Figure 3.3).

Neither mineral composition nor particle shape appears to have any significant effect on sand movement or accumulation. Any solid, non-cohesive particle, natural or human-made, that falls within the above-mentioned range is technically sand, including dry granular snow which can be built up by the wind into dune-like drifts. Although sand can be composed of various minerals, quartz makes up the bulk of the world's eolian sand grains. This dominance is primarily due to the widespread distribution of quartz-containing rocks and to the relatively chemical inert nature of quartz. Unlike other particles, quartz sand grains resist both mechanical and chemical breakup into smaller sizes (Bagnold 1941).

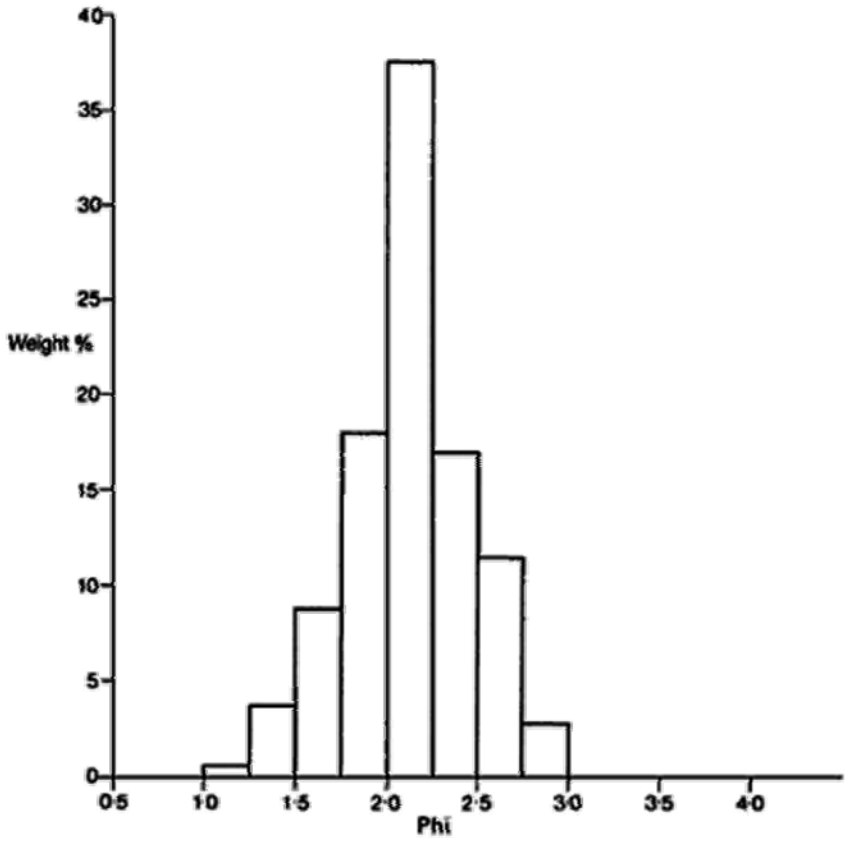

Figure 3.2: Grain Size frequency histogram of a sample of foredune sand, sieved at quarter-phi intervals, illustrates wind transported grain size narrow frequency. (modified after Pye and Tsoar 2009).

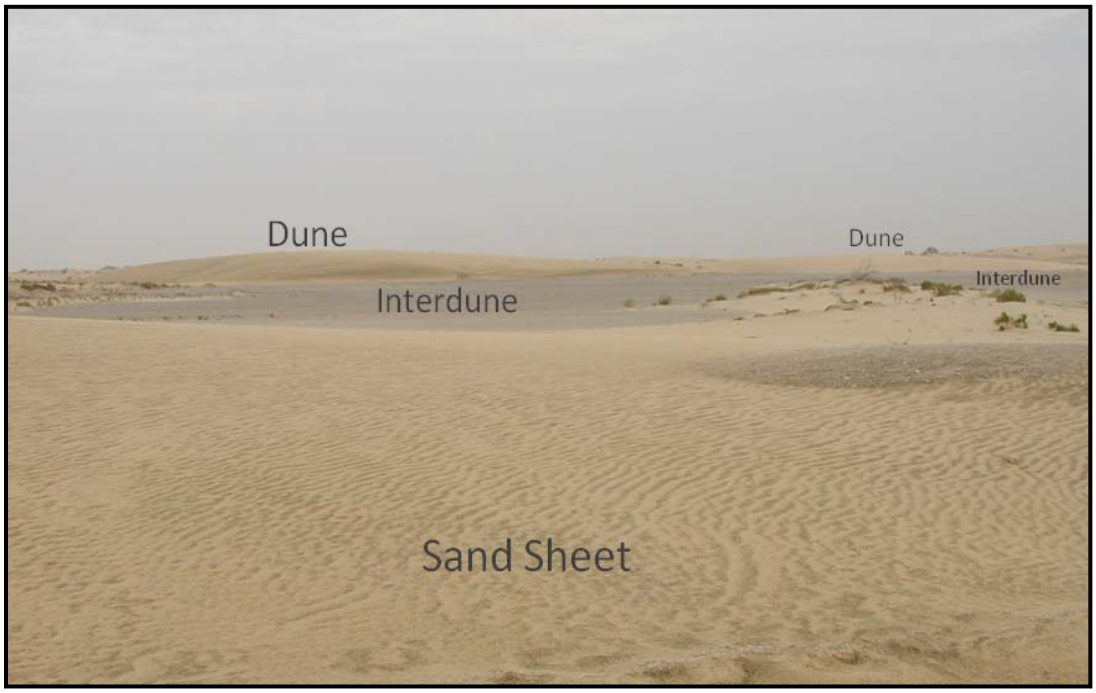

Figure 3.3: Photograph from modern eolian setting showing different eolian deposits (dune, sand sheet, and interdune) accumulations, (Half-moon Bay, Dhahran, Saudi Arabia).

The wind is only capable of transporting dry sediment. Because fine silt and clay particles take a relatively long time to settle even in air, the turbulent action of the wind tends to keep them in suspension over large distances, and the greater part is finally deposited in more humid areas outside the primary desert basin as loess, or over sea (Glennie 1970).

Wind-transported sand derives in part from chemical weathering and from the fracturing of rock surfaces by rapid temperature changes and the abrasive action of wind-blown sand (Glennie 1970). It has long been known that eolian sands can be transported across the distances of entire continents (e.g. Fryberger & Ahlbrandt 1979), so that identifying the source area for a particular dune field or erg is not necessarily easy.

Wind effectively separates sediment finer than about 0.05 mm (silt) from coarser sediment and transports this finer sediment long distances in suspension. Except at unusually high wind velocity, coarser sediment is transported by traction and saltation close to the ground (Figure 3.4a and b). Saltation is a particularly important mode of wind transport, aided by downslope creep of grains owing to impact of saltating grains as they strike the bed. Wind appears to be especially effective in transport of medium to fine sand and finer sediments, but coarse particles (up to 2 mm or larger) may also undergo transport by rolling and surface creep under high-velocity wind (Boggs 2001).

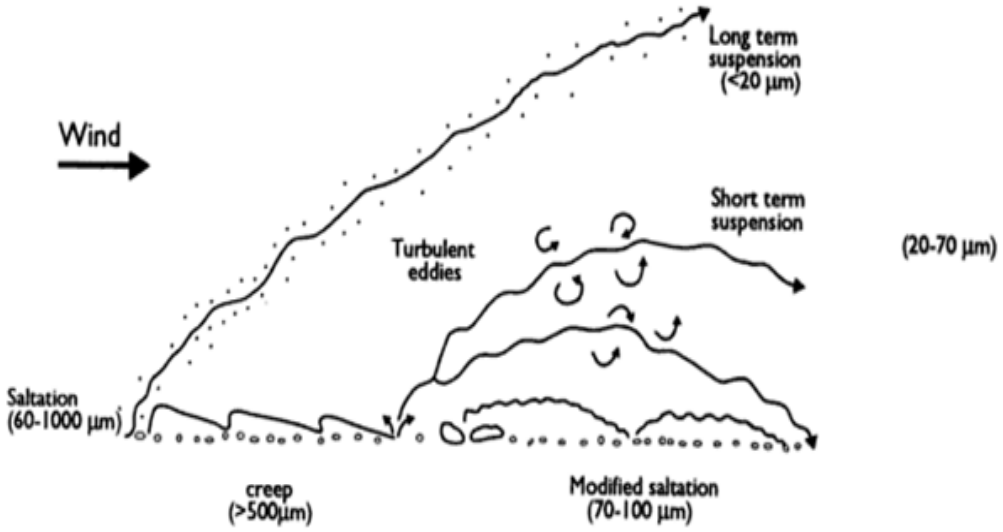

Figure 3.4a: Modes of eolian sediment transport (modified after Pye 1987).

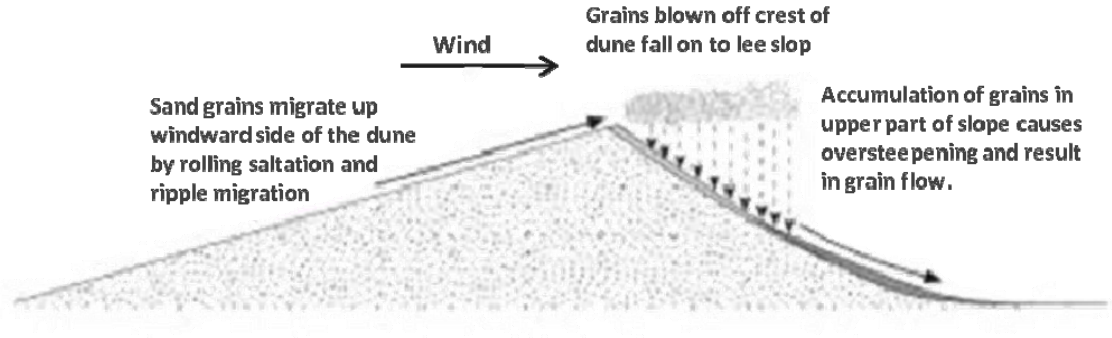

Figure 3.4b: Wind-blown sand moves up the gentle upwind side of the dune by saltation or creep. Sand accumulates at the brink, the top of the slipface. When the buildup of sand at the brink exceeds the angle of repose, a small avalanche of grains slides down the slipface, grain by grain the dune moves downwind (modified after Nicholas 2009).

Two primary factors are necessary for the accumulation of sand into sand sheets and dunes: 1) an adequate supply of sand, and 2) wind strong enough and persistent enough to move the sand (McKee 1979). If these two conditions are met, large quantities of sand can be transported hundreds and even thousands of miles (Fryberger and Ahlbrandt 1979).

For accumulation to occur, a decrease in the downstream transport rate and/or a decrease in concentration of sediment over time must occur, regardless of whether accumulation is from the bedload or the suspended load (i.e. loess accumulation).

By definition, eolian dune sands are deposited above the water-table (Boggs 2001). Preservation of eolian dune deposits can only take place when the sediments are permanently buried below an erosional base-level, which can be thought of as the post-depositional water-table. Thus, any sediment deposited during migration of dunes across a desert will only be preserved as the lower part of the dunes that is subsequently contained below the water table, (Boggs 2001) (Figure 3.5). Preservation can take place by basin subsidence, water-table rise, or a combination of the two. Thick eolian accumulations can occur in fault-controlled, rapidly subsiding basins as is the case in the south-west United States (Collinson 1978), and on stable cratonic areas like the Rub Al-Khali in Saudi Arabia, where the basin subsidence is slow compared to rifted, fault-bound basins.

Only rarely are complete dunes captured in the rock record. Varying degrees of preserved dune topography have been reported buried by marine or other

sediments (Eschner & Kocurek 1986 &1988; Fryberger 1986; Chan & Kocurek 1988) or buried beneath lava flows (C1emmensen 1988), but typically dunes are represented only by their basal portions that were progressively deposited over relatively long periods of time (Kocurek 1991).

3.2.2 Eolian Sand Stratification

Stratification in eolian dune facies is a function of the dune type and its processes of growth and movement (Fryberger 1990).

The basic deposit of an eolian sand dune is a set of cross strata, which is formed by depositional processes on a dune through time. That migrating bedforms, like dunes, produce sets of cross strata has been realized since Sorby (1859), but analytical studies of these did not occur until Allen (1963, 1968, 1970). Much of the present-day theory, which follows from Allen, has been collected by Hunter (1977) and Rubin & Hunter (1982) (Figure 3.6).

In general, however, dune deposits contain the steepest cross-bedding due to included avalanche strata. The complexity of the cross-bedding increases with increasing complexity of the wind regime. Dune types range from transverse dunes, through barchan, to linear, to star dune (Fryberger 1990).

The characteristics of interdune deposits are determined by moisture content, in addition to the associated dune type. Thus, they include wet interdune, damp interdune, dry interdune, and playa lake deposits. Sand sheets are found anywhere there is mobile sand, but are commonly a marginal facies to dune complexes and contain gently dipping or flat lying strata (Fryberger 1990) (Figure 3.5).

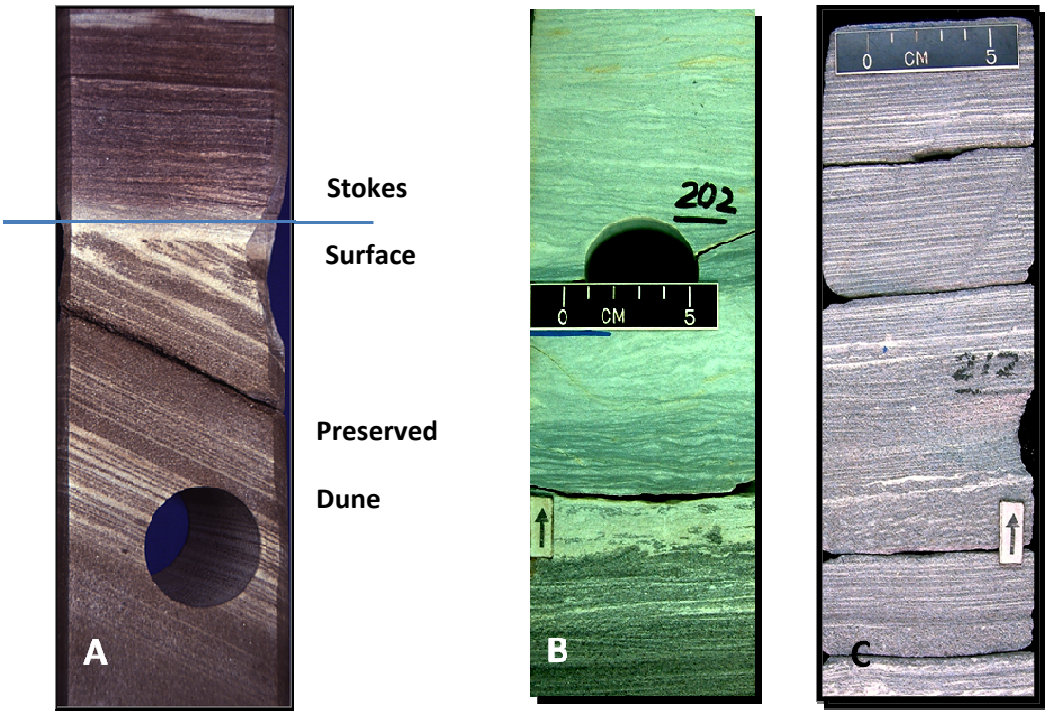

Figure 3.5: Core photographs from the study areas illustrating the main eolian depositional facies A: Showing preserved dune facies deposits below the paleo-water table. Note the abrupt upper horizontal termination of pronounced eolian dune cross-bedding. This is a "Stokes surface" and is overlain in this example by a sand sheet facies. It represents a rise through the dune deposits of the paleo-water table. B: Silty sandstone with irregular laminations that are associated with interdune setting, are overlain by flat laminations of sand sheet deposits. C: this example is showing well developed low-angle to flat wind ripple lamination of the eolian sand sheet depositional facies.

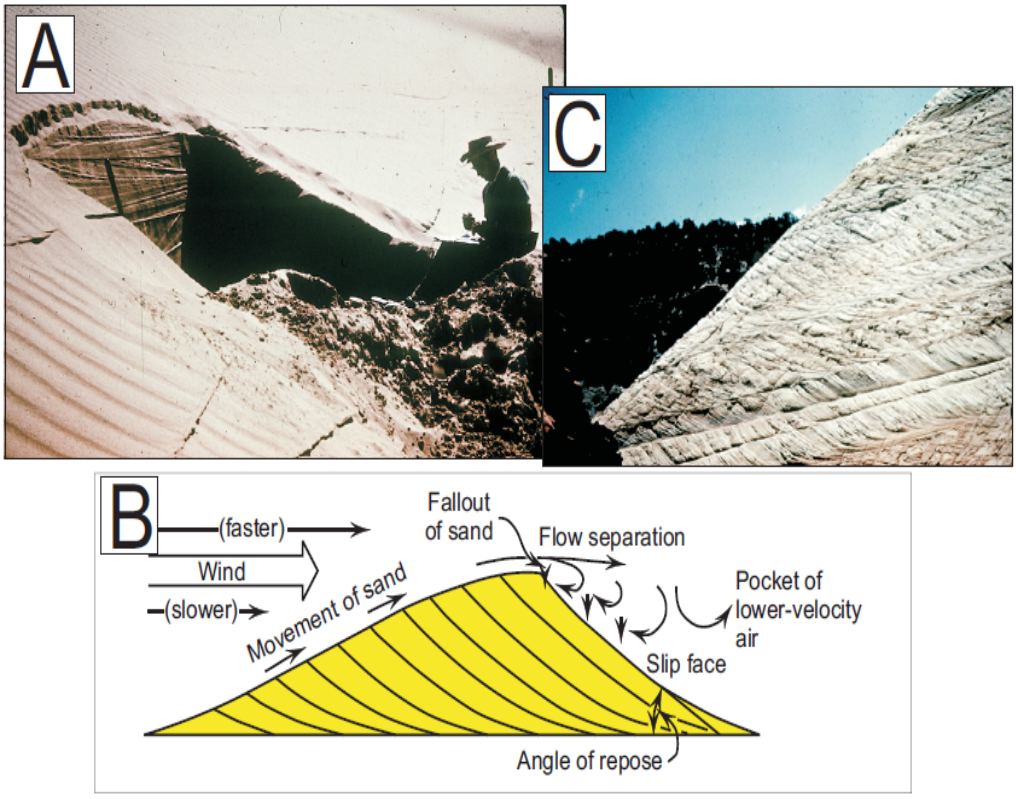

Figure 3.6: (A) The geologist in this picture has excavated the face of a sand dune. Note the different angles of the cross-beds. This indicates that the sand dune formed in an area of alternating wind directions. (B) Schematic cross-section that illustrates the movement of sand grains to form sand dunes. Grains move across the top of the windward side of the dune and fall over the steeper lee side. Over time, the continual downwind movement of grains causes the entire dune to migrate. (C) Windblown eolian sedimentary rock. Direction of transport of the sand by the wind wasleft to right, as shown by the orientation of the dune's cross-stratification (Slatt 2006).

3.2.3 Eolian Sand Dunes

Desert dunes occur in a variety of morphologic types, each of which displays a range of sizes (height, width and spacing) (Lancaster 1995). Eolian bedforms range in scale from small ripples to transverse and longitudinal dunes 0.1-100 m high to complex dunes, called draas, with heights of 20-450 m (Wilson 1972). Barchans, barchanoid ridges, and transverse dunes form under the influence of unidirectional winds. They have single slip faces and appear to represent a gradational series corresponding to an increase in sand supply (McKee 1979a). Parabolic and blowout dunes have one or more slip faces. They are related to the preceding group of dunes, but their development is controlled by vegetation cover. Dome dunes are circular in plan view and have no definite slip faces. They may originate by modification of barchanoid dunes by strong winds. Linear dunes, also called seifs or longitudinal dunes have nearly symmetrical ridges, and reversing dunes have asymmetrical ridges; both types have two slip faces (Boggs 2001). Linear dunes form in areas of uniform sand accumulation under generally high-velocity winds of variable directions. Reversing dunes, in which slip faces form on opposite sides at different times, result from a close balance between opposed winds (McKee 1979b). Star dunes are huge stellate dunes up to 450 m high, with a high central peak and radiating arms and commonly with superposed complex or compound dunes. They have three or more slip faces and apparently form under intense, multidirectional wind systems in areas of high sand-drift potential (Fryberger and Dean 1979) (Figure 3.7).

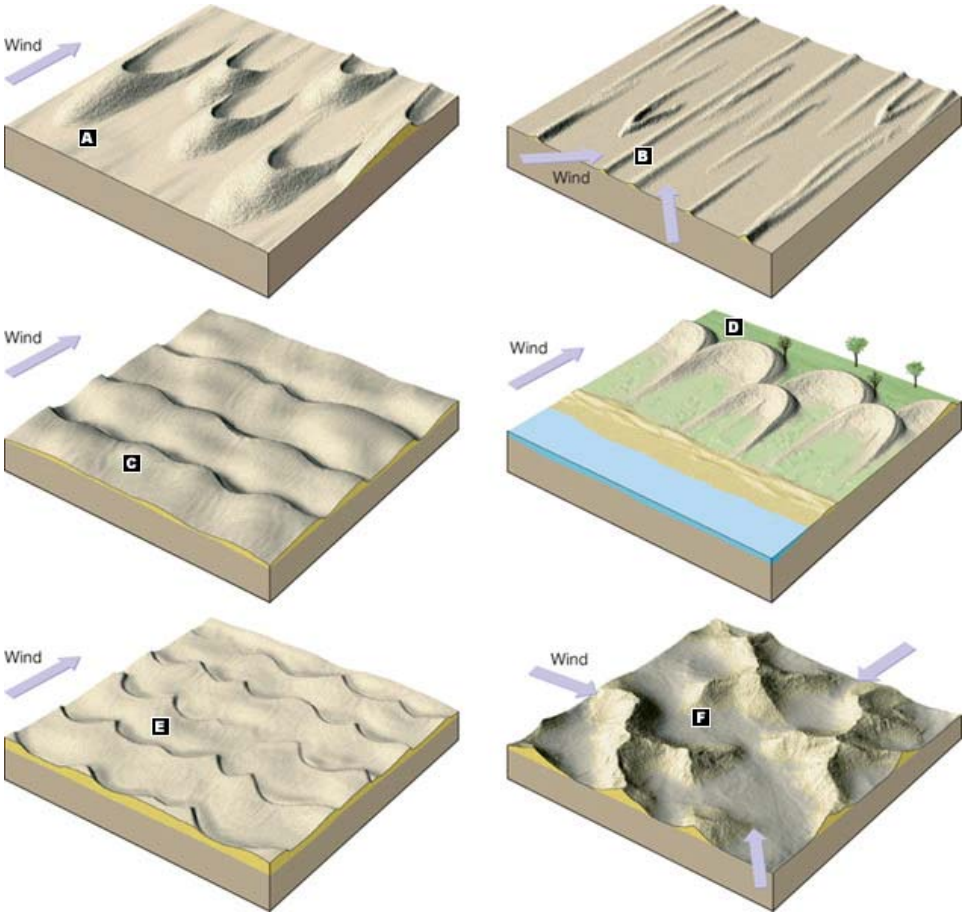

Figure 3.7: Basic eolian bedforms as related to the number of slipfaces; A: Barchan dune; B: Longitudional dune; C: Transverse dune; D: Parabolic dune; E: Barchanoid ridge dune; F: Star dune. This terminology follows that used by McKee (1979) for ground studies of eolian deposits (modified after Brookfield 2011).

3.2.4 Internal Structure of Sand Dunes

The most common characteristic feature of an eolian sand dune is the presence of a steep slip face and a gentle dipping windward side (Reineck & Singh 1975). The height of the dunes depends on the strength of the wind and the grain size. The rate of deposition is zero at the summit of a dune, reaches a maximum on the lee slope, and thereafter falls to zero again at the far end of the lee slope (Bagnold 1954). This fact results in faster advance of the upper part of the slip face than the lower part. This causes an over steepening of the slip face. If the maximum angle of repose (34º) is exceeded, the mass of the sand shears, an avalanche takes place, and a slip face is formed. This process is repeated every time maximum angle of repose is exceeded. On the windward slope, sand grains move upward by the processes of saltation and surface creep and are deposited on the upper part of slip face from where they avalanche. This process causes forward migration of sand dunes (Reineck & Singh 1975).

Cross-bedded units of sand dunes are made up of avalanche laminae of the slip face and wind ripple laminae “pin-stripe” lamination. Foreset laminae are steeply inclined, and angle of dip usually varies between 25 and 34º. Near the base of slip face, foreset laminae tend to flatten out. Individual foreset laminae are rather thick, 2-5 cm, and are less well defined than the horizontal laminae (Inman et. al. 1966; Sharp 1966). McKee (1966) gave a detailed account of cross-bedding in sand dunes. The bounding surfaces of the cross-bedded units are erosional and planar. Thus, most of the cross-bedded units are of planar type. Tabular shapes are more common than the wedge-shaped units. Wedge-shaped cross-bedded units are

produced if there are changes in wind direction. The bounding surfaces are nearly horizontal or dip in an upwind direction at low angle in the upward part of a dune. Near the slip face, bounding surfaces are rather steep (15 to 25º), dipping in a downwind direction (Reineck & Singh 1975) (Figure 3.8a,b) and (Figure 3.9).

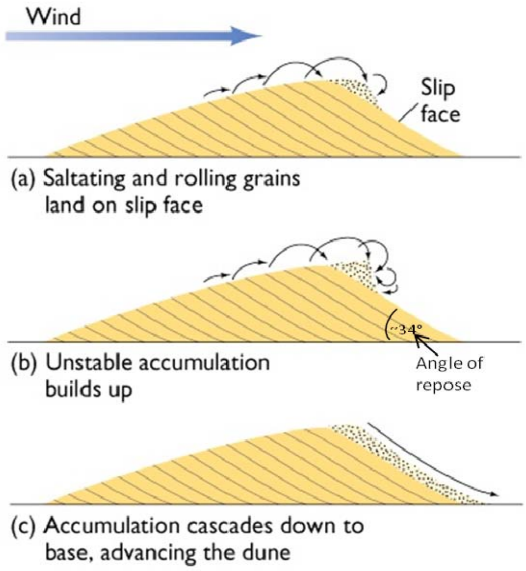

Figure 3.8a: Cartoon diagrams showing the mechanism of transport and accumulation of a sand dune. Note (1) the wind direction from left to right, thus the dune migration direction is to the right, and (2) once the grains accumulating at the top of the dune exceed the angle of repose, which is (34°), the grain will move downward forming a new bed at the lee side of the dune. (http://hsb.iitm.ac.in/~jm/ARCHIVES/Mar-April04/articles_files/sanddunes.html)

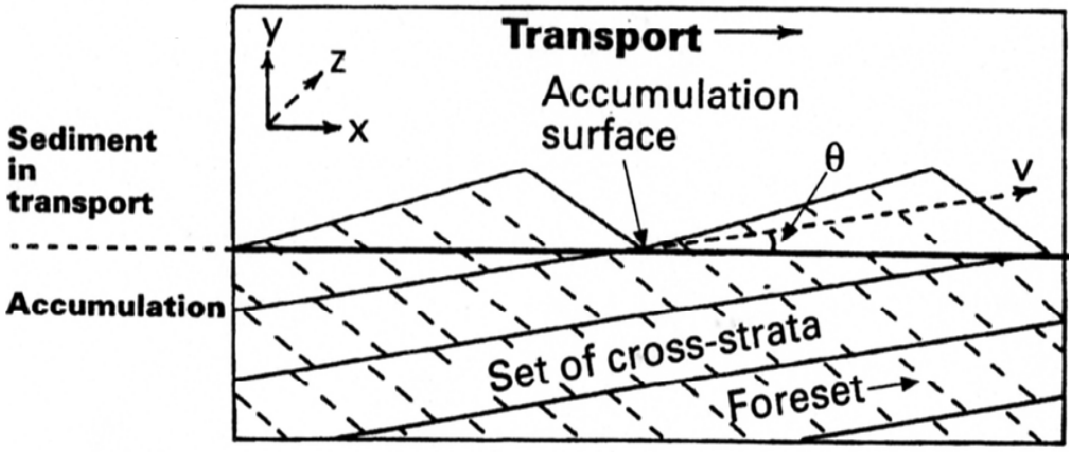

Figure 3.8b: Cartoon diagram showing the generation of sets of cross strata by migrating and climbing dunes shown in cross-section (x, y), where all transport is in the x direction and a unit width (z) is representative. Note the lines between the different sets are “bounding surfaces”, which are erosional surfaces within or between sets of cross strata (modified from Kocurek and Havholm 1993).

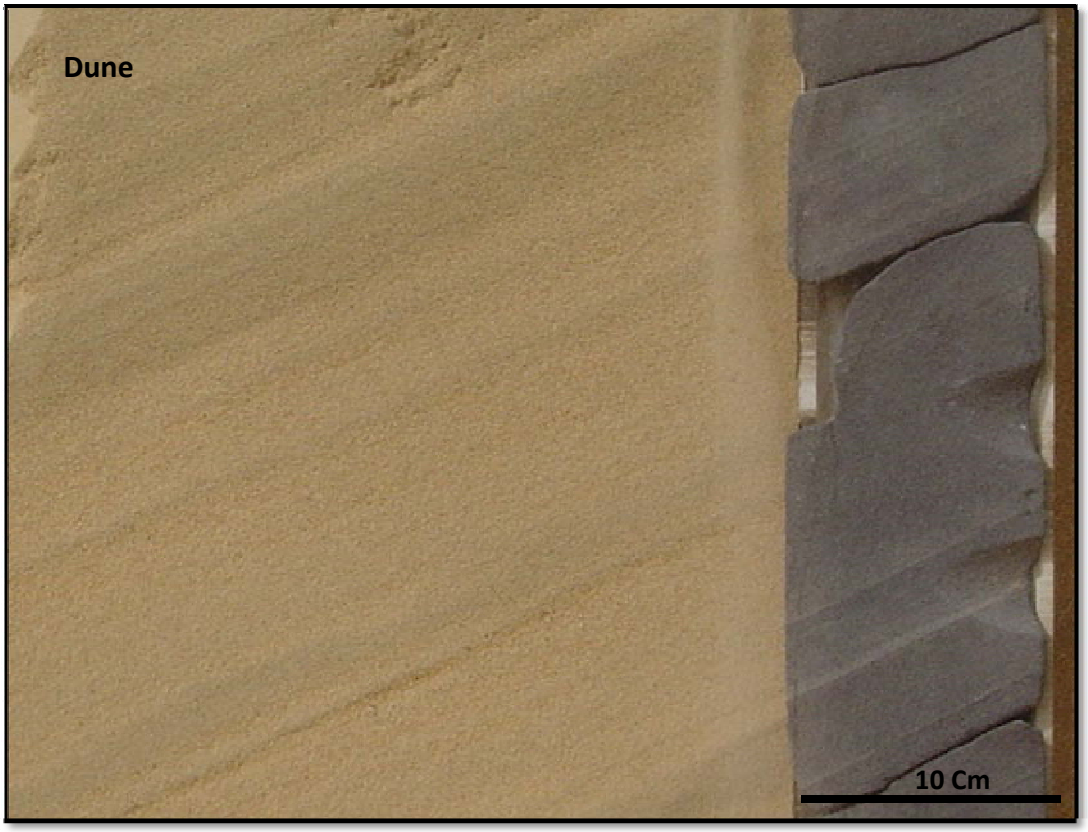

Figure 3.9: Trenched section through a modern sand dune, showing a comparison between ancient eolian deposits (core sample- well D1) and modern eolian deposits. Note the high angle grain size segregation lamination and the cross stratification similarity (Half-moon Bay Dhahran, Saudi Arabia).

3.2.5 Interdune

Interdune areas occur between dunes and are bounded by dunes or other eolian deposits such as sand sheets (Figure 3.3). Interdune deposits are characterized by thin units of roughly horizontal, thinly-bedded very fine sandstone. These may show ripple cross-lamination, poorly defined, thin horizontal bedding with silty drapes, desiccation cracks, deformed laminae, and rare bioturbation (Collinson 1978). They are ascribed to interdune setting where a variety of both wind and aqueous processes may operate (Kocurek 1981; Adams and Patton 1979).

Interdunes may be either deflationary (erosional) or depositional (Boggs 2001). Very little sediment accumulates in most deflationary interdunes except coarse, granule-size lag sediments that may show rippled surfaces and inverse grading. Deflationary interdunes are preserved in the rock record as a disconformity overlain by thin, discontinuous, winnowed lag deposits. Sediments deposited in depositional interdunes areas can include both subaqueous and subaerial deposits, depending upon whether they are deposited in wet, dry, or evaporite interdunes (Ahlbrandt and Fryberger 1981). All interdune deposits are characterized by low-angle stratification (<10°), because they are formed by processes other than dune migration (Boggs 2001) (Figure 3.10).

3.2.6 Sand Sheets

Sand sheets usually occupy very large areas of desert country. They are flat to gently undulating bodies of sand that commonly surround dune fields (Boggs 2001) (Figure 3.3). They are typically characterized by low to moderately dipping

(0-20°) cross-stratification and may be associated in some parts with ephemeral stream deposits. Sheet-sand deposits may also contain gently dipping, curved, or irregular surfaces of erosion several meters in length; abundant bioturbation traces formed by insects and plants; small-scale cut-and-fill structures; gently dipping, poorly laminated layers resulting from adjacent grainfall deposition; discontinuous, thin layers of coarse sand intercalated with fine sand; and rare intercalations of high-angle eolian deposits (Ahlbrandt and Fryberger 1982; Kocurek and Nielson 1986; Schwan 1988) (Figure 3.11).

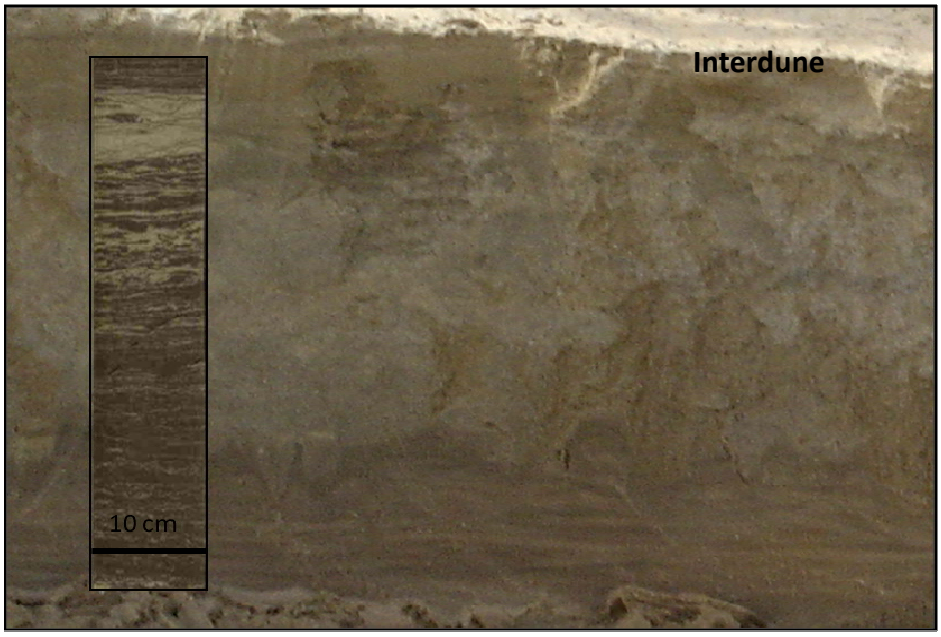

Figure 3.10: Trenched section through a modern interdune facies and a 4" subsurface core, showing comparison between modern and ancient interdune deposits from core (well B1). Note the horizontal laminations and the adhesion ripples and water-lain deposits (Half-moon Bay Dhahran, Saudi Arabia).

Figure 3.11: Trenched section through modern sand-sheet deposits, showing a comparison between modern eolian sand-sheet deposits and ancient sand-sheet deposits from core (well C1). Note the low angle lamination compared to eolian dune deposits (Half-moon Bay Dhahran, Saudi Arabia).

3.3 STUDY AREA DEPOSITIONAL FACIES

A total of 1096 feet of core from four fields was described in detail in this study (Appendix1). The studied cores display five distinctive litho-facies: 1) High-angle cross-bedded sandstones, 2) low-angle to flat laminated sandstones, 3) irregularly laminated sandstones, 4) irregularly laminated, silty sandstones, and 5) poorly sorted, patchy carbonate cemented sandstones. These various depositional facies occur with a high degree of repeatability throughout the Unayzah-A reservoirs and were recognized in all of the studied wells. The facies association showed widespread evidence of deposition under arid to semi-arid conditions, very commonly in a wind-dominated, eolian setting.

3.2.1 High-angle Cross-bedded Sandstones

Description: This litho-facies consists of fine- to medium-grained sandstones with very well rounded and frosted grains of quartz sand occurring in high-angle, grain size-segregated cross laminations typically with foreset dips over 25º. This facies is seen in all of the studied wells, although in varying proportions. The cross-laminations may show very close (mm-scale), and commonly inversely graded, 'pin-striped' spacing (*sensu* Fryberger and Schenk 1988) (Figure 3.12). Alternatively, they may be a few centimeters thick, representing gravity sliding/grain flow lamination down the dune slip faces. The basal set (dune toe) of cross-bedded sand stone generally display lower dip angle and in several places show a degree of deformation. This litho-facies represents eolian dune cross-bedded sandstones, and

is well displayed in all the cored wells. These cross laminations in many places are abruptly truncated by a horizontal surface that is overlain by flat-laminated sandstone. These cross-bedded deposits are also readily identified on downhole image logs, which allows this facies to be recognized in uncored wells (see following chapter).

Interpretation: The closely spaced pinstripe cross lamination and the textural characterization of these sandstones are interpreted as wind ripple laminations (subcritically climbing translatent strata: Kocurek and Dott 1981) which formed on the slip face of sand dunes. The thicker cross laminations are grain flow cross strata and represent gravity sliding down the dune slip faces. The horizontal surfaces that sharply truncate the eolian cross-bedding are attributed to the rising paleo-water table (Stokes surface) (*sensu* Stokes 1968; Fryberger et al. 1988; Melvin et al. 2010a) (Figure 3.12).

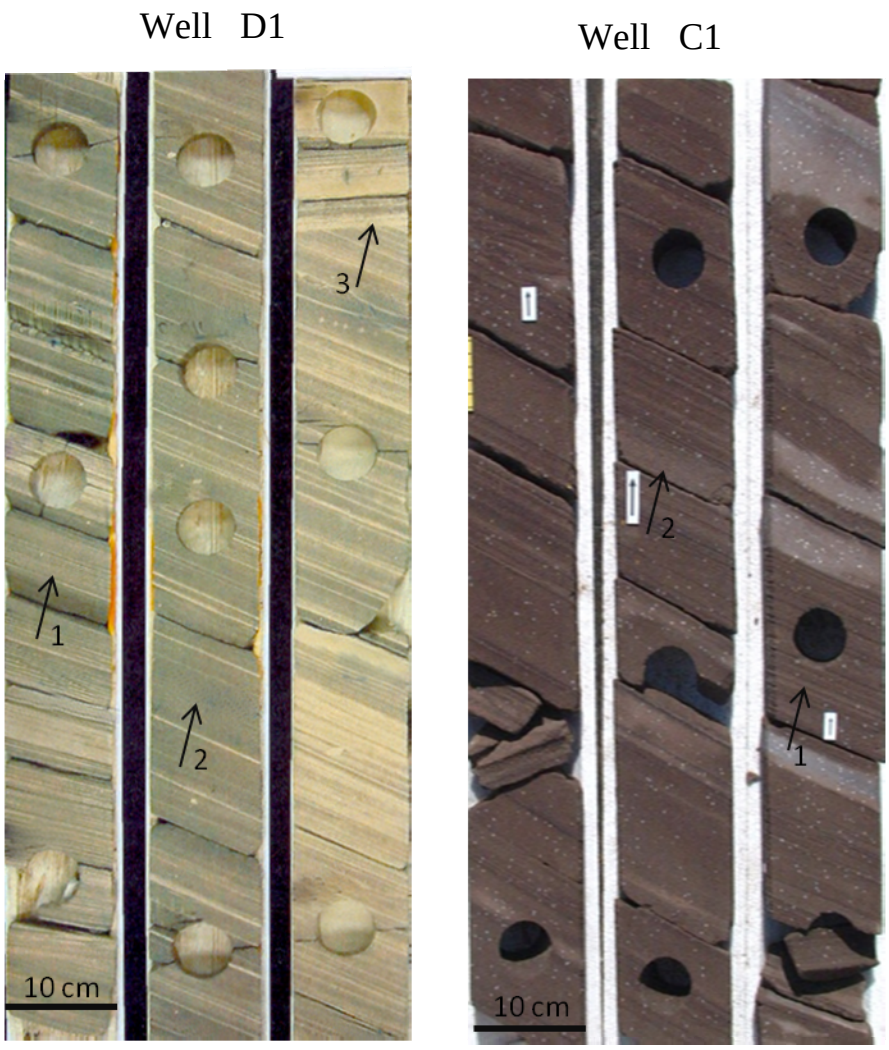

Figure 3.12: Sandstones of the Unayzah-A, showing well developed eolian dune cross stratification. Closely spaced, 'pin-striped' wind ripple lamination is very well displayed (arrow1); thicker laminations reflecting grain flow on the dune's lee slope are also well preserved (arrow 2), The horizontal surface truncating the dune cross strata at (arrow 3) is a "Stokes Surface" reflecting rising paleo-water table through the dune deposits and is overlain in this example by flat, laminated, silty sandstone (interdune facies). Note the patchy distribution of the post-depositional white nodules of anhydrite in well C1.

3.3.2 Low-angle to Flat Laminated Sandstones

Description: This depositional litho-facies consists of fine to medium-grained sandstones, with very well rounded, well sorted and frosted grains of sand that occur in very low-angle to flat grain size segregated laminations (Figure 3.13). They are seen in all of the cored wells in varying proportions. Flat-based lenses of medium-coarse sand were also observed within these deposits. Many lamina-sets show a pin-striped appearance, which is also identified in image logs. Lamination disruption has been locally observed and very low-angle truncations was also observed in several places, which separates different sets of low-angle laminated sandstone.

Interpretation: Based on the observed characteristics, mainly the occurrence of the "pin-strip" low-angle to flat laminations (*sensu* Fryberger et al. 1979), and by comparing these characteristics to modern analogs (Figure 3.14), it can be concluded that this facies represents eolian sand sheet deposits. The local sediment lamination disruption that occurred by plant rooting in most cases is a strong indication of the close water table, which is expected in the eolian sand sheet deposits.

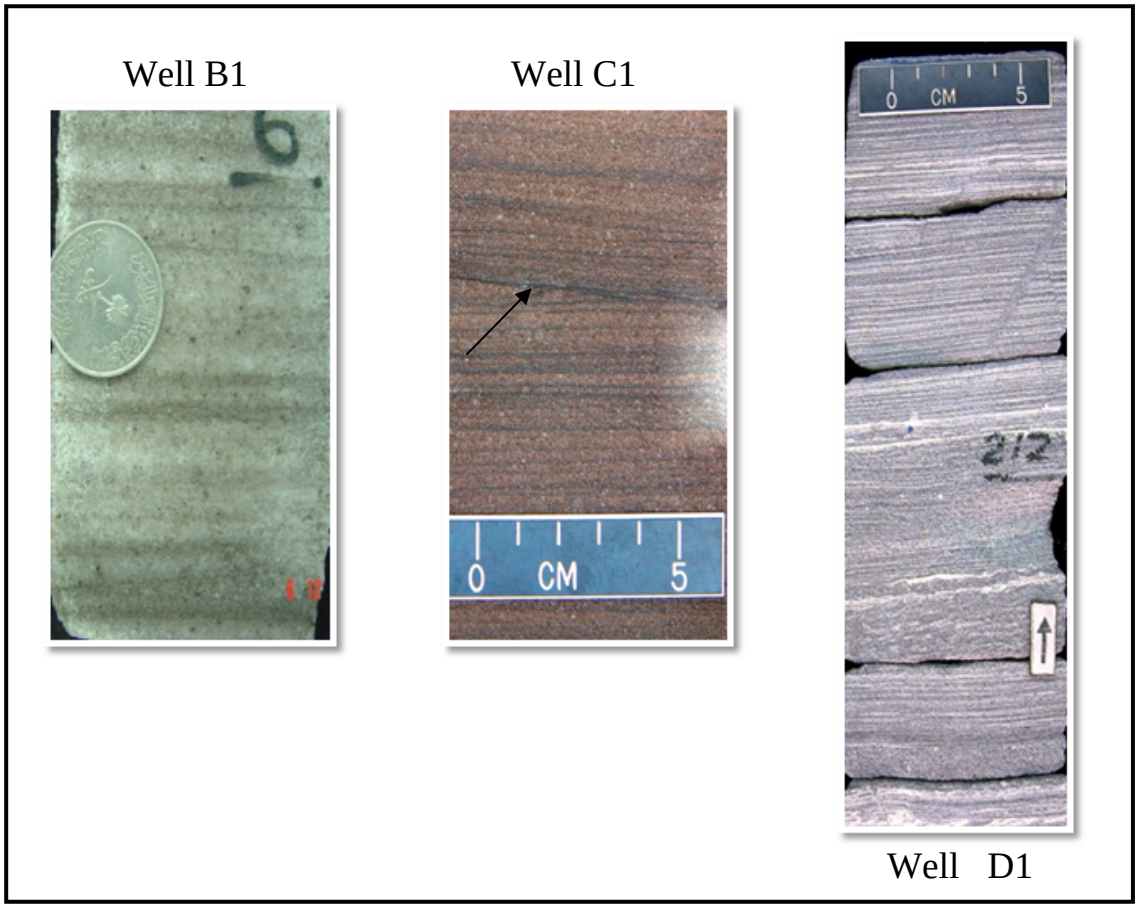

Figure 3.13: Core photographs illustrating different eolian sand sheet deposits encountered within the Unayzah-A member in the study areas. All of them showed fine- to medium-grained sandstone with flat to low angle lamination (and rare crinkly-laminated interbeds). Note: (1) the grain size segregation lamination varies in thickness in well B1, (2) the very low-angle truncation of the lamina-sets (arrow) in well C1, and (3) the clear flat to very low “pin-striped” grain size segregation lamination in well D1.

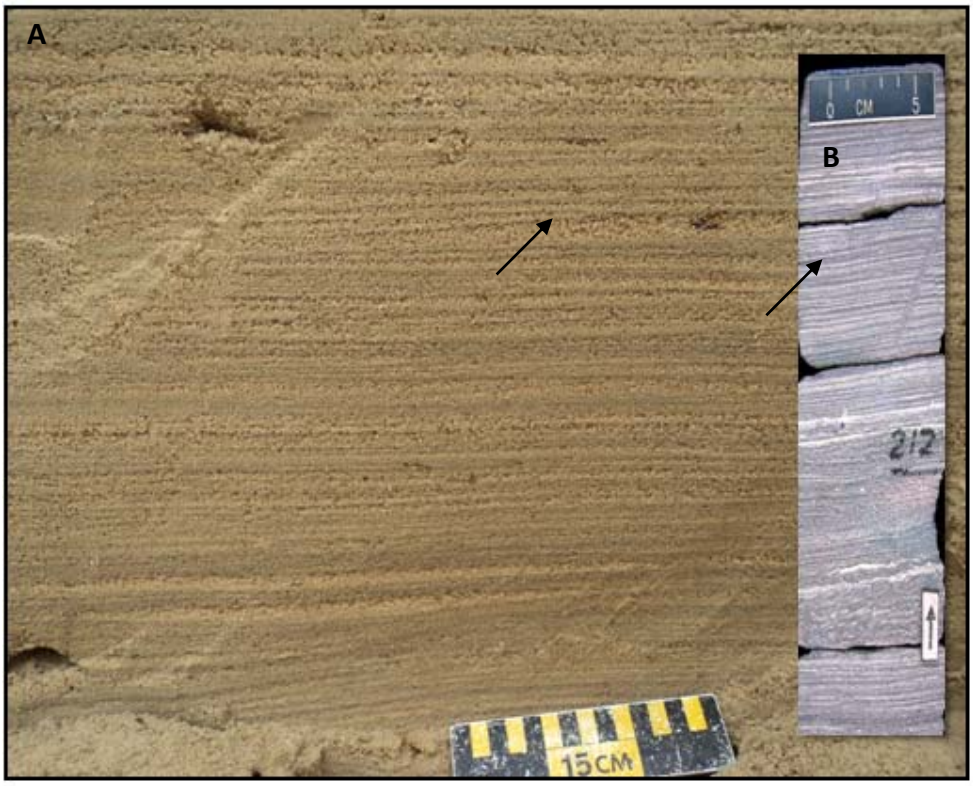

Figure 3.14: Photographs showing a comparison between modern and ancient wind ripple lamination of the eolian sand sheet depositional facies. (A) Modern trenched section through a sand sheet deposits (Half-moon Bay, Dhahran) showing a very well developed flat "pin-strip" grain size segregation lamination. Note the low-angle truncation of the lamina-sets (arrowed). (B) Core photographs from well D1 showing a very low-angle wind ripple lamination interpreted as sand sheet deposits. Note the very well developed "pin-stripe" grain size segregation lamination and the low-angle truncation (arrowed).

3.3.3 Irregularly Laminated Sandstones

Description: This facies is common throughout the Unayzah-A member in the studied areas, although it varies in proportion among the investigated wells. It is generally characterized by fine to medium grained, moderately sorted sandstones showing irregular to disrupted, crinkly and variably continuous laminations and very thin (cm-scale) beds with well-developed adhesion ripple laminations (Figure 3.15).

Interpretation: The pronounced presence of the crinkly laminations and the well-developed adhesion ripple laminations indicate that this facies was formed in a damp interdune or sandy sabkha environment (*sensu* Fryberger et al. 1988; Melvin et al. 2010a). Generally, the occurrence of adhesion ripple laminations suggests that the sediments were laid down in a damp surface (cf. Kocurek and Fielder 1982) and in close proximity to the paleo-water table.

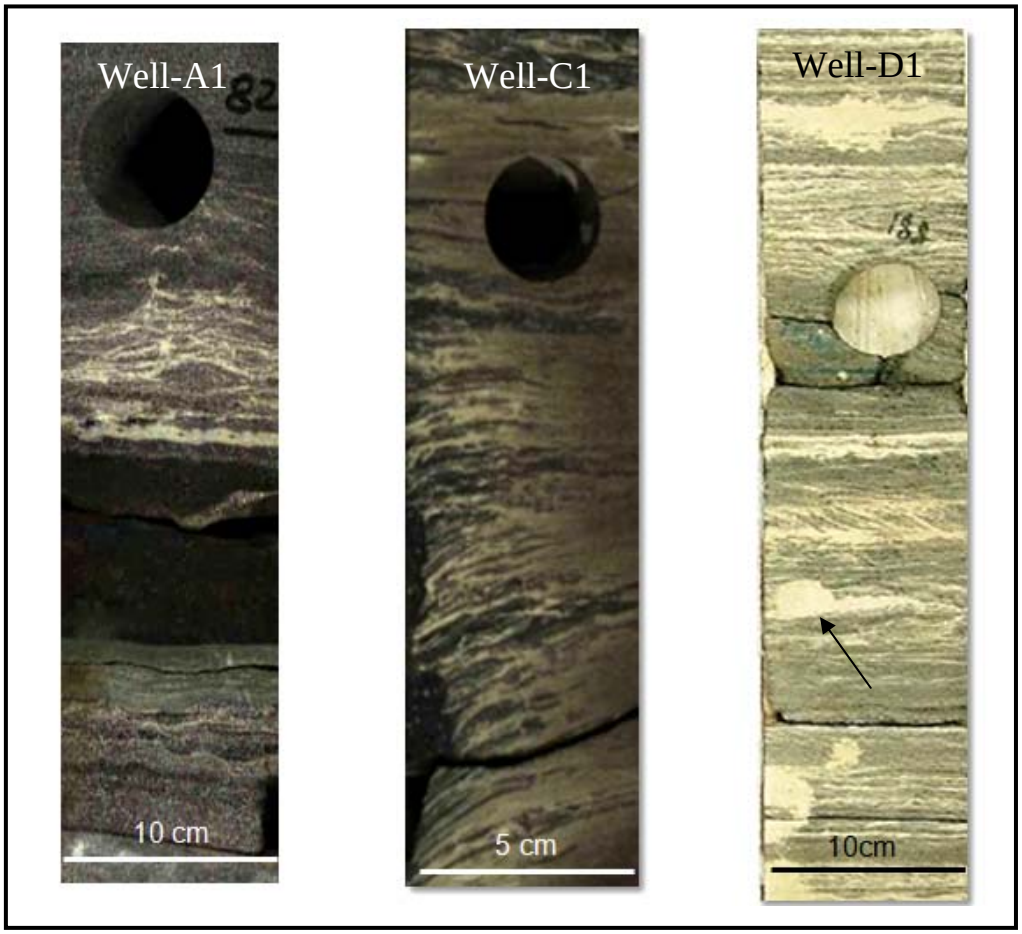

Figure 3.15: Core photographs illustrating representative features of the damp interdune environment encountered throughout the Unayzah-A member in the studied wells. They are all fine to medium grained, moderately sorted sandstones dominated by irregular crinkly laminations that are associated with damp interdune setting. The well developed adhesion ripples are indication of a sabkah environment. Note the white patches of anhydrite cement (arrow) that are usually related to sabkah type environments.

3.3.4 Irregularly Laminated, Silty Sandstones

Description: These rocks are silty, very fine-grained sandstones showing variably continuous and crinkly lamination that is locally disrupted. Small-scale ripple cross-lamination is seen in places, but desiccation features are common. These sediments generally occur in thin beds comprised of thin siltstone and very-fine silty sandstone. This facies was observed in all the cored wells but in varying proportions (Figure 3.16).

Interpretation: In general the very fine-grained and silty nature of these sediments reflects deposition under a relatively quite environment, interpreted here as ephemeral lakes. Also, the presence of the ripple cross-lamination and the siltstone beds suggests subaqueous deposition. The observed desiccation cracks indicated that the water body was very shallow and the sediments were subjected to exposure from time to time. This facies is interpreted as wet interdune.

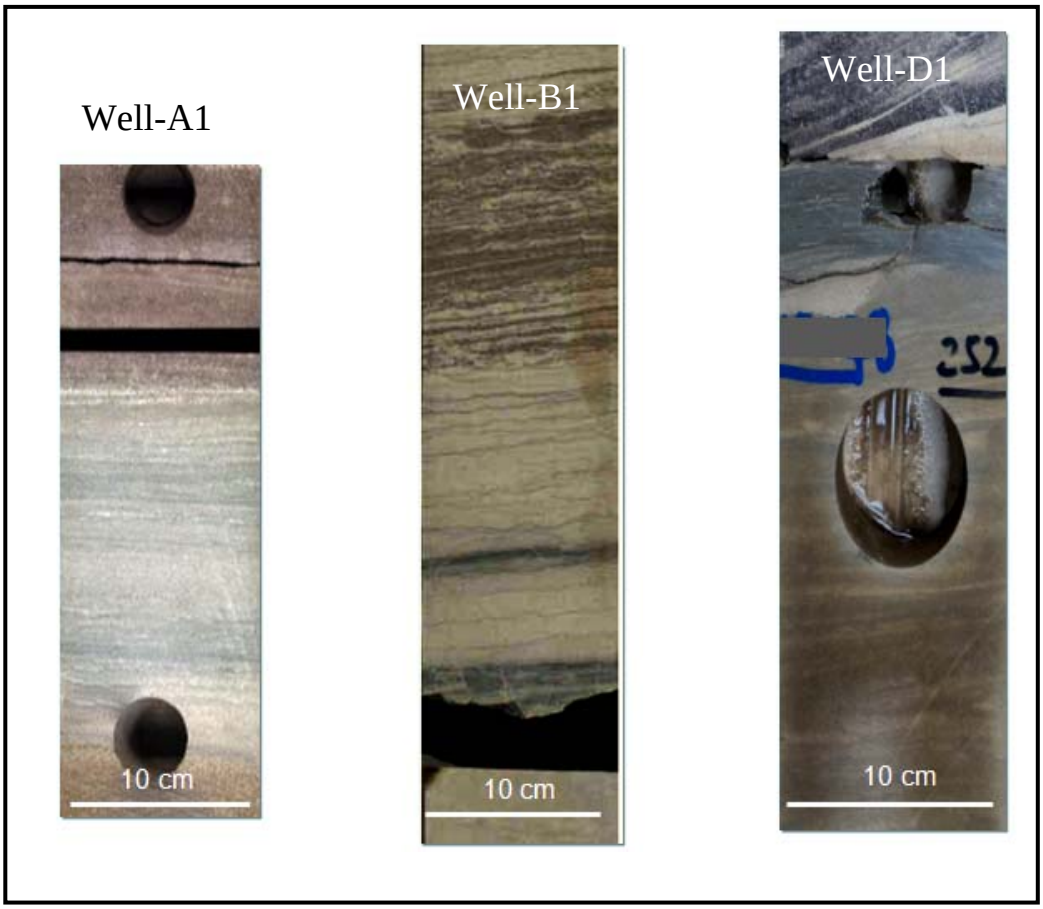

Figure 3.16 : Core photographs from the studied area illustrating the Unayzah-A playa lake deposits or wet interdune. Note that all the examples are dominated by the very fine grained, silty sandstone and siltstone units. Also Note (1) the irregular to crinkly lamination in well A1 and B1. (2) In well D1, the fining upward of very fine-gained sandstone into siltstone, which indicates deposition under subaqueous conditions such as shallow ephemeral lake environment. This facies is overlain in this example by high-angle lamination eolian dune facies. (3) The indistinct desiccation cracks structure in the upper part of well B1, which is an indication of the close water table.

3.3.5 Poorly Sorted, Patchy Carbonate Cemented Sandstones

Description: These rocks are poorly sorted, very fine- to medium-grained sandstones, with patchy carbonate cementation, and varying degrees of disrupted texture and brecciation. These deposits may be as thick as 5 feet, and it was recognized at a number of localities within the eolian-dominated Unayzah-A member. They are generally thin and less conspicuous, occupying only a small part of the section, and they were observed mainly in the upper part of the Unayzah-A member (Figure 3.17).

Interpretation: The high degree of disruption within the sediment is due to plant rooting in most cases (see the modern analog, Figure 3.18), and the presence of the carbonate cement suggests that this facies represents paleosol horizons that were formed in very close proximity to the paleo-water table.

Figure 3.17: Core photographs illustrating examples of the paleosol deposits that were recognized in the Unayzah-A member in the studied area. In general, these facies are recognized by the pronounced poorly sorted and heavily disrupted sandstones. Note the mottling in well B1, which indicates plant rooting and a shallow water table. And the disrupted and brecciated sandstone in well D1.

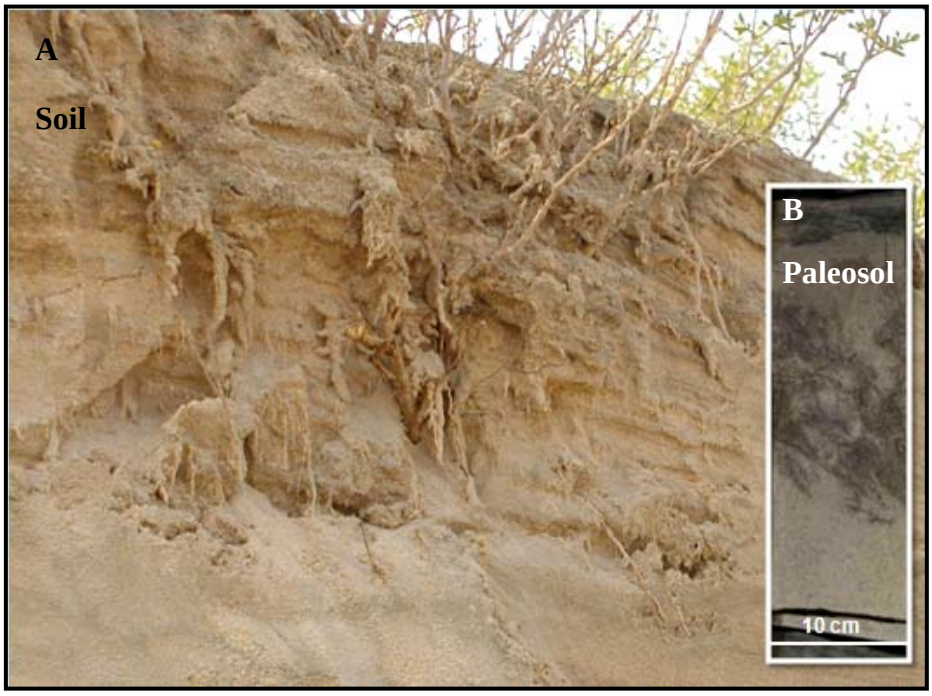

Figure 3.18: Photographs showing a comparison between modern soil deposits and ancient soil deposits (paleosols). (A) Modern trenched section through an arid eolian deposit (Half-moon Bay, Dhahran) showing very disrupted sediment caused by heavy plant rooting through the original sand sheet deposits. (B) Core photographs from well B1 showing poorly sorted sandstone with distinctive cement color mottling that is due to plant rooting.

3.4 FACIES ASSOCIATION

The Unayzah-A member in the studied area is characterized by five depositional facies.

High-angle cross-bedded sandstones (eolian dunes) that vary in thickness and abundance throughout the studied wells (Table 3.1). They are comprised of bed-sets of cross-bedded sandstone and are abruptly truncated by flat to irregular laminated very fine-grained and silty sandstone interpreted as Stokes surfaces (after Stokes 1968). These surfaces represent the change from dry to wet conditions and the rise in paleo-water table and mark the termination of eolian dune deposition (Figure 3.19) (see the detailed cores descriptions in Appendix 1). The stratigraphic significance of the identification in the core of these Stokes surfaces was emphasized by Melvin et al. (2005 and 2010a). This facies represents the highest percentage (46%) among the five facies, which indicates the dominance of the dry eolian depositional system (Chart 3.1).

Low-angle to flat laminated sandstones (sand sheet) facies. This facies is comprised of bed-sets of low-angle, grain size segregated, lamination sandstones, with a developed pin-striped appearance, that suggests a wind-ripple migration (*sensu* Melvin et al. 2010a). These characteristics compare favorably with features seen in other documented eolian sand sheet deposits (*sensu* Fryberger et al. 1979).

Irregularly laminated sandstones (damp interdune) facies. This facies is characterized by irregular to crinkly laminated sandstone with locally well developed adhesion ripple lamination. These characteristics suggest deposition in

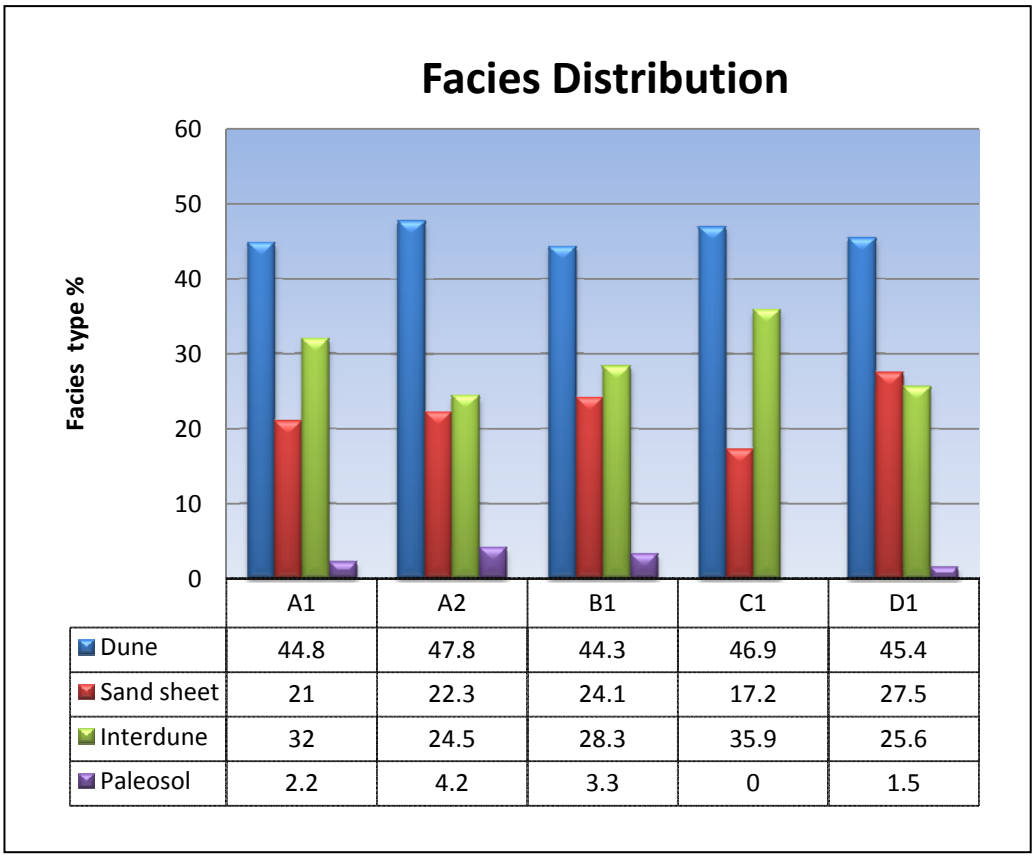

	A1	A2	B1	C1	D1
Dune	44.8	47.8	44.3	46.9	45.4
Sand sheet	21	22.3	24.1	17.2	27.5
Interdune	32	24.5	28.3	35.9	25.6
Paleosol	2.2	4.2	3.3	0	1.5

Table 3.1: Showing the recognized Unayzah-A facies distribution in the cored wells. Note the very similar average values for the different sand facies between wells. *The wet and damp interdune facies have been combined in this chart.*

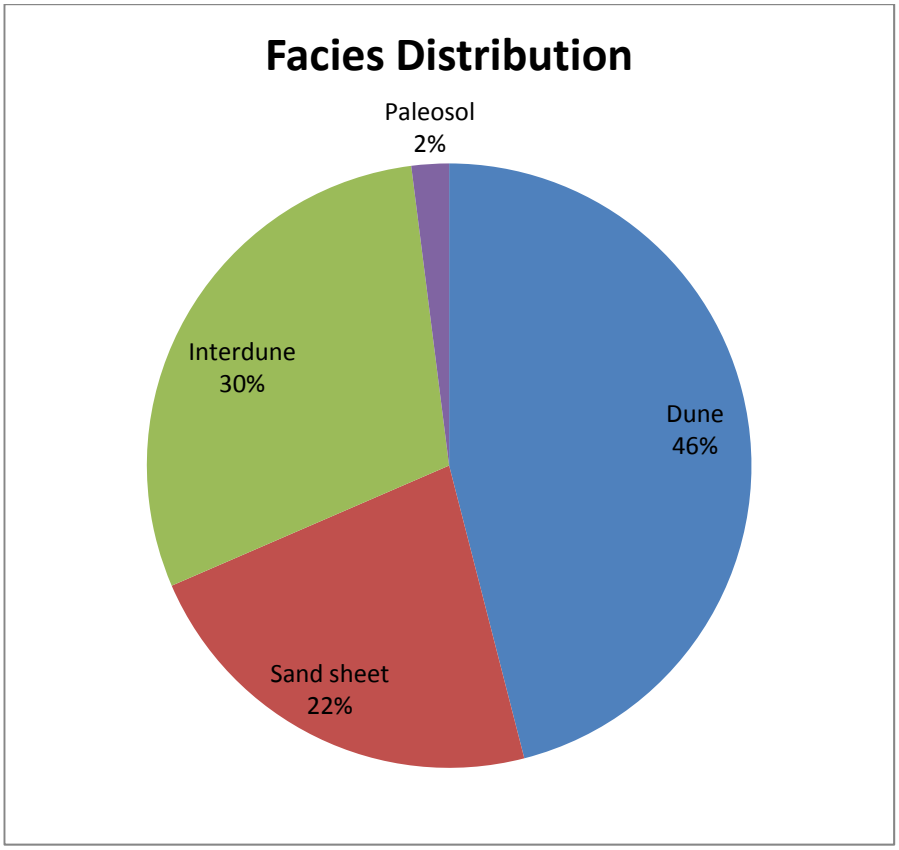

Chart 3.1: Showing the average Unayzah-A eolian facies distribution in the cored wells. Note that the eolian dune and the interdune (wet and damp interdune facies combined) facies are the dominant facies, which suggests an arid to semi-arid depositional environment.

a damp environment. Given the association of these deposits with the previous described facies, which were deposited in an arid depositional environment, this sediment was also deposited under an arid eolian setting and the presence of the adhesion ripple reflects deposition close to the paleo-water table.

Irregularly laminated, silty sandstone (wet interdune) facies. This facies is generally recognized by the finer gained-silty sandstone that shows a strong sediment disruption and the presence of the ripple cross-lamination in some localities. This reflects deposition under wet conditions that can be associated with either ephemeral lakes at the margin of eolian setting, or a rise in the paleo-water table. Both conditions are likely to take place within a desert environment.

Poorly sorted, patchy carbonate cemented sandstone (paleosols) facies. This facies is recognized mainly at the top of Unayzah-A member in the wells. These sediments showed a high degrees of texture disruption that occured mainly due to the plant rooting, which is associated with the close paleo-water table.

The above described eolian and eolian related deposits occur commonly throughout the Unayzah-A member in the studied cored wells. The mutual association and the relative abundance relative of these facies did not vary significantly among the studied wells.

From the previous discussion the various depositional facies seen in the Unayzah-A member in the study area can be assigned to a mix of arid to semi-arid eolian depositional facies (Figure 3.13). This mixed facies association is interpreted as an eolian erg-center system and erg-margin deposits (*sensu* Mountney and Jagger 2004). Within these facies a number of cyclical changes (*sensu* Aktas et al 2000) in

the paleo-water table was recognized based on the identification of the Stokes surfaces, particularly in the core, as well as on image logs (see following chapter). And the general association of the various facies was recognized throughout the Unayzah-A member in the studied wells (Figure 3.19).

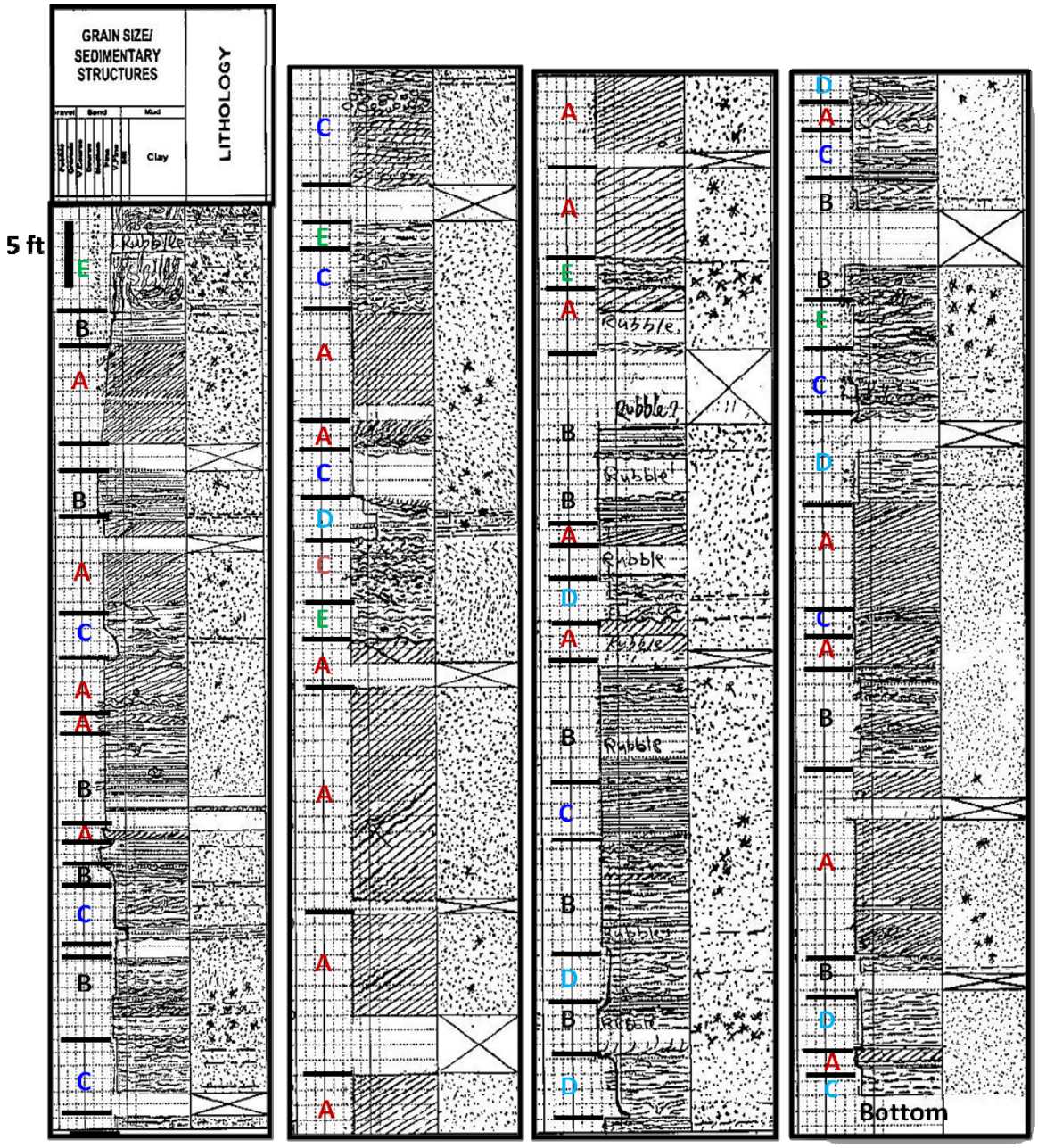

Figure 3.19: A core description log through 272 ft of core in well D1, extending from the bottom to the top of the Unayzah-A member, representing the various facies identified in the eolian facies association of the Unayzah-A in the studied wells. Note the abrupt horizontal upper terminations of the cross-bedded facies in many places. The facies are identified as follows: A**:** Dune; B: Sand sheet; C: Damp interdune; D: Wet interdune; E: Paleosols.

CHAPTER 4

IMAGE LOG STUDIES

4.1 INTRODUCTION

The potential usefulness of images recorded from the borehole wall to improve reservoir characterization has long been recognized (see Appendix 2) (Zemanek et al. 1969). Only recently, however, has progress in measurement technology, transmission, and processing allowed us to have high-resolution images of sufficient and reliable quality that can enhance our understanding and interpretation of our reservoirs.

Micro-resistivity image logs are rich in data, and provide valuable information for reservoir characterization. These borehole imaging techniques are capable of providing continuous and detailed observations of formation properties. Conventional downhole logging techniques provide data of low vertical resolution (generally 30 cm to 1m), whereas borehole imaging techniques have been developed to identify sedimentologic and structural features with a resolution down to 0.3 cm. Image logs can therefore bridge the gap between conventional logs and core (Figure 4.1).

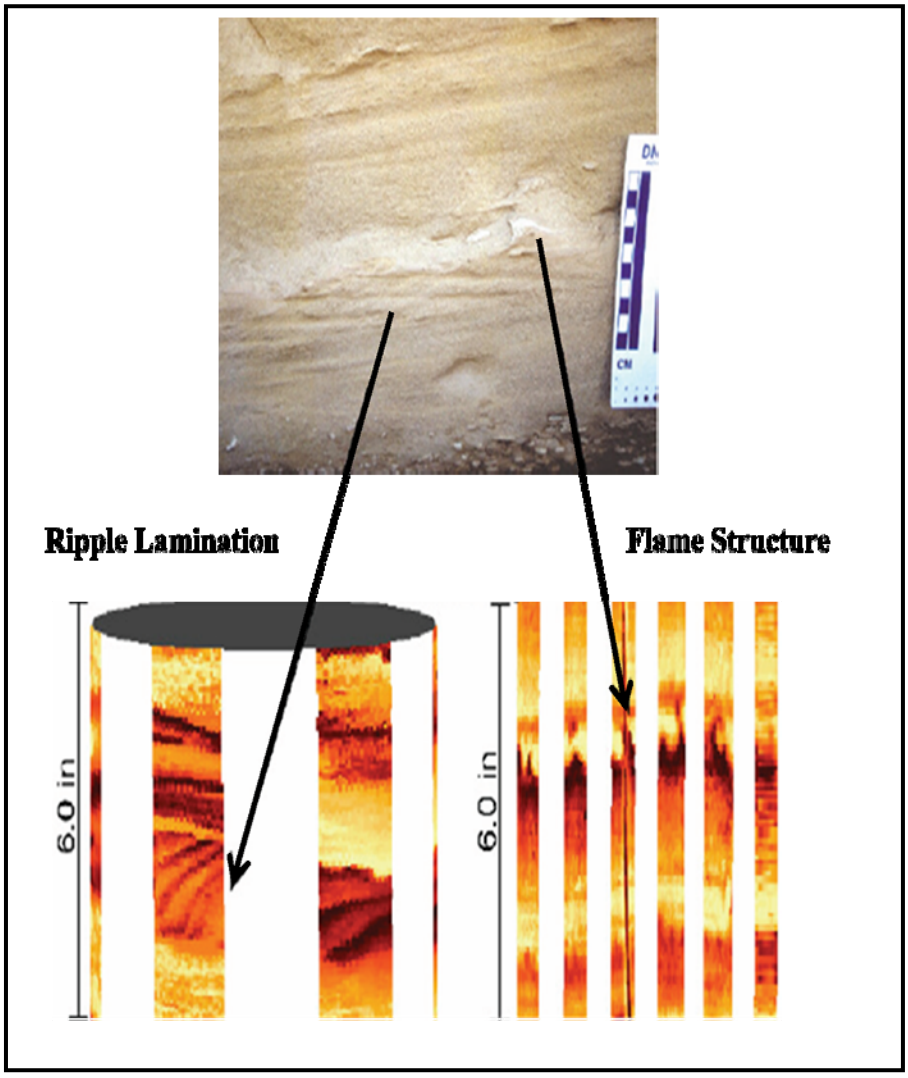

Figure 4.1: Comparison of core and borehole image logs showing small features that cannot be seen by conventional wireline logs (Modified after Witton 1999).

4.2 BOREHOLE IMAGING

Borehole images provide electronic pictures of the rocks and fluids encountered in the wellbore, and are derived from electrical (resistivity), acoustic, or video devices that are lowered into the well. Electronic images are oriented, they have high vertical and lateral resolution, and they provide critical information about bedding dip, paleocurrent direction, fractures, faults, unconformities, vuggy and fracture porosity, and other geological features. Case studies have shown that borehole images are best used in conjunction with other available wellbore data, such as other logs, cutting, cores, and production data (Hurley 2004).

The most common borehole image devices are based on acoustic and electrical measurement techniques (Luthi and Banavar 1988).

Electrical resistivity logging measurements characterize a rock volume some distance into the formation beyond the wellbore wall. In contrast, acoustic imaging measurements represent borehole wall or casing surface imaging only. The practical consequences of this difference is that electrical devices are capable of resolving smaller features than acoustic devices (Stephen 1999).

Electrical borehole images are based on dipmeter technology that has been commercially available since the 1950s (Bigelow, 1985a; Gilbreath, 1987; Adams et. al. 1987). Figure 4.2 is an illustration of the tool configuration and the basic principles behind dipmeter logs. Modern electrical borehole imaging tools are highly

sophisticated dipmeters. The imaging tools have microresistivity electrodes arranged around the tool on pads that are pressed against the borehole wall.

New digital wellbore-imaging tools (Table 4.1) provide a wealth of geologic data previously obtainable only from cores. Although spatial resolution of features visible on the images is lower than that of a core, it is widely recognized that these images can resolve major geologic structures penetrated by the well and can provide data where core is absent.

Company	Trade Name	Number of Pads	Number of Electrodes
Schlumberger	FMS (Formation Microscanner)	4	64
Schlumberger	FMI (Formation MicroImager)	8	192
Halliburton	EMI (Electrical Micro Imaging Tool)	6	150
Baker Atlas	STAR (SimulTaneous Acoustic and Resistivity Imager)	6	144

Table 4.1: Electrical borehole imaging tools.

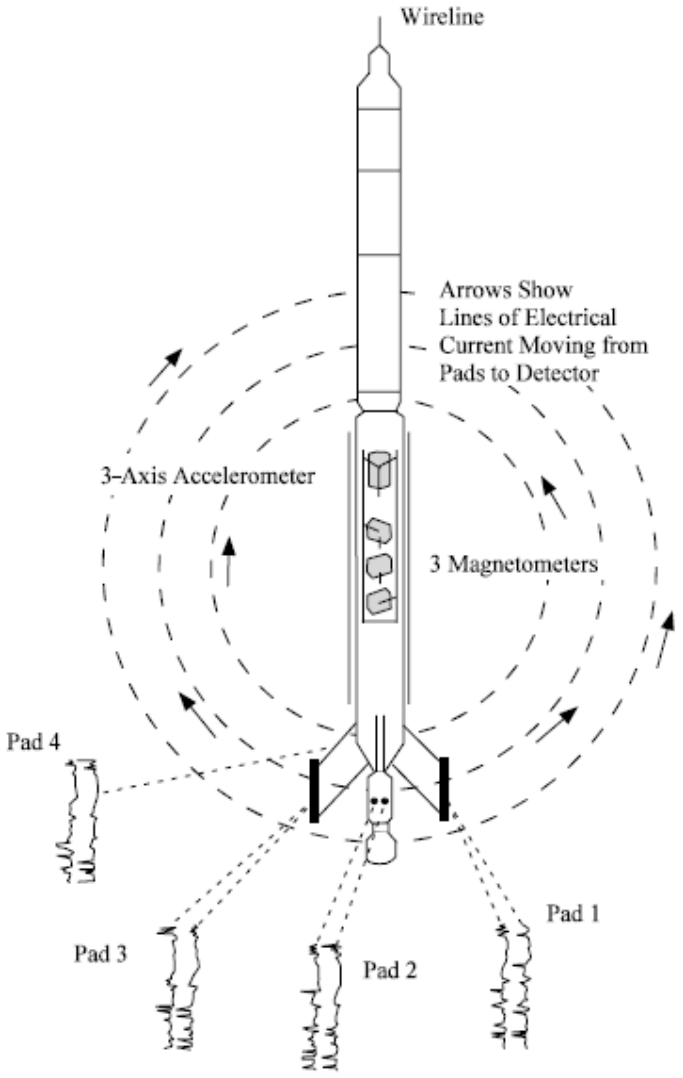

Figure: 4.2: The basic principle of electrical dipmeter tools is illustrated in this diagram of Schlumberger's SHDT (Stratigraphic High Resolution Dipmeter tool). Two measuring electrodes on each of four pads generate eight raw electrode traces, as shown on the bottom. Magnetometers measure borehole deviation. Accelerometers record the high frequency tool speed variation that occurs as the tool is being run. Formation dip is computed from planes that fit through correlative peaks and troughs on the speed correlated electrode trace. Caliper logs record borehole diameter between pads 1 and 3 and between pads 2 and 4. After Schlumberger (1983) and Hocker et al. (1990).

Borehole images are created by assigning color maps to different “bins” or ranges of resistivity values. Colored pixels are then arranged in their proper geometric position around the wellbore. By convention, low resistivity features, such as shale or fluid-filled fractures, are displayed as dark colors. High resistivity features, such as sandstone and limestones, are displayed as shades of brown, orange, yellow, and white (Hurley 2004).

Two types of processed borehole images are available: static and dynamic (Figure 4.3). Static images are those which have had one contrast setting applied to the entire well. They provide useful views of relative changes in rock resistivity throughout the borehole. Dynamic images, which have had variable contrast applied in a moving window, provide enhanced views of features such as vugs, fractures, and bed boundaries. Dynamic images bring out subtle features in rocks that have very low resistivities, such as shales, and very high resistivities, such as carbonate and crystalline rocks (Hurley 2004).

Sedimentologic interpretations are aided by the fact that the intrinsic lower resolution limit of borehole images is on the order of 0.2 in (5mm) (Hurley 2004). Sedimentary structures, such as fluid-escape features, ripples, cross bedding, and imbricated clasts can be identified and studied. Observations may provide important information regarding paleocurrent, facies, and depositional environments (Luthi and Banavar 1988; Carr et al. 1997; Witton 1999). Thinly bedded sands and shales with bedding thickness on the scale of 2 to 20 in (5 to 50 cm)are below the resolution limits of most conventional logging tools. However, such thin-bedded successions have been successfully resolved and quantified using

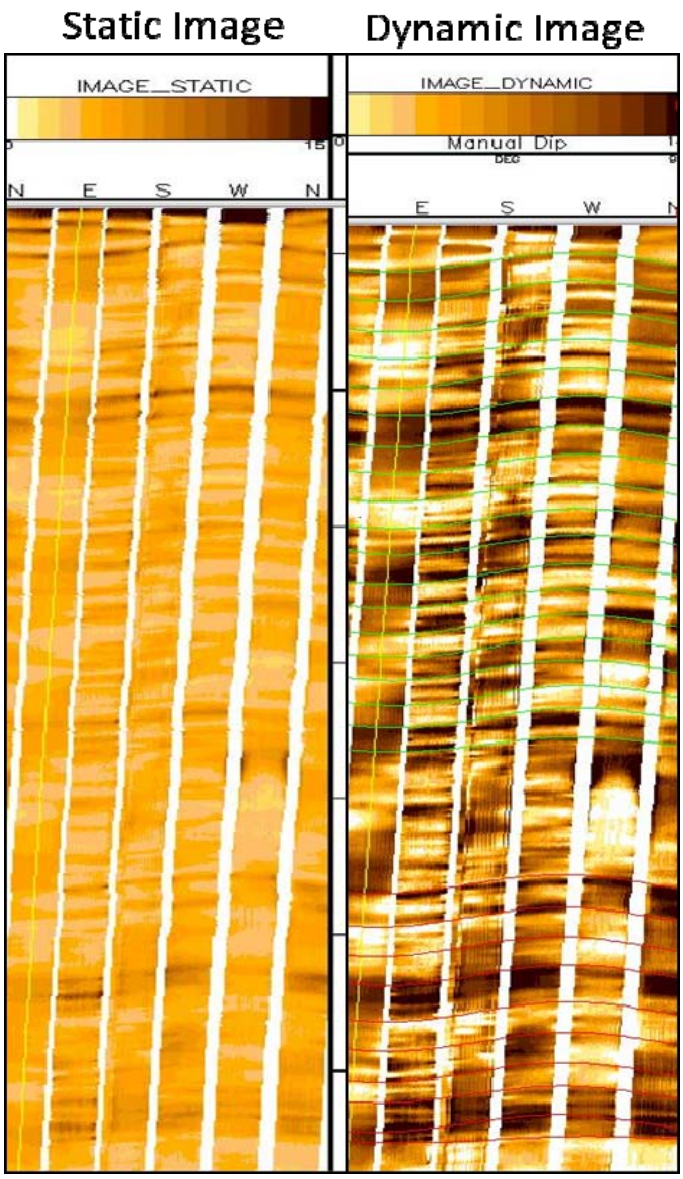

Figure: 4.3: Examples of representative electrical borehole images showing the static and dynamic images quality differences. The static image illustrates the gross variation in the parameter being measured through the succession. Dynamic images using small data windows enhance small scale data variations allowing the interpreter to visualize sedimentary and structural fabrics that are not associated with large variations.

borehole images (Sovich et al. 1996). Such analyses have led to better estimates of net to gross reservoir thickness and improved volumetric calculations (Reid and Enderlin 1998).

Eolian reservoirs exhibit significant compartmentalization and variations in directional permeability caused by the processes taking place during the accumulation of sediments within an eolian system (Carr-Crabaugh et al.1996). Dipmeter data can clearly reveal the occurrence of cyclic dune and interdune deposits and distinguish lateral and longitudinal dune types, which may have different reservoir characteristics. Lateral-type dunes--barchan, transverse, and parabolic are elongate perpendicular to the wind direction and are characterized by cross-bedding with a generally unimodal distribution of dip azimuths relative to the wind direction. Longitudinal, or seif, dunes are elongate parallel with wind direction and are characterized by a bimodal distribution of cross-bedding dip azimuths relative to the the wind direction (Nurmi and Hepp 1979).

4.3 EOLIAN BEDDING AND IMAGE LOGS

Eolian sands are deposited when the velocity of the driving wind is reduced to the point where it can no longer transport the sand.

Barchan and transverse dune sand accretion, influenced by winds of moderate velocity and uniform direction, results in the building of oval mounds that have their highest point in a downwind direction. As the height of an individual sand patch becomes greater, the lee slope increases until it reaches the angle of repose for

dry sand, at about 34°, and a slip-face (or avalanche slope) forms. This situation seems to be reached at a minimum slip-face height, for what may now be called a dune, of about 30 cm. Sand grains are transported up the windward slope of the dune. Any tendency to exceed the angle of repose of the lee slope causes sand to avalanche down the slip-face until the slope of 34° is regained. The largest and roundest grains are found at the bottom of the slope (Glennie 1972) (Figure 4.4).

Transport direction inferred from cross-bed dip is one of the most important applications of cross-bedding analysis in the determination of paleocurrent (Rubin, 1987). The most diagnostic feature for eolian dunes facies is a “clean” low API gamma log, and the corresponding dip motif on the dipmeter log is a “blue” pattern in which the upward increase in dip commences opposite to the short muddy interval of gamma curve (Selly,1978). This corresponds to the sub-horizontal toeset of the dune on which any clays settle out. This passes up into the clean gamma interval with uniform high angle foreset dip (Figure 4.5).

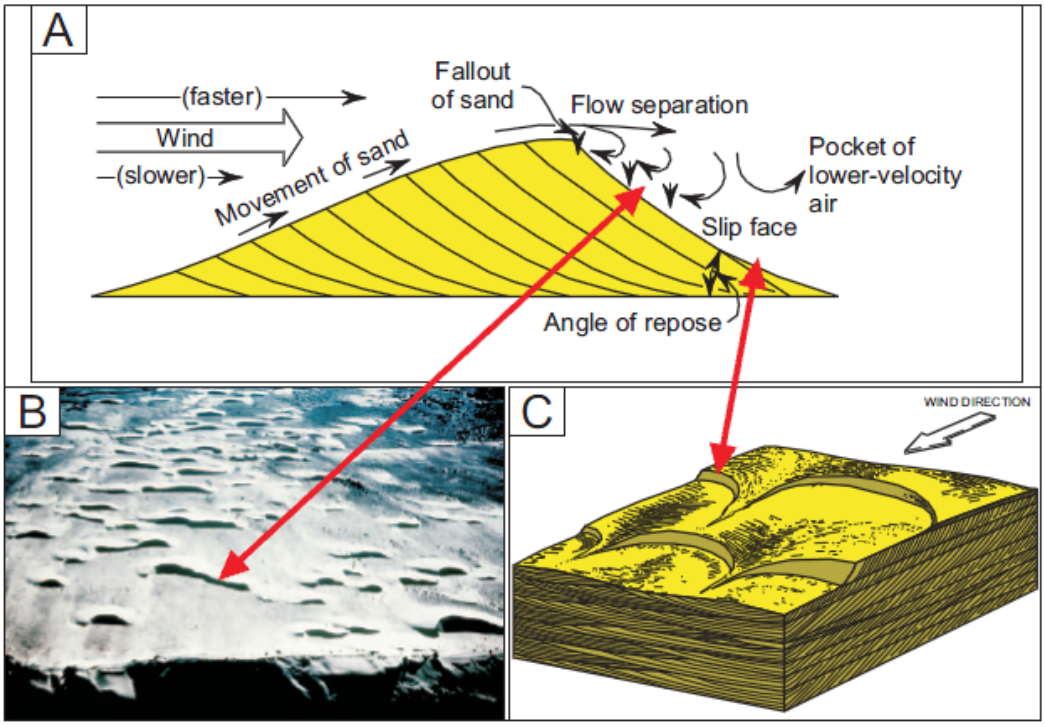

Figure 4.4: Illustration of how sand dunes migrate. (A) the wind is blowing from left to right. Individual sand grains move up the windward face of the dune and over the crest of the dune to the leeward side or slip face. Cross-beds form internally within the dune as a result of the downwind and lateral movement of the sand. In side view, it is possible to determine the direction of wind transport by noting the direction of dip (downward) of the cross-beds. (B) the leeward side of the dune is the downwind side. (C) in an orientation perpendicular to the wind direction, the internal sedimentary structures may be more lenticular than they are in the direction parallel to the wind. After Weber (1987), (from Slatt 2006).

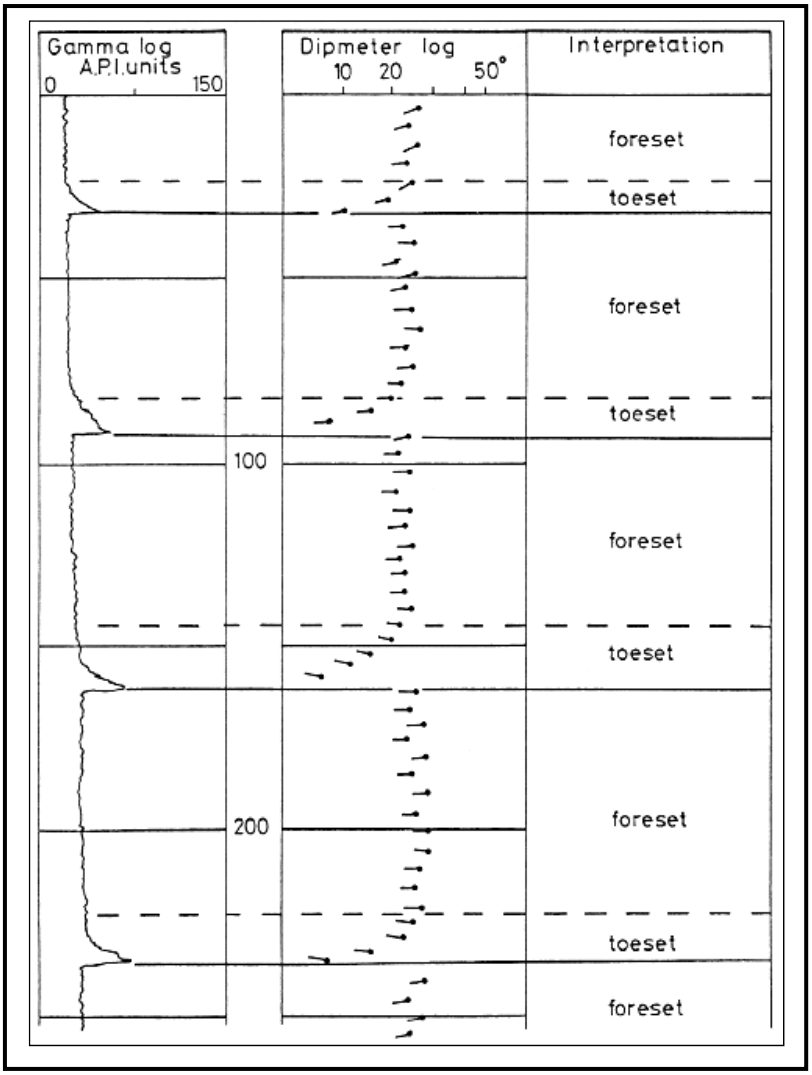

Figure 4.5: Gamma ray log and dipmeter log patterns for a borehole, through eolian dune deposits, showing the response of dip meter reading (tadpoles) and the gamma-ray response though staked eolian dune facies deposits. Note: (1) The low gamma-ray log reading at the main body of the dune facies (foresets), which indicates clean sand deposits, and the high log response at the bottom of each dune (toesets), which indicates interdune deposits. (2) The change of the dip meter log reading from high (above 20) in the dune body (foresets), to very low (~0^{o}) at the base of the dune (toesets) (after Selley1978).

4.4 PALEOCURRENT APPLICATIONS

Electrical image logs produce a ‘picture’ of the formation that allows geological interpreters to identify a variety of structures within the wellbore (e.g. sedimentary cross-bedding, fractures etc.). This kind of detailed geological information was previously only obtainable from cores. Whereas core provides the geologist with a physical sample of the formation, electrical image logs provide a unique dataset which, in particular, can be used to derive extremely detailed information on the orientation (dip magnitude and direction) of sedimentary structures that cut across the borehole (Serra 1989). Good quality image log-derived orientation data can be superior to that gathered by any other method, even outcrop measurements (Goodall et al. 1998).

The image log (dipmeter) is an extremely useful device for recognizing and interpreting eolianites in the subsurface. Most eolian cross-beds steepen upward and the combination of the spread of dips and their mean values is useful in interpreting ancient dune bedforms and thus, sandstone geometry. Stratigraphic interpretation from dipmeter data (Bigelow 1985e; Gilbreath 1987) involves looking for steepening or shallowing upward patterns in bedding dips. Combined with core, other log signatures, and isopach maps, such interpretations can lead to new well locations (Grace and Newberry 1998). Bourke et al. (1989), Hocker et al. (1990) showed that sedimentologic and stratigraphic interpretations from core and other logs can be combined with dipmeter results to improve reservoir characterization in

clastic rocks. Hurley (1994) showed that boundaries between dip domains can be subtle angular discordance between overlying and underlying sedimentary strata.

Sedimentological modeling of an eolian reservoir is desirable because the depositional characteristics, including facies, strongly affect many aspects of these reservoirs at all scales of interest. A routine core/image log analysis and modeling of the depositional facies, dune types, and their effective transportation direction is possible. This analysis can then be used in defining the areal extent and distribution of cross-bed reservoir units.

Cross-bedding analysis is an indispensable technique for interpreting sedimentary deposits. Cross-bedding is an important indicator of depositional environments, paleoflow velocities, and paleocurrent direction (Rubin 1987). Moreover, cross-bedding provides information about how modern bedforms behave, how they migrate, how they change in morphology, and how they interact with other bedforms. This type of information is particularly valuable for bedforms whose behavior cannot be observed, either because they migrate or change shape too slowly, or because they are active in environments where repeated observations cannot be made (Rubin 1987).

D. B. Loop et al. (2004) utilized dip direction data from Colorado Plateau eolian sandstones to provide important clues to planetary-scale atmospheric circulation during much of Pangaea’s existence. This study indicated that eolian cross-strata should receive more attention in future palaeogeographic and palaeoclimatic reconstructions.

Thus, an understanding of bedding characteristics in ancient eolian deposits has many applications, and it provides a valuable tool for the eolian sandstone reservoirs analysis and modeling.

4.5 IMAGE LOG DATA IN THE UNAYZAH-A

High resolution electrical borehole images of Unayzah-A sandstones clearly reveal a vertical succession of different eolian bedding facies. In this study, borehole image logs from 21 wells were processed and interpreted using GeoLog software (Paradigm Geolog®) (Figure 4.6). The data were loaded and their quality evaluated through software processing and ground-truthing using core data. The dip magnitudes and dip azimuth were analyzed from the image logs. In addition, electrofacies analysis was employed from image logs through calibration with core data to diagnose the facies type.

4.5.1 Data QC and processing

In this study different types of image logs were used (FMI, FMS, EMI and STAR). A total of 21 wells were selected from 60 wells which have image logs in the studied fields. The selection was based on the well location and image log data quality (see appendix 2, image log data).

The data was processed using the following workflow:

1. Look in the row data
2. Check inclinometry format
3. Check speed correction accelerometers, it should be constant with hole condition

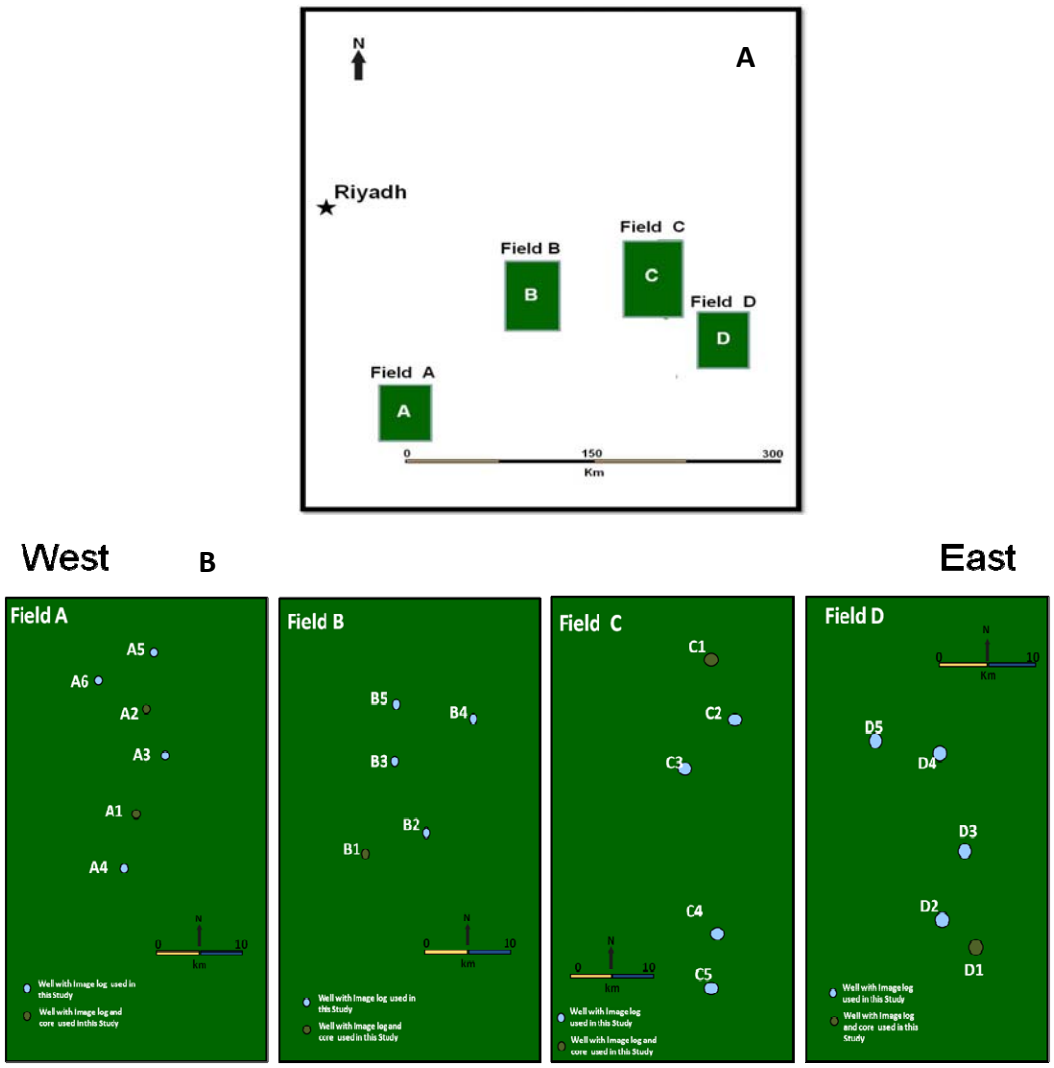

Figure 4.6: Location maps. (A) Map of east-central Saudi Arabia (note Riyadh's location) showing the general location of the studied fields (A, B, C and D). (B) Maps showing a zoom-in on the selected fields and the location of the studied wells in each field.

4. Horizontal equalization removes stripes and DB's
5. Static normalization & dynamic enhancement
6. Image display; white resistive, black conductive
7. Check gamma-ray and calipers on depth
8. Run side by side correlation automatically as a first check on the dip data
9. Pick dips manually and merge with the image displays

The dynamic normalization of the images uses the high and low values for microresistivity from a narrow "window" of data (3 feet) and then re-scales all of the values between 0 and 100%. This can artificially enhance the changes found at shale interfaces and serves to highlight bedding surfaces. A "static normalization" takes the entire data set (sometimes over 100s of feet) and again re-scales the data to the 0 and 100% values of the highest and lowest values found in the entire logging run. This subordinates rapid local changes in microresistivity to more general changes, and preserves the gross lithologies such as sand and shale intervals.

After processing, log quality controls were applied to increase the accuracy and reliability of the data, these involved checking:

- No abrupt lateral shifts of the azimuthal images
- No mirror imaging between pads/flappers
- Constant color scaling of the images
- Borehole drift and azimuths match the well trajectory
- Calculated dips make sense and sinusoids match image
- Calipers, gamma-ray should match reasonably and match litho changes

4.5.2 Dip Determination

The process of drilling a borehole through a cross-bedded, sedimentary formation exposes these structures in 3-dimensions. The orientation of such features can be recorded from borehole image logs and subsequently the image-derived dip data provide a unique record of internal bedform geometries (Goodall et. al 1998), (Figure 4.7).

On image logs from vertical holes, horizontal sedimentary laminae appear as flat surfaces, whereas dipping foreset structures appear as sine-waves (Figure 4.7). The sine-wave amplitude indicates the dip magnitude, and the low point of the wave describes the dip direction (azimuth). The interpreter can interactively match a sine-wave to the sedimentary structure shown on the image to derive a very accurate dip and azimuth value (Adams et al. 1990). Once the interactively picked dip data have been collected it is possible to classify each dip according to the sedimentary feature that it represents. After the dips have been classified, the dip types can be interrogated separately using statistical analysis, and they can be displayed on stereograms or rose azimuth plots.

In reservoir rocks which contain important paleotransport (paleowind) information (e.g. cross-bed orientation) it is critical that these orientation data are measured accurately. The technique presented in this study depends heavily on hand-picked dips in borehole images. This technique increased the quality of the measured dip data and accurately reflected the subtle cross-cutting relationships of the bedding planes.

The dip and dip direction of individual bedding planes represent a combination of original bedding-plane orientation and generations of structural overprinting. Structural dips should be determined in lithologies that were likely to be flat-lying at the time of deposition. The core study (chapter 3) indicates that within the Unayzah-A member, one facies is expected to contain flat-lying lithologies, the interdune accumulations. Interdune deposits can be identified in high-quality images by conductive appearance and the flat (~0°) wavy-bedded nature of the individual laminae (Figure 4.8).

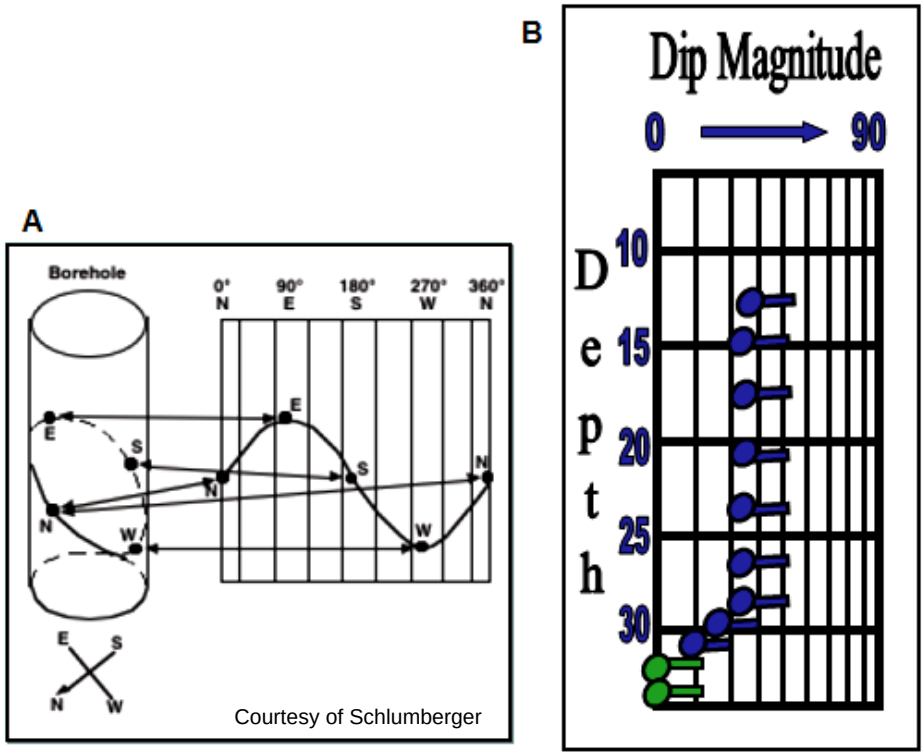

Figure 4.7: (A) Illustrates the creation of a 2D sinusoid of a dipping plane imaged form the original 3D vertical borehole. The dip azimuth is located at minimum sine-wave. In this example, the dip azimuth is to the west (270º). (B) Shows a display of the dip and azimuth data in a logarithmic scale. In this example, the dip of the blue (tadpoles) is 25º and the dipping azimuth is to the East. Note: the head of the tadpole represents the dip-angle and the tail represents the dip direction (azimuth).

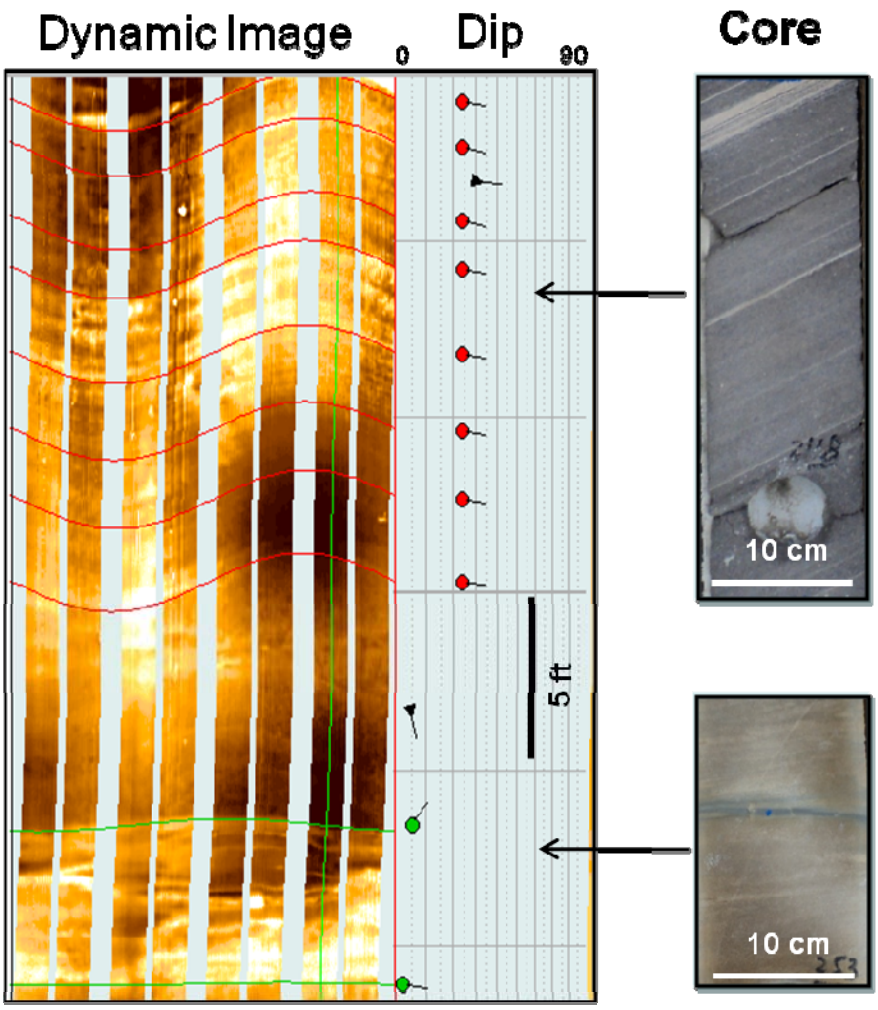

Figure 4.8: Shows examples of dynamic image log data and core photos illustrating the high-angle lamination from eolian dune facies and the low-angle lamination from interdune facies. Note: (1) The sine-wave amplitude in the dynamic image log data represents high angle laminations of eolian dune facies. The dip data to the right of the image shows the dip and azimuth of the imaged dipping planes. (2) The upper core photo shows the distinctive high-angle grain-size segregation laminations of eolian dune facies. These are represented in the image log data by the high amplitude sine-waves. (3) The lower core photo shows the interdune flat laminations, note the flat gray siltstone bed in the middle of the photo which is represented in the image log data by the flat green sine-wave.

4.5.3 Image log Data Problems

During the analysis of the data some problems were encountered. At the A2 well (EMI data) the image data quality was poor and could not be trusted. Due to the poor hole conditions, and poor pad contact these data could not be recovered by further processing (Figure 4.9). In this case an alternative well with image log data from the same field was used for the paleowind investigation.

At the C2 well (FMI data), the dip reading was very high (above 34º), which indicated a problem either in the data or in the image log processing. The data was reprocessed using GeoLog and GeoFrame software, but both gave the same result. Further investigation and QC showed that there were no problems with the data quality itself, but that the hole was deviated about 7º according to directional survey data, plus there was 5º of structural dip. The data was reprocessed and the survey data was aligned with the hole azimuth and the structural dip was removed, as a result, the well dip data showed general dip reading ranges of between 20°-30°, which is in the normal dip range for eolian dune deposits (Figure 4.10).

At the C1 well (STAR data), the data was processed perfectly with no problems, however the interpreted dip data showed consistent orientations to the northwest, which was completely different to every other image log across the Unayzah-A in the entire study area. This could be a true geological anomaly, but the overwhelming body of data (which has a dominant dune foreset dip direction toward the east-northeast-see Chapter 5) suggested this was unlikely.

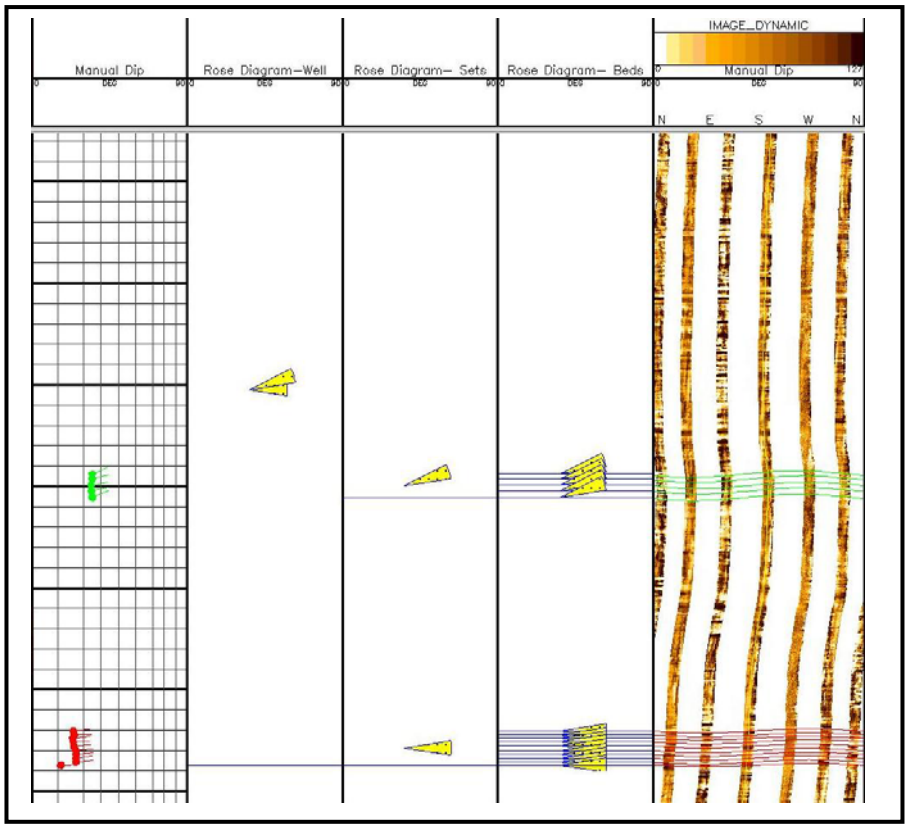

Figure 4.9: Dynamic image snap-shot from well A2 illustrating the low quality of the image log. This is mainly due to the poor hole conditions caused by hole breakout. Note: the lamination fuzzy appearance that reflects bad tool contact to the borehole surface. This resulted in a very low quality image. Very few sine-waves were picked in this well.

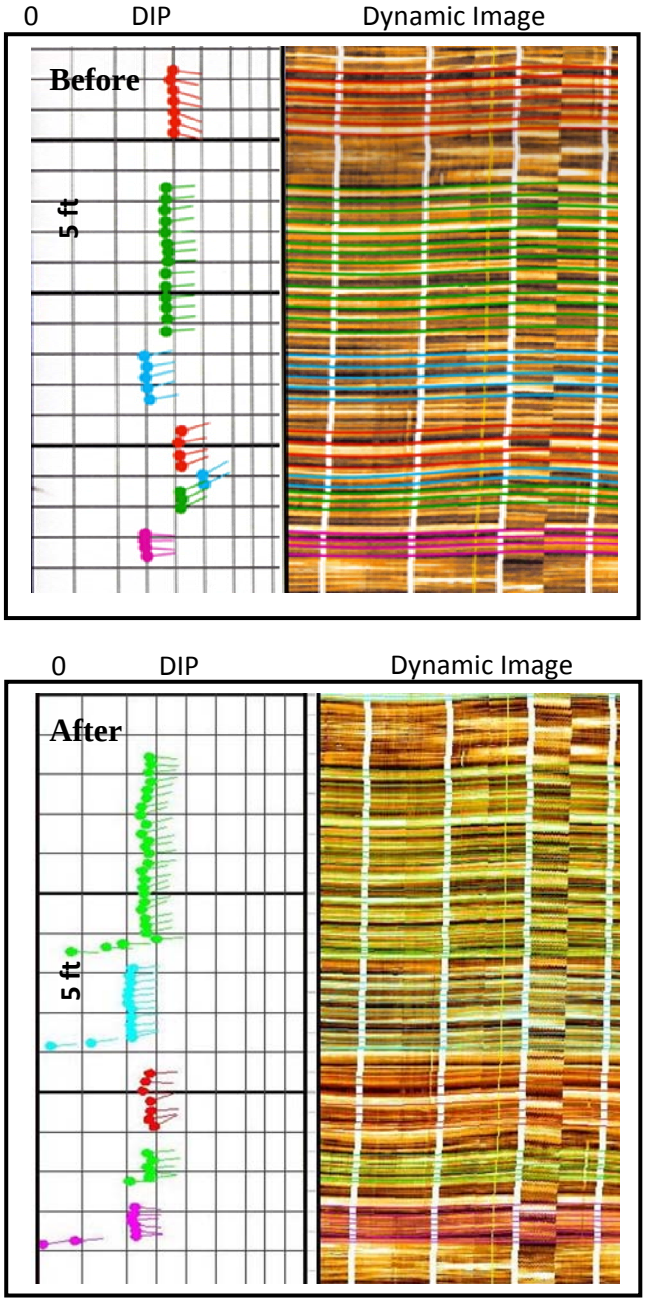

Figure 4.10: Dynamic image snap-shots from well C2 illustrating the data before and after correction. The first image shows the image and dip data after it was processed for the first time, note the dip data before the correction. The dip reading is extremely high for dune deposits (40°-50º), indicating a problem in the processing. The second image shows the same data after re-processing and removing of the hole deviation and structural dip. Note the dip data for the same intervals is now between (20º-30°).

The data was reprocessed again using Recall (Baker Hughes image software) and the results were exactly the same. Furthermore, the orientation data was of good quality as can be seen on the magnetometer QC plot.

Based on the data quality checks, it appeared there are no errors in the orientation data. Since processing the data with different software produced the same results and there was no clear problem with the data, this suggested we needed to review the raw acquisition data.

Additional extensive data QC was carried out within Aramco's Geological Technical Services Division, to investigate the data problem. Their findings were that the magnetometer and accelerometer cross-plots provided by Baker agreed with those produced in house. This indicated that the issue was most likely related to (1) the data channel naming conventions, (2) data processing software issues, or (3) the inclusion of an orientation offset. Review of all these possibilities showed that the difference in the computed dip orientation appeared to be due to the Pad 1 allocation. The spurious Baker data could be reproduced by rotating the Pad 1 to match the in-house Pad 3 (e.g. Baker Pad 1 to in-house Pad 3, Pad 2 to Pad 4, Pad 3 to Pad 5 etc). Once the image curves were named in the correct order the features and orientation data were then found to match (Figure 4.11).

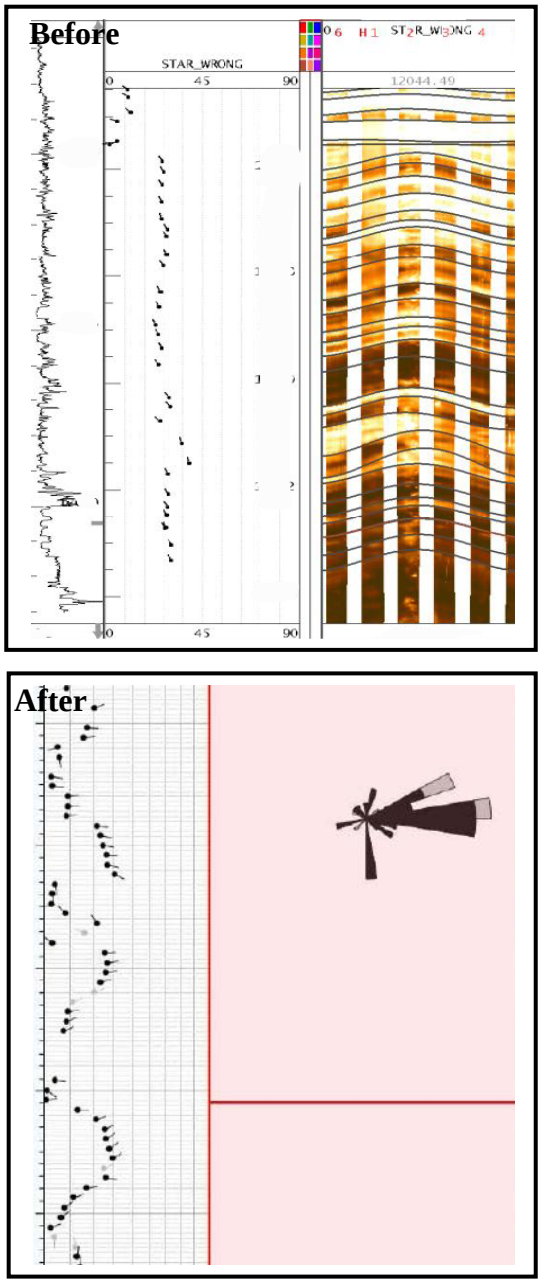

Figure 4.11: Snap shots from well C1 illustrating the well dip data before and after correction. The first image is shows the dip data (note the tadpoles tail direction) oriented toward the north-west. The second image shows the dip data after it was re-processed and corrected, note the general east dip trend of high angle bedding of the stacked eolian dune deposits. The rose diagram illustrates the general bedding trend to the east.

CHAPTER 5

RESULTS & CONCLUSION

5.1 INTRODUCTION

Eolian sandstones were amongst the first to be studied for paleocurrent directions (e.g Brinkmann 1933; Shotton 1937) and their recognition has been important in the definition of paleoclimates and in the testing of paleo-magnetically determined reconstruction of global paleogeography (e.g., Bigarella 1972; Robinson 1973) (Collinson 1986).

The combination of sedimentological information from conventional core studies with that from images is a highly complementary process. Core provides an effective means of “calibrating” or “ground-truthing” image logs to increase interpretation confidence beyond cored intervals.

Image log and core integration is a powerful tool in recognizing the various eolian lithofacies within the Unayzah-A member. Image logs alone provided detailed facies information within the eolian reservoir once the ‘ground-truth’ had been established with core. In this study, 4000 ft of borehole image logs, and 1096 feet of core were described and interpreted, and used: 1) to confirm and evaluate the

eolian depositional setting, and 2) to investigate the paleowind direction during the deposition of the Permian Unayzah-A eolian facies.

5.2 FACIES DETERMINATION AND DATA GROUND-TRUTHING

Dipmeter tools record a large amount of dip data. However, the geological or sedimentological origin of these recoreded dips cannot be determined in isolation. In order for these data to be interpetable, the dips need to be filtered and classified. These steps cannot be achieved without integration of the dip meter log with core sedimentology and conventional log data.

The studied cores (discussed in Chapter 3) from the selected wells revealed clearly that the Unayzah-A member in each area/field is composed of arid to semi-arid eolian depositional facies, represented mainly by: 1) high-angle laminations of eolian dunes, 2) flat to low angle lamination sand sheets and 3) flat irregular-crinkly laminated interdune deposits (wet and damp). These litho-facies were also identified in the studied image logs (Figure 5.1).

Electrical image logs, as discussed in Chapter 4, provide a picture of the formation which makes the identification of complex sedimentary structures within the wellbore, such as cross-bedding, easier and more reliable. In this study an extensive interpretation was conducted on image logs to identify facies and dip data.

Based on the image log texture, the following “bedding facies” were distinguished: high-angle cross-bedded, low-angle cross-bedded and horizontal lamination, which reflects dune, sand sheet and interdune facies, respectively.

Image-defined bedding facies correlated well with core lithofacies (Figure 5.1). High-angle cross-bedding (20º-34º) corresponds to eolian dune deposits as suggested by the core studies, low-angle (generally between 0º-20º) cross-bedding corresponds to sand sheet deposits, the horizontal laminated facies corresponds to sand with thinly laminated and disrupted bedding which represents interdune deposits (Figures 5.2 and 5.3).

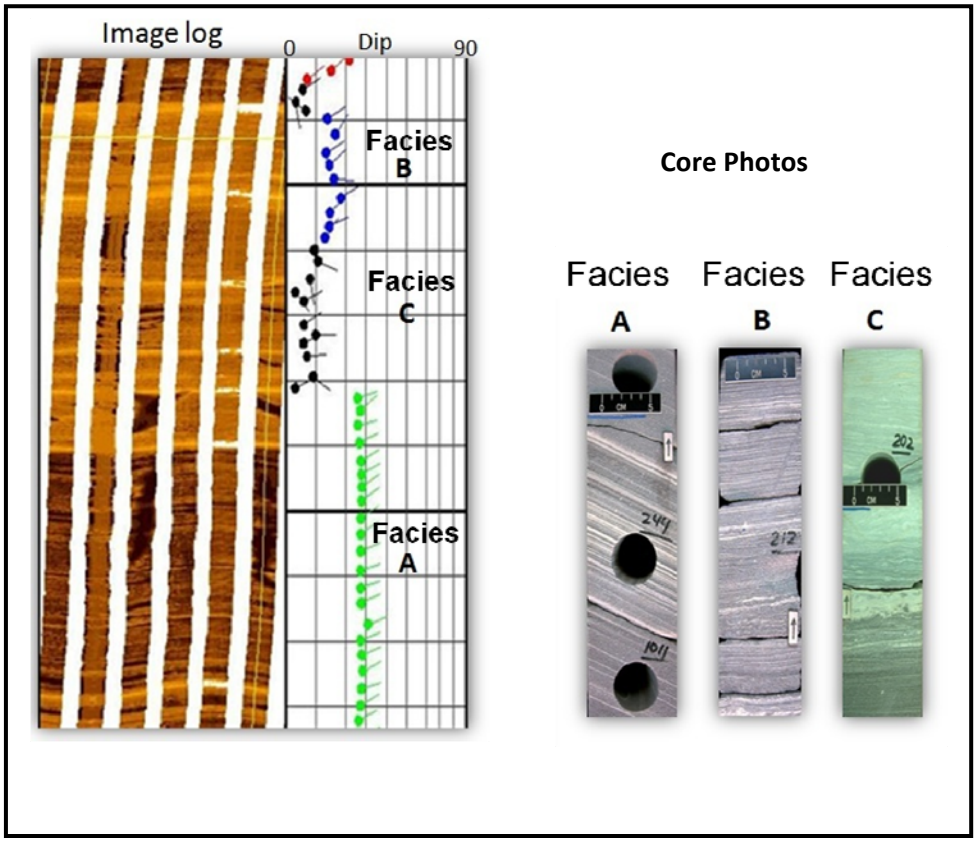

Figure 5.1: Image log and core photos from the studied cores showing a correlation between image log and core data. The core photos illustrate the different facies encountered in the Unayzah-A member. Facies A represents the eolian sand dunes deposits, facies B represents the sand sheet deposits and facies C represents the interdunes deposits. The image log data shows the equivalent dip data for these facies. The dip data above 20° (green tadpoles) represents the eolian facies, the dip data between 10°-20º (blue tadpoles) represents the sand sheet deposits and the dip data between 0°-10° (black tadpoles) represents the interdune facies. Note the eolian facies dip direction orientation is to the east-northeast.

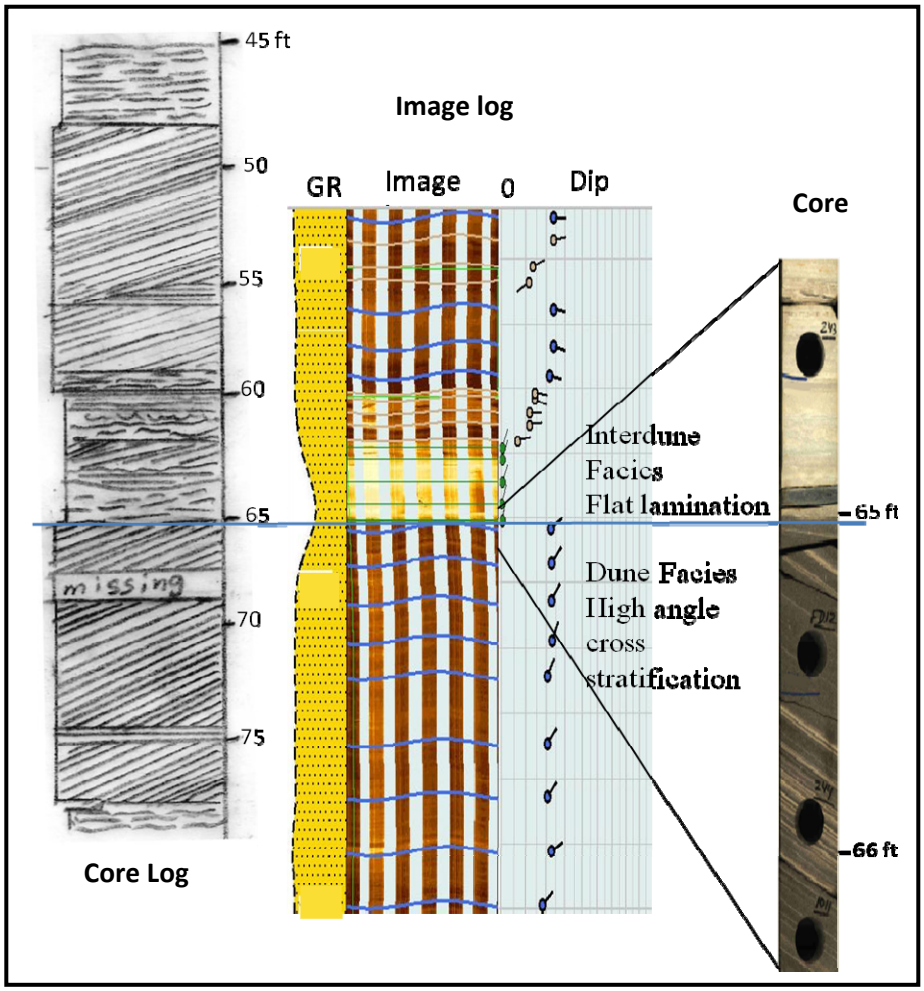

Figure 5.2: Image log-core calibration from field D illustrating the eolian dune and interdune facies from core and image log data. The lower part of the core photo (below 65 ft) shows the high angle eolian dune facies cross-stratification. The upper part of the photo (above 65 ft) shows the flat laminated (zero dip) eolian interdune facies. The image log along with the dip data shows the high angle eolian dune facies cross-stratification with the high dip reading and the interdune facies with the low (0º) dip reading. The core log is showing 35 ft of eolian deposit succession, from the same well, illustrated by several stacked eolian dune and interdune facies. Note the abrupt truncation of the eolian facies at depth 65 ft, which represent the Stoke surface (the paleo-water table).

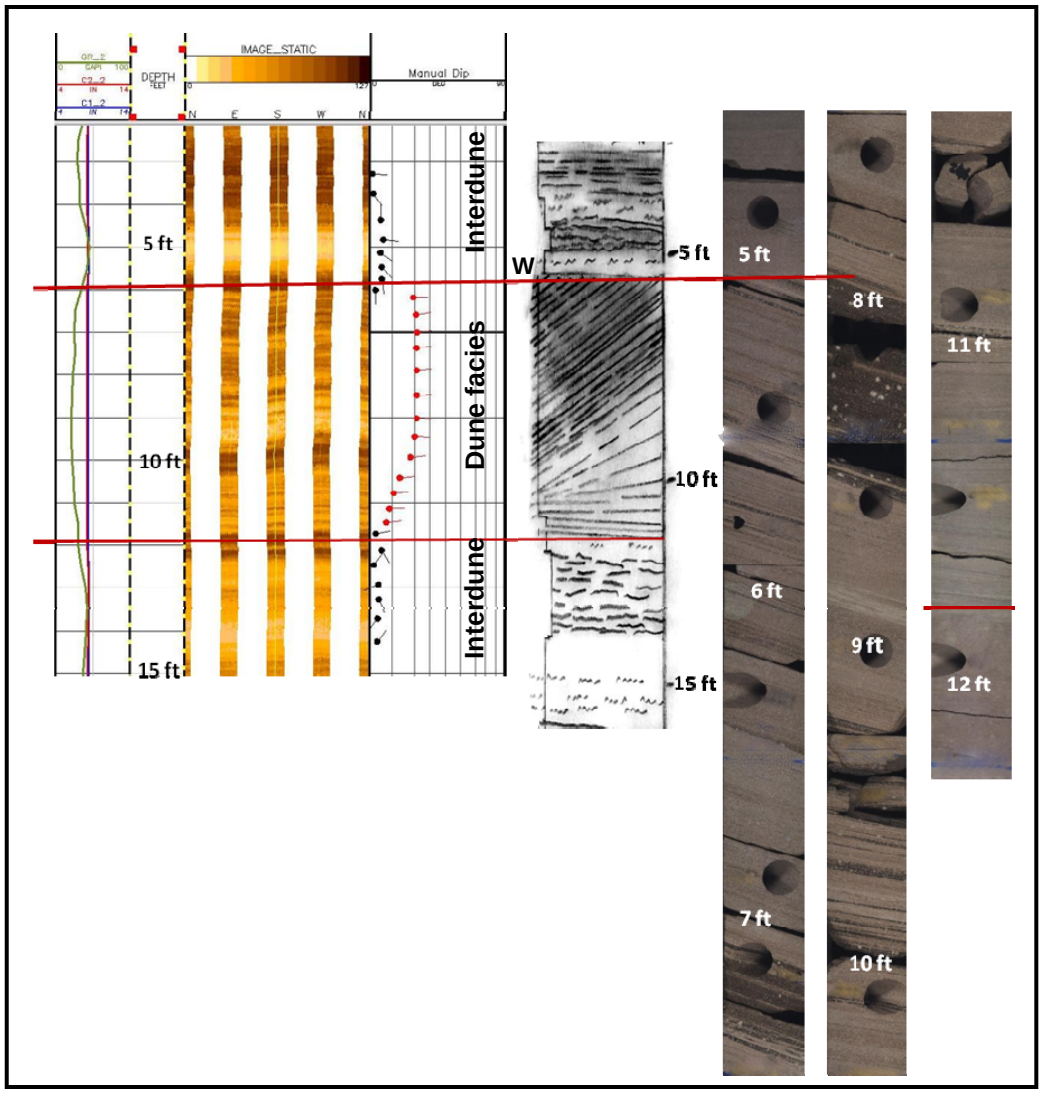

Figure 5.3: Calibration example of an image log and the corresponding core across a 13-ft interval from well A1. This shows the correlation between core and image log data for the eolian dune deposits, high angle cross-stratification and the interdune flat-irregular laminations. Note (1) The high-angel dip data and low-angle dip data, which reflects the dune and interdune facies respectively. (2) The different orientation of the interdune dip data and the dominant east direction of the dune deposits. (3) The clear abrupt truncation of the dune facies seen on both the core and image log at (W), which represents the paleo-water table. (4) The GR (green curve on the left of the image log) response to the eolian and interdune facies, high across interdune deposits due to the high content of argillaceous materials, and low in the clean sands of the dune deposits.

5.3 PALEOWIND INVESTIGATION

The slip faces of eolian dunes generally face down-wind, so by measuring the direction of dip of the cross-beds formed by the migration of eolian dunes, it is possible to determine the direction of the prevailing wind at the time of deposition (Nichols 2009).

The paleowind investigation was based mainly on dip data that were picked manually across all the dune facies in the studied wells (see example Figure 5.4). This required examining over 4000 feet of image log data. A hierarchical approach was employed to analyze the data (Figure 5.5) whereby the eolian dune cross-bed paleowind azimuthal data were:

i) Recorded appropriately for each identifiable bed

ii) Averaged within each bedset within each well

iii) Averaged among all bedsets over each well

iv) Averaged among all wells over each field and the data represented on a rose diagram

v) And finally, averaged over the four studied fields and the results were represented on a rose diagram

From the spectrum of the dunes bedding dip and azimuth it was then possible to determine the dune type and paleowind direction and variability.

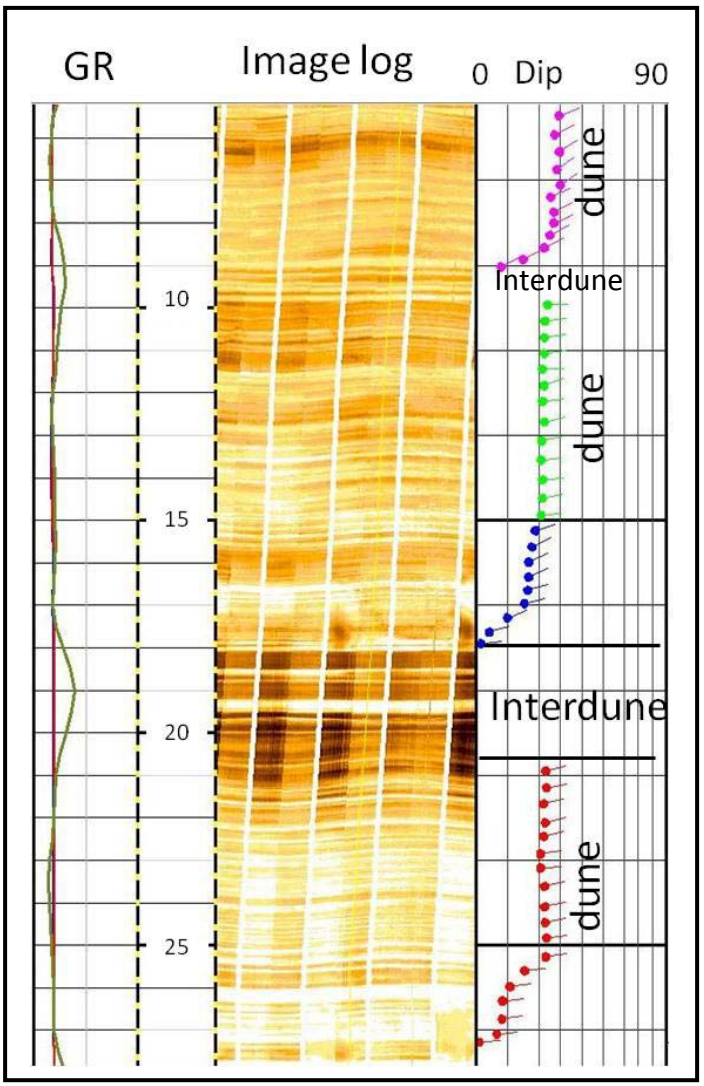

Figure 5.4: Borehole image log data across the Unayzah-A member in well A1 illustrating a pronounced eolian dune deposit and the associated dip and dip direction. Note (1) The low GR reading across the dune facies and higher readings across the interdune deposits, (2) The high dips across the dunes and the low dips at the bottom of the dunes, which reflects the presence of the silty interdune deposits. And most importantly, (3) the dominant dip direction, across all the picked dunes (reflected in the "tadpole" plots), towards the east-north east direction.

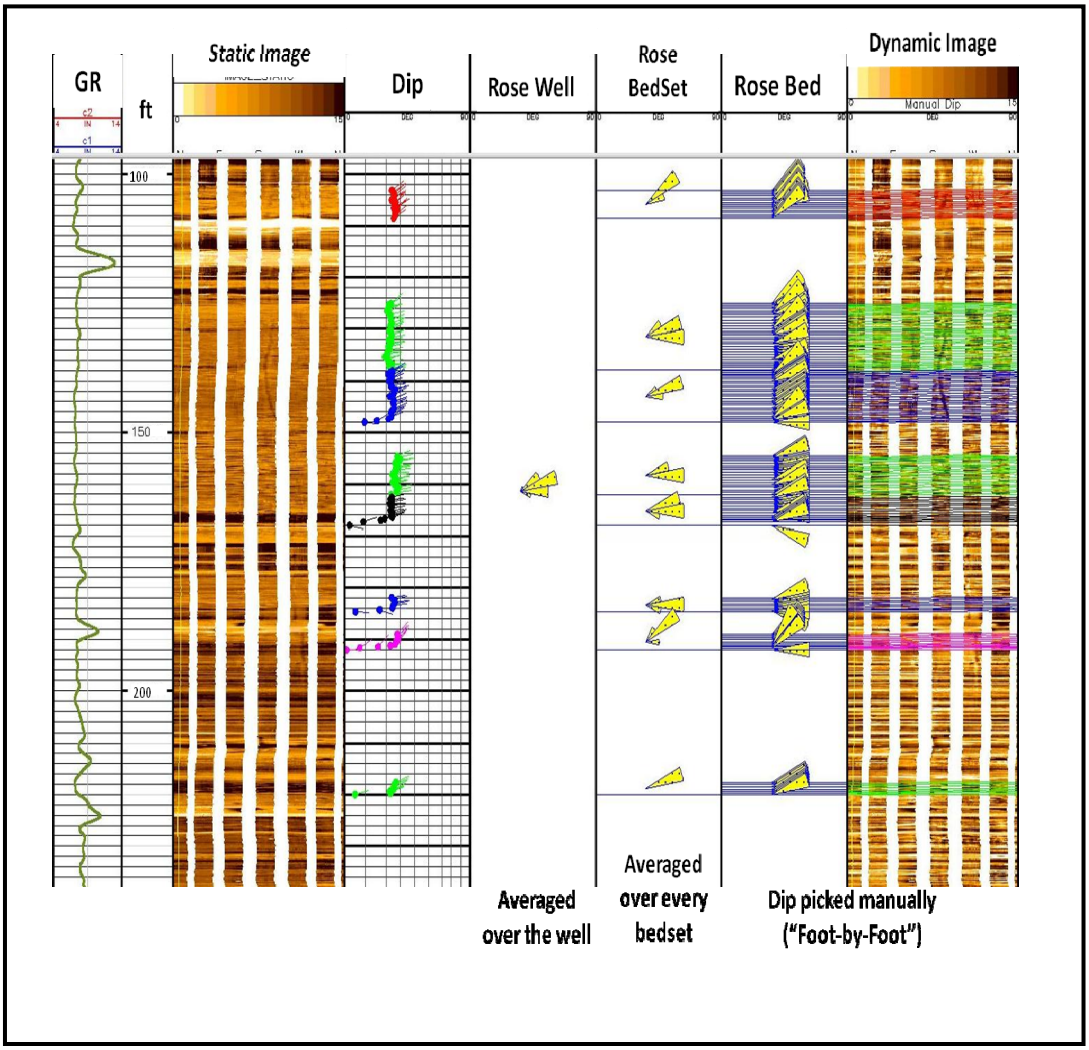

Figure 5.5: Interpreted high resolution borehole image log data illustrating thehierarchical approach used to investigate the paleowind direction across the Unayzah-A member, utilizing the eolian dune facies bedding azimuth data. Note the well-averaged data displayed on rose azimuth plots showing east-northeast paleowind direction (present day orientation).

5.4 DUNE TYPE DETERMINATION

Since the work of Bagnold (1941), additional important contributions to the study of eolian sands have been made in the field by Sharp (1963; 1966; 1978), Sharp et al. (1978) and McKee (1979a), among others. Important work has also been done in the application of aerial photography (Smith, 1968) and Landsat imagery (Fryberger and Dean 1979; Breed and Grow 1979), and in the study of erg morphology.

The starting point for all aspects of desert dune geomorphology is the identification and description of different dune types (Lancaster 1995). Dune morphology and occurrence appears to be controlled primarily by regional wind regime characteristics, especially directional variability (Lancaster 1995) (Figures 5.6a & b).

The relationships between eolian dune morphology and wind regime stems from the study of simple dunes and the facing directions of the slipfaces with respect to the generalized wind directions (Schenk 1990). Quantitative analysis of wind data and dune morphology has demonstrated that the larger eolian features visible on satellite imagery can be related to regional wind data as follows: barchan and transverse dunes characterize areas of least wind variability; linear dunes characterize areas of greater wind variability; and, star dunes characterize areas of complex wind regimes (Schenk 1990). Barchan, barchanoid, and transverse dunes have one principal slipface and commonly develop in a unidirectional wind regime (Mckee 1966) (Figure 5.6a & b).

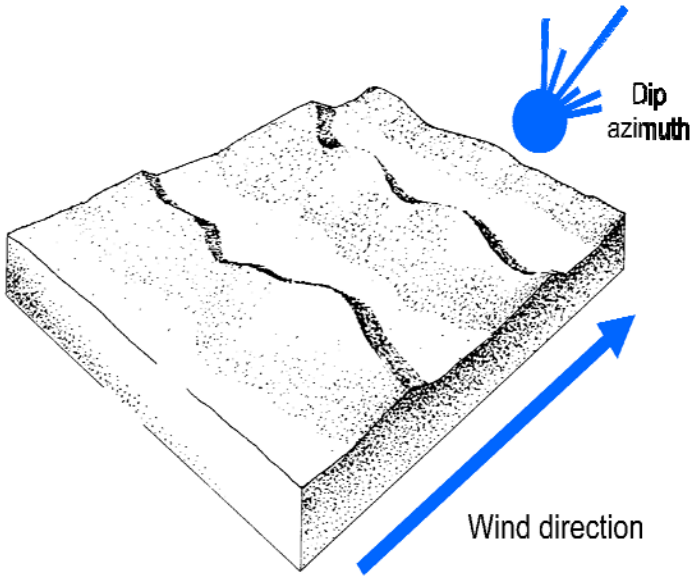

Figure 5.6a Barchanoid ridge dune schematic showing the slipface orientations that develop with a dominant wind direction. The sinusoidal dune crest and corresponding slipface orientation is generally perpendicular to the dominant wind direction. The resulting dipmeter data would show a wide unimodal slipface dip azimuth (modified after McKee 1979).

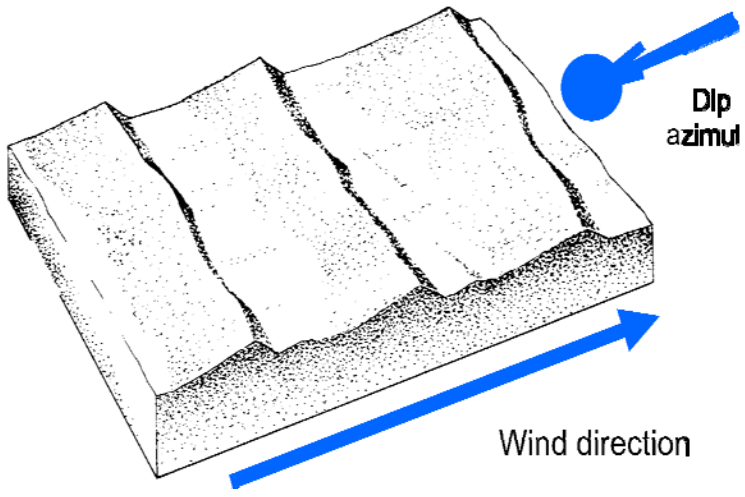

Figure 5.6b: Transverse dune schematic showing the orientation of the dune crest and corresponding slipface perpendicular to the dominant wind direction. The resulting dipmeter would show a narrow unimodal slipface dip azimuth (modified after McKee 1979).

5.5 RESULTS

Paleo-transport analysis is a valuable sedimentological tool in reservoir and basin characterization. Such interpretations can be derived using borehole images and core. Modern computer systems allow the visualization and analysis of oriented borehole images. Such images can be interpreted in the same manner as a core, with the additional benefit of interactive picking of features on-screen, leading to a high confidence dip data set. Different features are picked using a classification scheme, suitable for the depositional environment, with resulting tadpoles and sine curves. Resulting data can aid in environmental interpretations and paleowind direction investigations throughout the study area**.**

5.5.1 Paleowind direction

The current study investigated the paleowind direction from the Unayzah-A reservoir dune facies according to a hierarchical method described previously.

As discussed previously in Chapter 3, the Unayzah-A sandstone is composed of a series of interbedded eolian facies. Among these, the eolian cross-bedded dune facies is composed of one or more sets of compound cross-strata. Each bedset is bounded by a significant bounding surface succeeded by interdunes and represents the deposits of one or more bedforms as the dune migrated and climbed through time (Figuer 5.7).

A total of 2813 image log data points (dips) were picked manually across the dune facies from the twenty-one selected wells (see image logs, Appendix 2). The

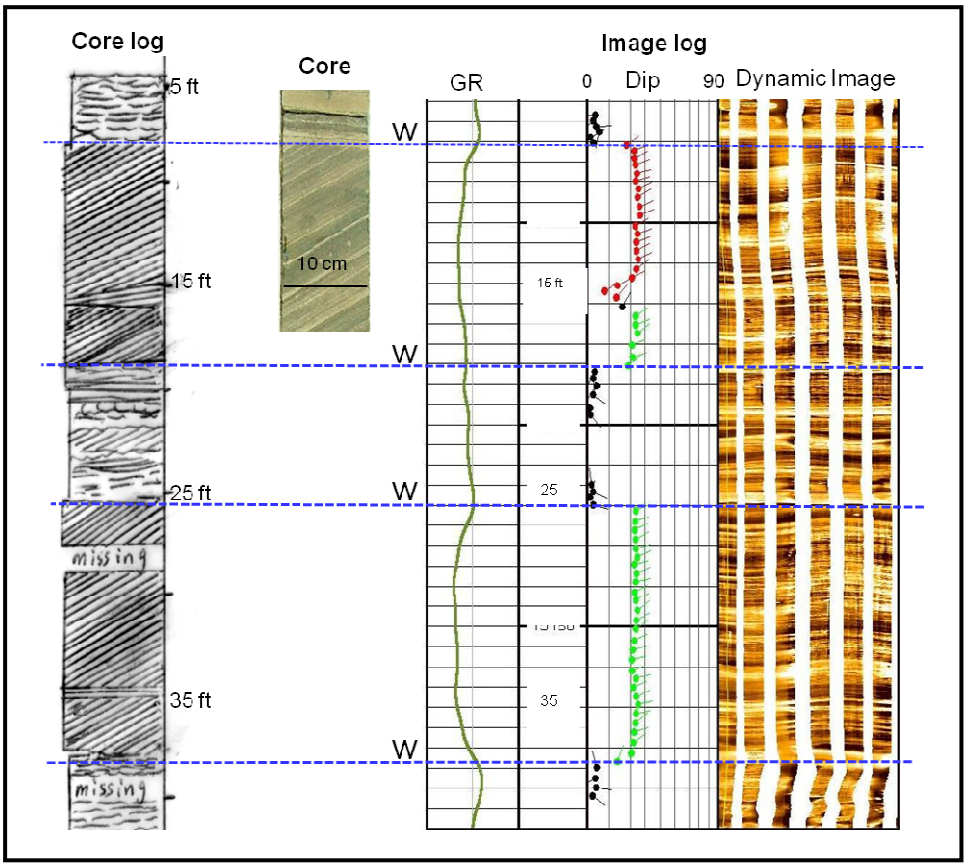

Figure 5.7: Image log-core correlation in Well D1 showing well-defined bed-sets of sandstone displaying high angle cross-laminations (dune facies) between 7-15 ft and low-angle laminations (interdune facies) between 5-7 ft. Cross-laminated bed-sets are terminated upwards abruptly and horizontally by “Stoke Surfaces” (blue dashed line), indicating a rising water table. Note the dominant unimodal eolian dune’s dip direction of east-northeast on the image log data.

histogram in Figure 5.8 illustrates the distribution of the image log data points. The majority of the data points are concentrated between 40 and 100 degrees, or in the east-northeast direction, which reflects the dominance of this orientation in all the studied wells. Then the data was averaged over each bedset, each well, andeach of the four fields. Finally, all the data were averaged over the entire study area.

The collected data was statistically analyzed for each field utilizing rose diagrams from two software packages, namely Rozeta (Figures 5.9 & 5.10), and Oriana (Figures 5.11& 5.12). The resultant azimuthal rose diagrams were then considered to represent the best indication of cross-bed orientations.

The Rozeta software represented the data by counting the numbers of azimuth data points every 10 degrees. The software statistical analysis (Table 5.1) revealed that the data point density in all the studied fields fall between 40 and 100 degrees, and the maximum number of points (88%) fall between 80-90 degrees (Figure 5.8). The total number of azimuth data points in this interval is 2481(88% of the total), which reflects very clearly a dominant paleowind orientation of east-northeast (present day) (Figure 5.9).

The Oriana software analyzes orientations and calculate a variety of the special types of statistics necessary for working with data measured in degrees. Oriana calculates circular measurements such as mean vector, and standard deviation, along with confidence intervals for the mean. The azimuth data analyzed using this software to increase the confidence in the analysis and improve the previous results from the Rozeta software. The statistical analysis of each field's

azimuth data revealed that the dominant paleowind orientation is to the east-northeast (present day) (Figure 5.11) with a clear concentration of the data between 80-90 degrees. The statistical mean of the azimuth data was calculated for each field and found to range between 67-76 degrees East. Then, all the data was averaged using the same software to generate one rose diagram representing the dominant direction for all the fields. The data shows clearly that the dominant direction is east-northeast (preset day) with mean value of North 72 degrees East (Figures 5.12).

The resultant rose diagrams for the studied wells were plotted on the location map to indicate and evaluate the dominant paleowind direction in each well and for each field (Figures 5.13 and 5.14). The studied field's locations extend about 300 km from central Saudi Arabia (field A) to the eastern part of Saudi Arabia (Field D). The data revealed that a dominant trend was found in every well and in all the studied fields of east-northeast (present day). This indicates that the dominant wind direction during the deposition of these dunes, across the entire study area, was constant toward the east-northeast (present day).

Azimuth Data / Field	Total No. of data points	Azimuth Concentration	Azimuth Concentration No. of points	%	Highest Concentration	No. of points
A	681	40 º -100º	582	85	80º-90º	160
B	491	60 º -90º	346	70	80º-90º	130
C	798	60 º -100º	650	81	80º-90º	304
D	840	40 º -100º	695	82	60º-70º	186
All Fields	2813	40 º -100º	2481	88	80º-90º	735

Table 5.1: Shows the number of the image data points and the azimuth distribution, and concentrations, for all the studied fields. Note the point concentration is high between 40º-100º (east-northeast). Also note that the maximum number of points are between 80º-90º (east-northeast).

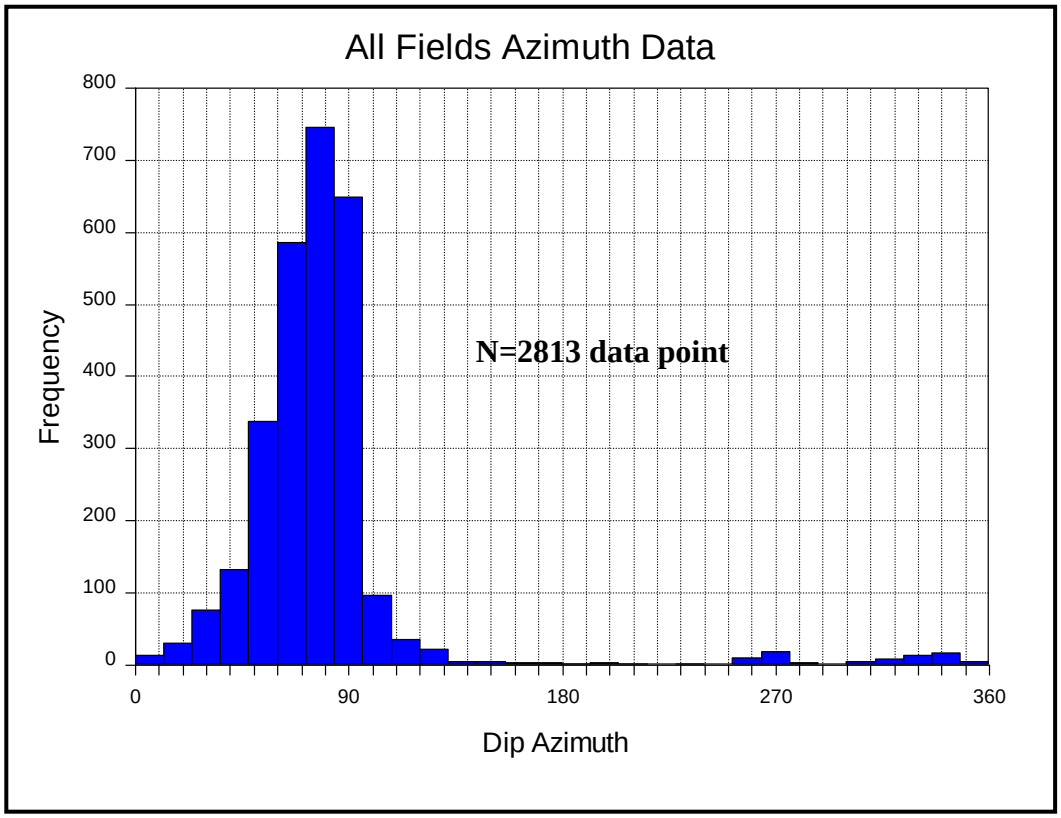

Figure 5.8: Histogram showing the total number of the data points (frequency) used in this investigation, and the frequency of each azimuth. The X axis represents the dip direction (azimuth) of each image log data point collected from the studied wells. The Y axis represents the number (frequency) of points for each azimuth. Note that the highest concentration of the dip azimuth data is between 40º-100º reflecting a dominant direction toward east-northeast.

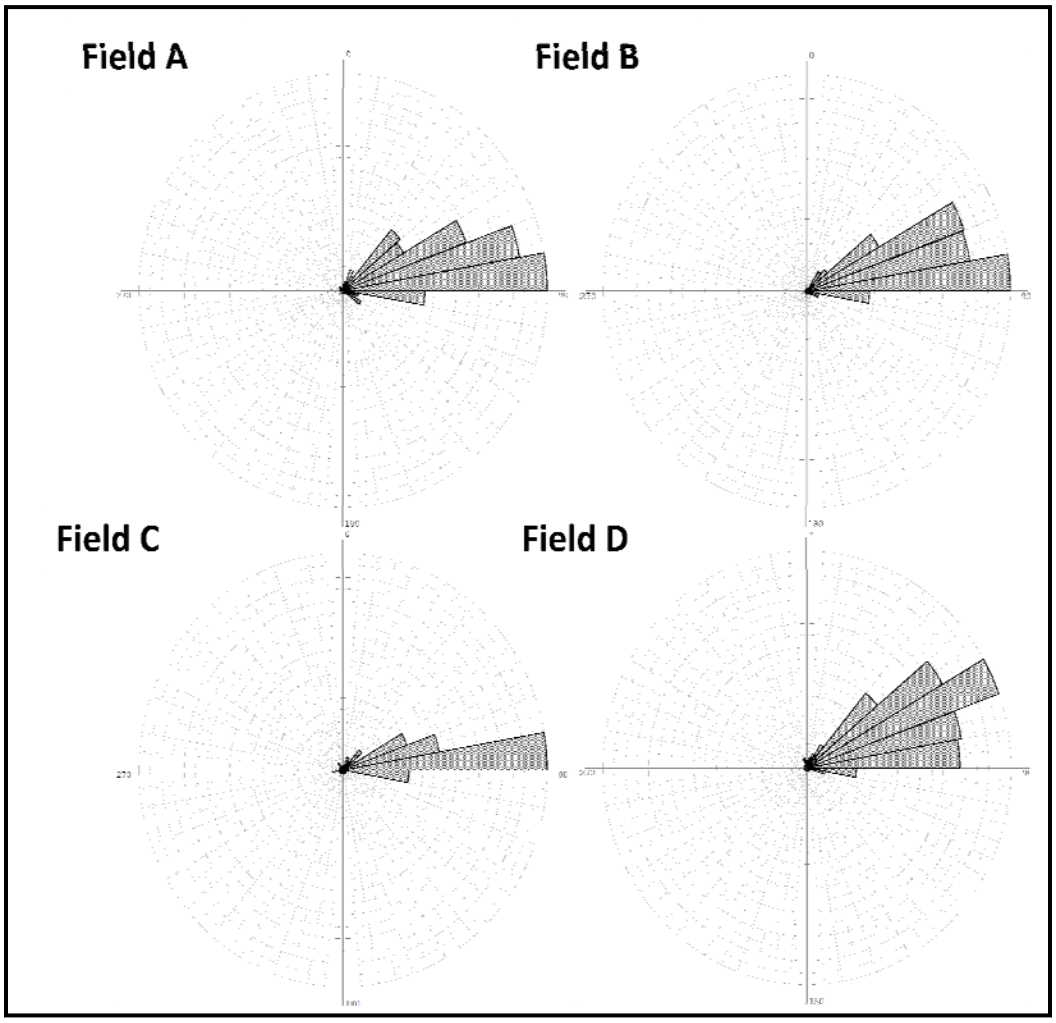

Figure 5.9: Rose diagrams (Rozeta software) showing the Unayzah-A dune sand's bedding dip azimuth data distribution for each field, which indicates the paleowind direction for each field. The data is showing a direction toward east-northeast (present day). Note: the data point concentration density is high between (40º-110º) which reflect the mean direction of the azimuth data.

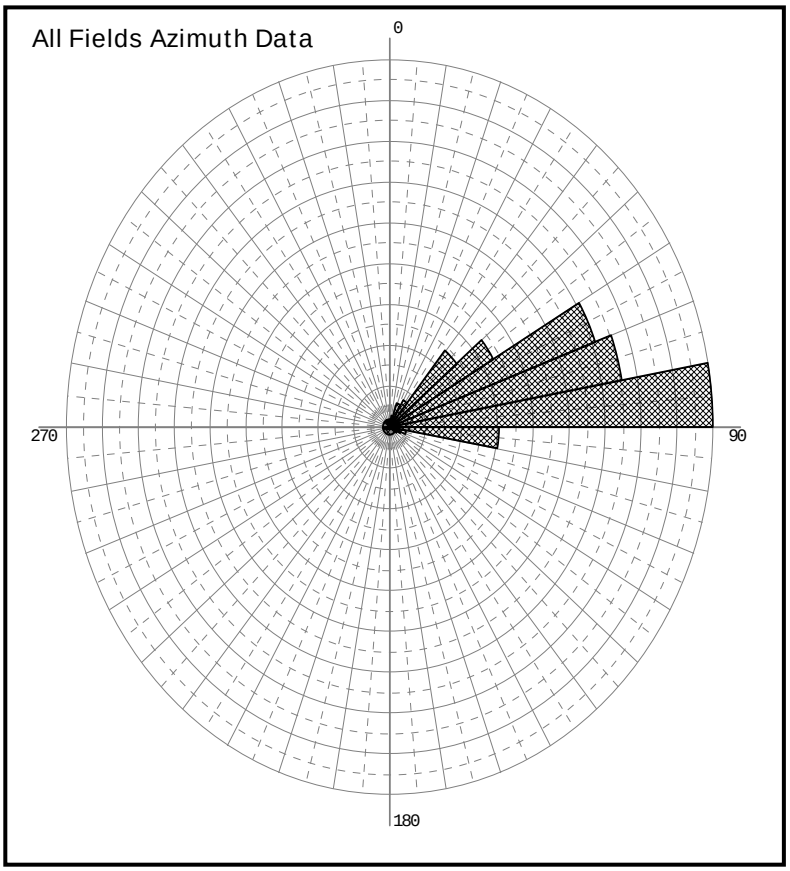

Figure 5.10: Rose diagram (Rozeta software) illustrating the Unayzah-A dune sand's bedding dip azimuth data distribution for the whole study area.It shows the dominant paleowind direction for the whole study area (four fields). The data indicates a wind direction toward east-northeast (present day) between (40º-110º), with a strong concentration (70.4%) between (60º-90º), and 26% of the points between (80º-90º).

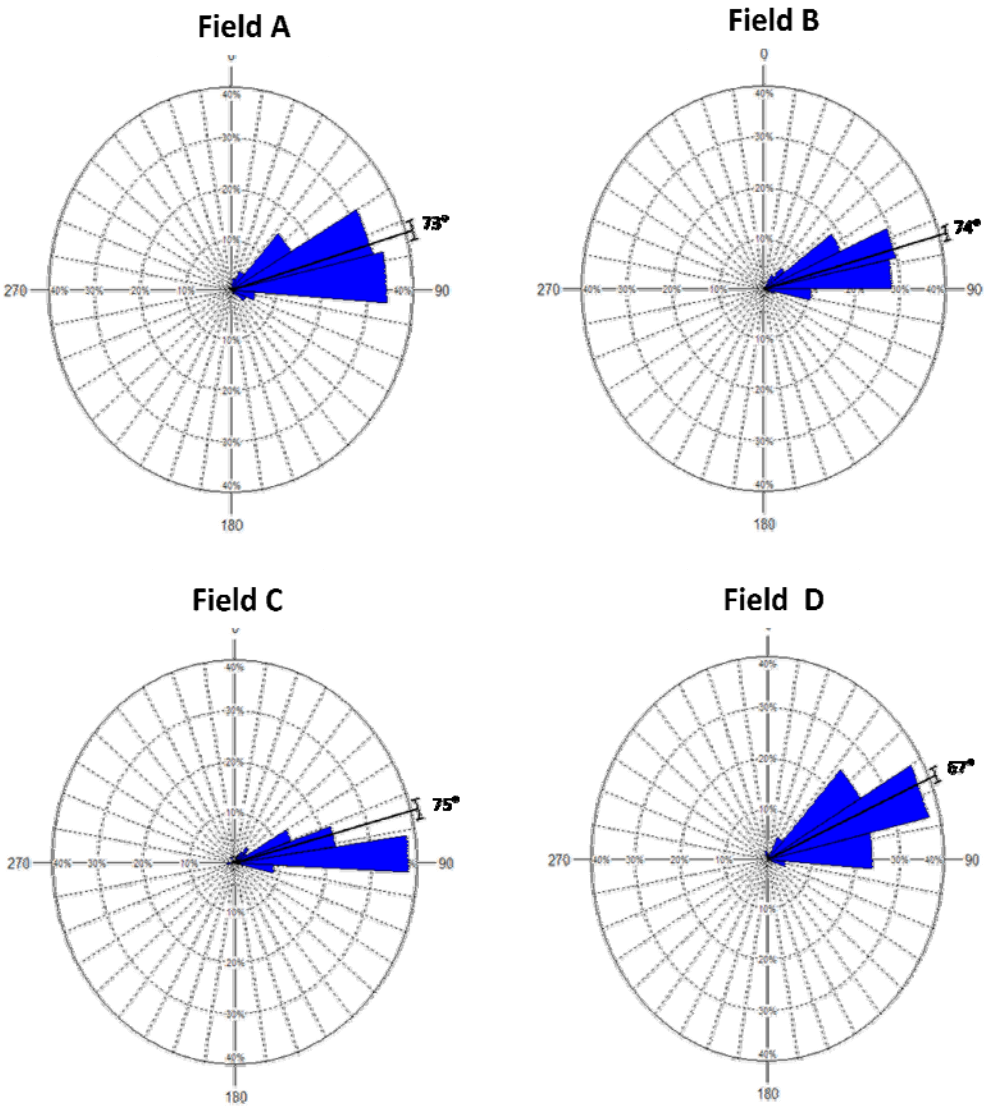

Figure 5.11: Rose diagrams (Oriana software) showing the Unayzah-A dune sand's bedding dip azimuth data distribution for each field, which indicates the paleowind direction for each field. The data is showing a unimodal and narrow orientation strongly concentrated between (60-90º). This indicates a dominant paleowind direction toward east-northeast (present day). Note the azimuthal mean values range between North 67-75 degrees East.

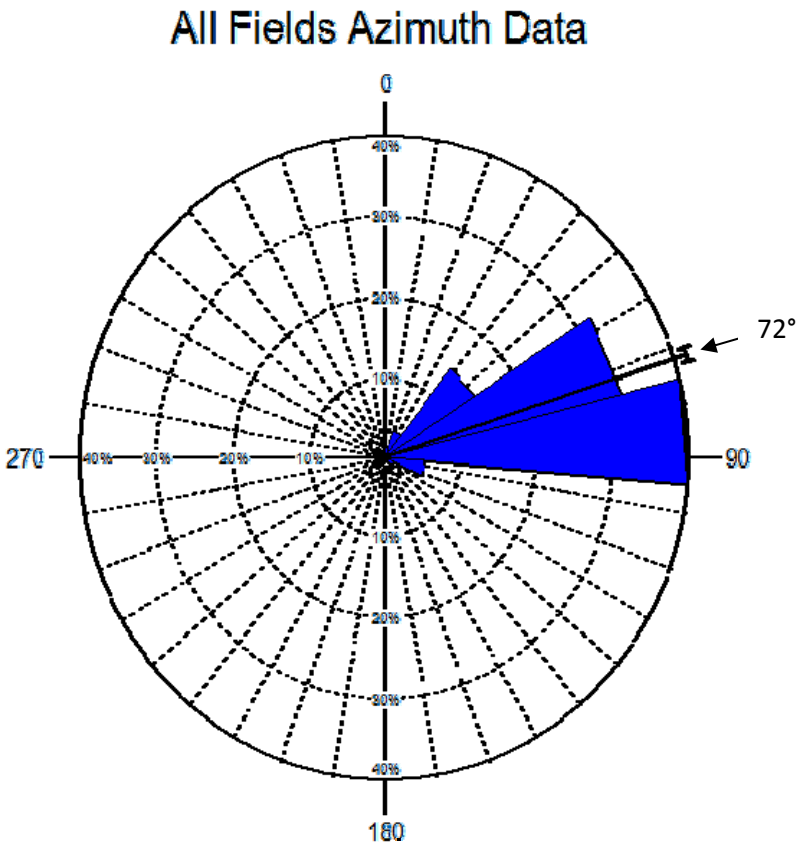

Figure 5.12: Rose diagram (Oriana software) showing the Unayzah-A dune sand's bedding dip azimuth data distribution for the whole study area. This shows the dominant paleowind direction for the four fields. The data indicates a direction toward east-northeast (present day). The data density is high between (40º-100º) with a strong concentration between (60-90º). The calculated mean value (arrowed) is 72°, which shows the dominant east-northeast orientation.

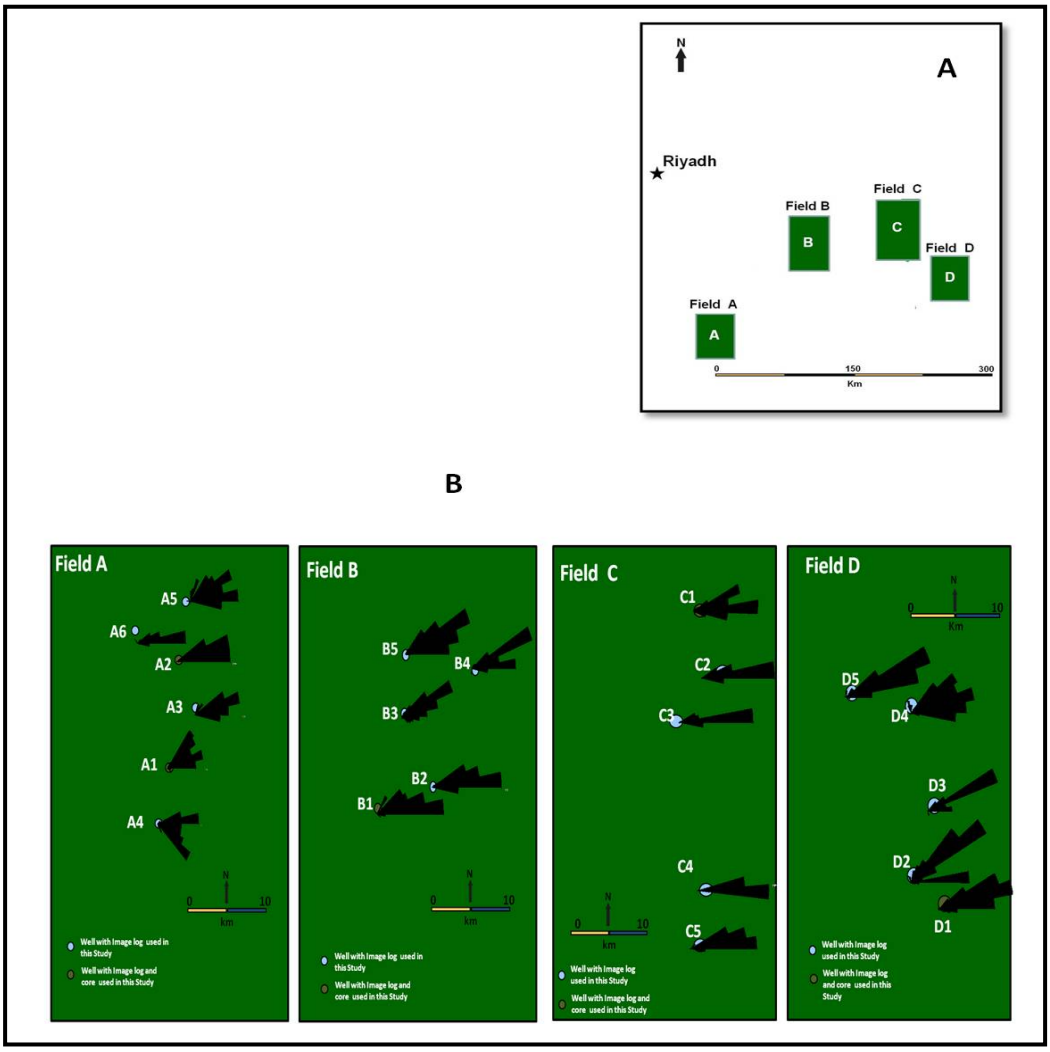

Figure 5.13: Location maps showing the general field and well locations. A: Shows the selected fields (A, B, C and D), note the location of Riyadh. B:Showing a close up of the selected fields and the wells used in this study. The azimuth data rose diagrams are posted at the well locations. Note the generally narrow and unimodal shape of the azimuth data, and the dominant orientation to the east-northeast (present day) in all the studied wells from Field A in central Saudi Arabia to Field D in eastern Saudi Arabia.

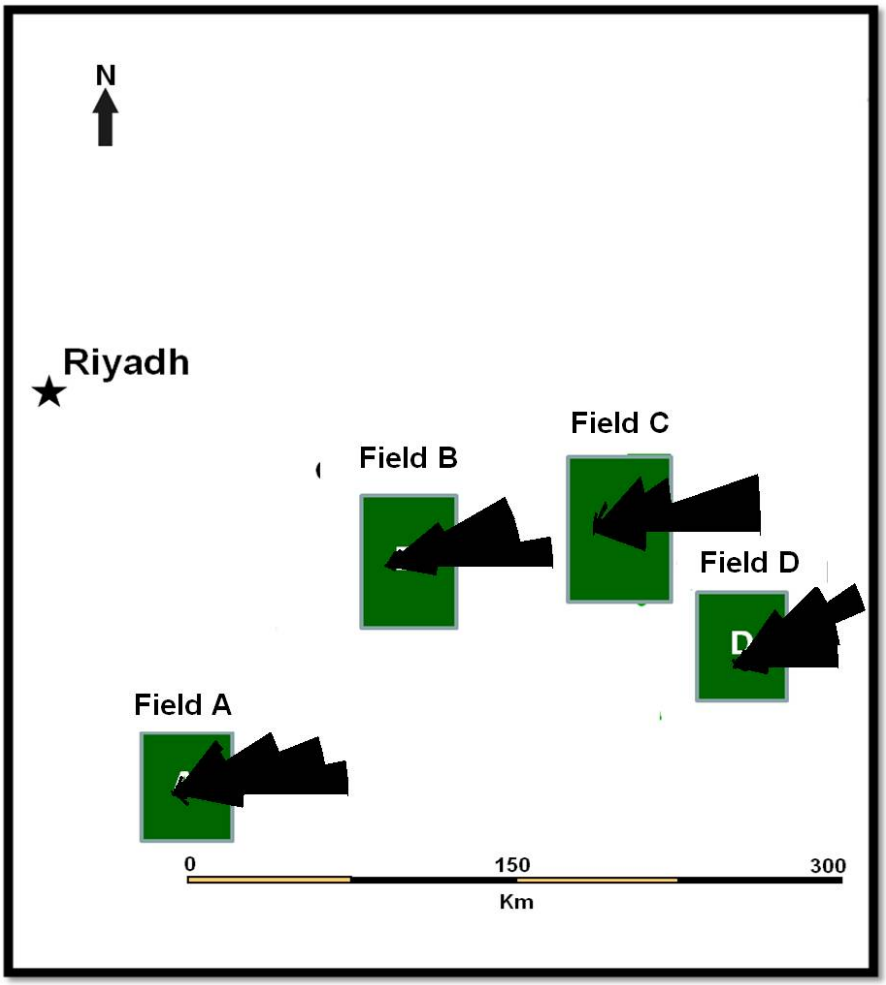

Figure 5.14: Location map of the study area showing the paleowind directions inferred from the dip azimuth data. Note: the dominant direction for the azimuth data is east-northeast (present day).

5.5.2 Dune Types

There are a several different types of modern eolian dunes that are classified by their external form. Dunes form in response to specific wind regimes of which four basic types are recognized (Fryberger 1979) (Figure 5.15).

Fryberger (1979), in a paper on dune forms and wind regimes, used satellite images and aerial photographs from various dune fields around the world to classify dune types based on dune morphology. He then related the classified dune types to a wind direction rose diagram derived from local wind monitoring stations within the study areas. He concluded that the measurement of a unimodal wind direction corresponded to a dune classification of transverse to barchanoid ridge dunes identified on the aerial photos and satellite images (Figure 5.16).

It is also possible to classify the dune types by the geometry of the internal cross-bedding that is produced by the geometrical characteristics of the advancing surface of each dune type (Nurmi 1985).

Figure 5.17 from Nurmi (1985) shows the basic premise of dip spectral analysis that each dune form has unique internal architecture, or dip patterns, and also unique azimuthal distributions of dip spectra.

The previously discussed rose diagrams and the statistical analysis of the measured azimuth data throughout the Unayzah-A eolian dune facies in the study area showed that 88% of the azimuth data lies between (80-90º), which reflects a dominant unimodal and narrow wind orientation (azimuth) across the entire study area.

Based on these observations, and the evaluation of the studied well dip data, it is noticeable that there is a clear decrease in the dip data readings throughout most of the interpreted dunes in the studied wells (Figure 5.18). Correlations of rose diagrams from bedset level to well and field levels (Figure 5.19), and their relationship to the dune forms (*sensu* Fryberger (1978) Nurmi (1985) and Nichols (2009) suggests that the majority of the Unayzah-A member dunes were made up of transverse dune types formed by a narrow unimodal wind regime.

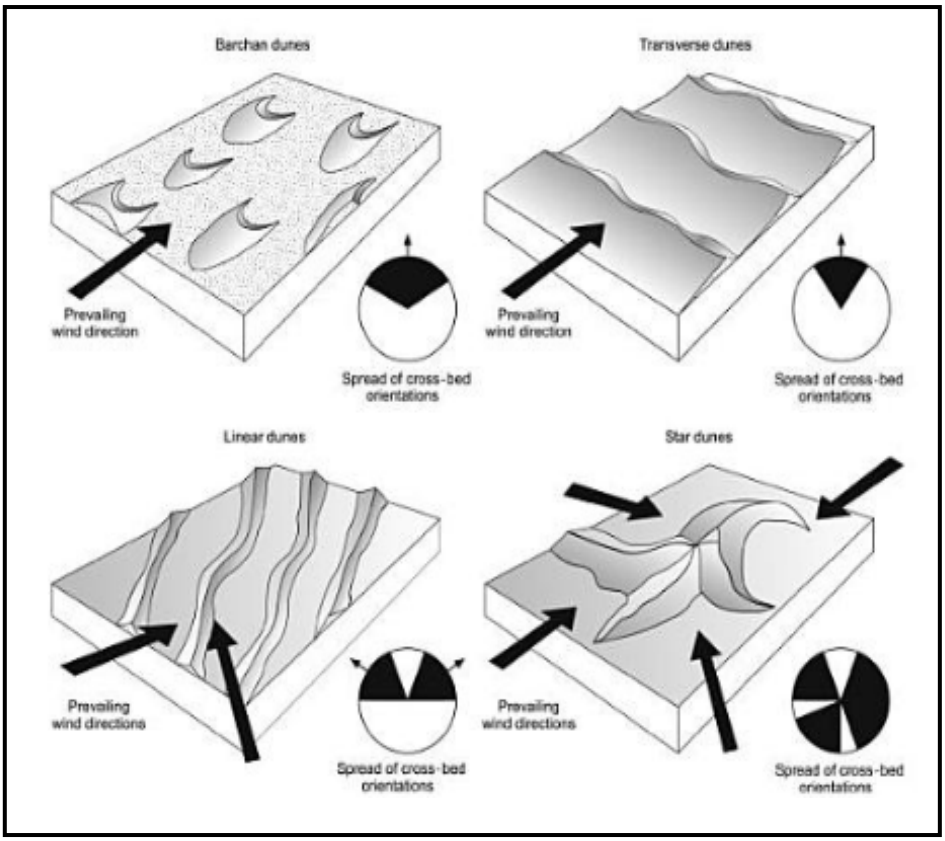

Figure 5.15: Four of the main eolian dune types. Their forms are determined by the direction of the prevailing wind(s) and the availability of sand. The rose diagrams indicate the likely distribution of paleowind indicators if the dune resulted in cross-bedded sandstones (after Nichols 2009).

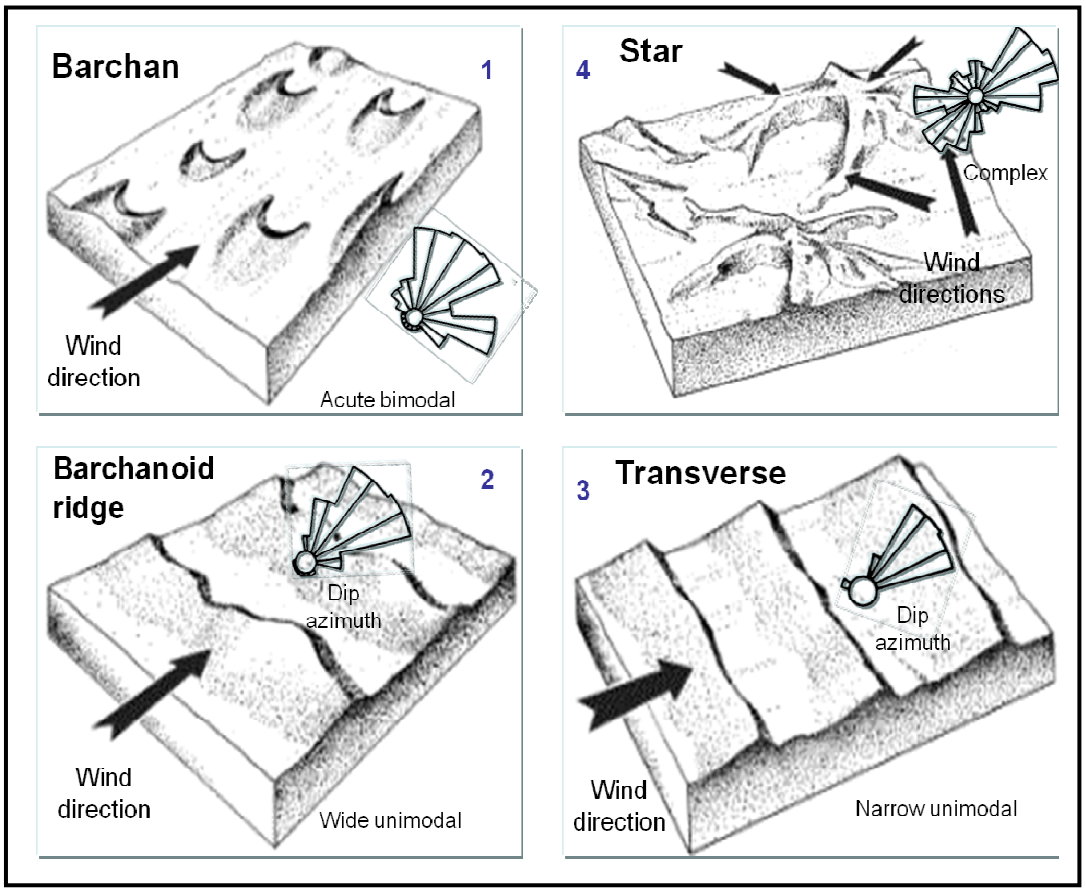

Figure 5.16: Dune schematics illustrating eolian dune forms from the classification of Mckee (1979a). These include barchan, barchanoid, transverse and star dunes. Rose diagrams from Fryberger (1978) are posted on the dunes showing the relationship of dune forms and wind regimes. As wind regime becomes complex (multidirectional), dune forms evolve into more complex forms with greater internal complexity, as expressed in the rose diagrams. Note the unidirectional orientation and the narrow window of the azimuth data that belongs to the transverse dune type. The major dune types modified after (McKee, 1979a) and the stereonet plots (rose diagrams) (modified after Fryberger (1978).

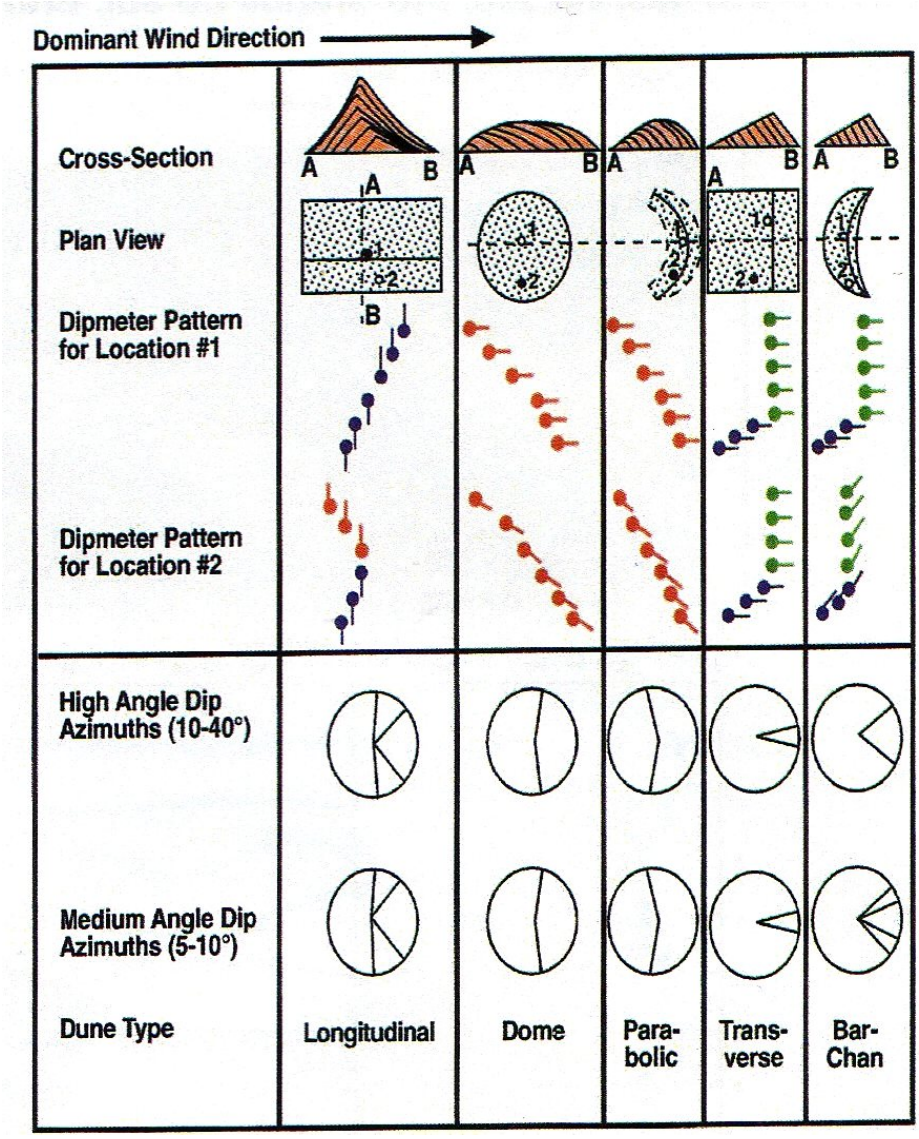

Figure 5.17: Dip characteristics of the basic dune types illustrating the dune forms internal structure and the corresponding dipmeter patterns in 2 location from plan view across the dune, and the resultant rose diagrams for each dune (the wind is blowing to the east). Note the decrease in dip data reading and the corresponding narrow unimodal azimuth data throughout the transverse dune type (After Nurmi, 1985). The dip pattern matchs well with the dipmeter data collected across the proposed transverse dune system in this study.

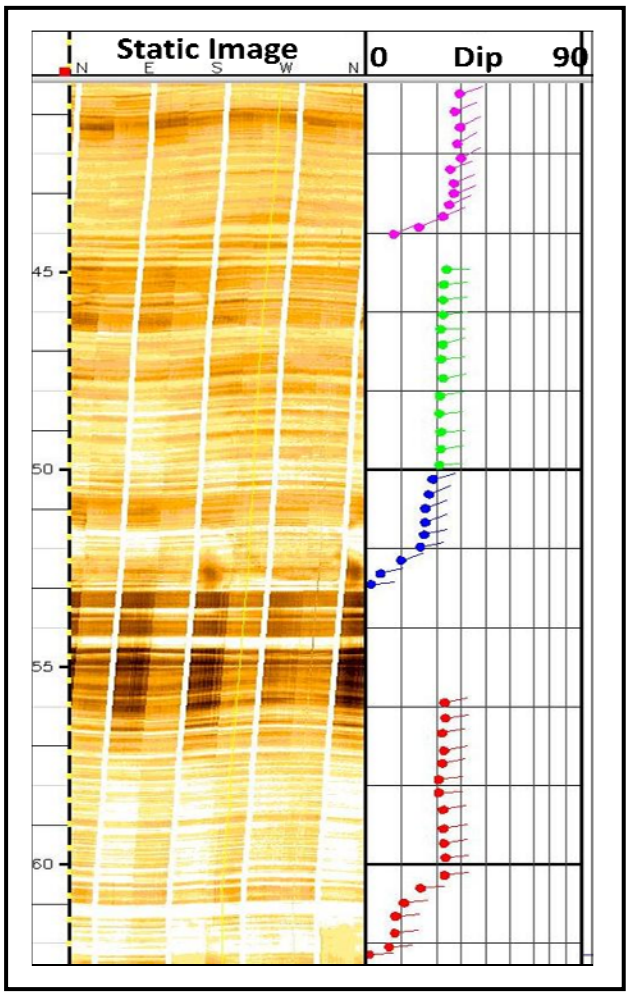

Figure 5.18: Image log and dip data across 23 ft of eolian dune facies observed in well D1. This shows a clear example of the descending appearance of the dipmeter data throughout the preserved dunes deposits and is similar to the transverse dipmeter patterns observed by Nurmi (1985).

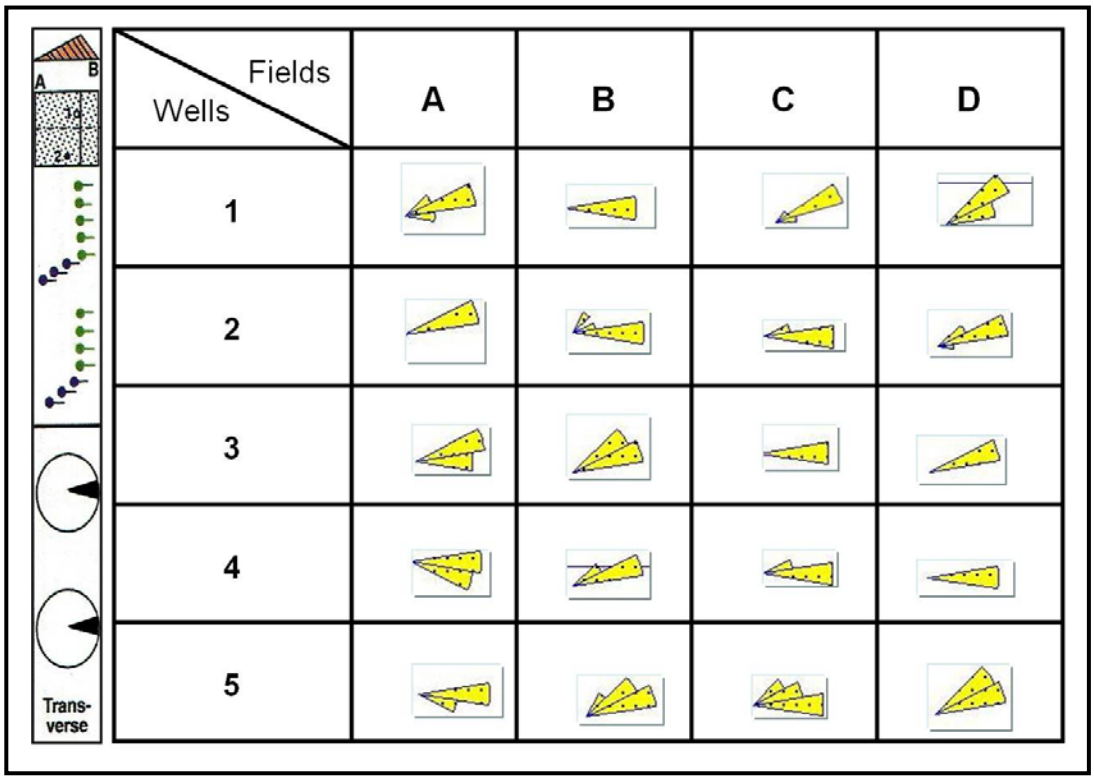

Figure 5.19: Rose diagrams from representative bedset data from the 20 study wells. This illustrates the narrow unimodal orientation of the analyzed azimuth data compared with the transverse dune internal structure azimuth data from Nurmi (1985) (column to the left of the table). Note the similarity in the narrow unimodal orientation of the azimuth data, which reflects the dominant transverse dune type in the Unayzah-A member.

5.6 PALEOGEOGRAPHIC IMPLICATIONS

D. B. Loop et al. (2004) utilized dip direction data from Colorado Plateau eolian sandstones to provide important clues to planetary-scale atmospheric circulation during much of Pangaea's existence. This study indicated that eolian cross-strata should receive more attention in future paleogeographic and paleoclimatic reconstructions.

The paleowind investigation throughout the Unayzah-A member in the studied fields reported a resultant mean vector of North 72° East, which reflects the dominant wind direction (measured present-day) (Figure 5.12). This proves to be exceedingly important when trying to position the Saudi Arabian peninsula geographically, in time, during the deposition of the eolian Unayzah Formation (Figure 5.20 a & b). The key is to honor the unimodal wind orientation derived from the prograding dune foresets recognized on image logs. The interrelated relationship of these types of results with current wind belts and paleogeography was not studied and it is generally beyond the scope of this study.

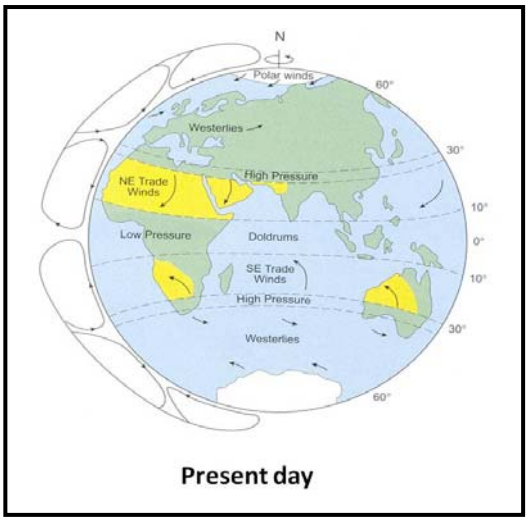

Figure 5.20a: Diagram showing the origin of the Earth's air-pressure system and the tropical Trade-Wind deserts (wind belts present day) (after Glennie, 2005**).**

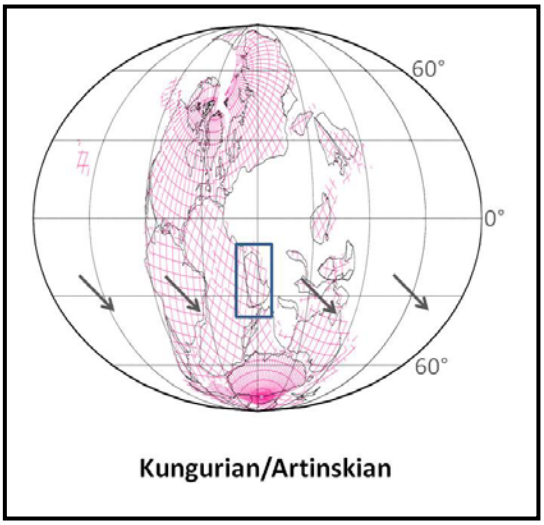

Figure 5.20b: Base map representing the plate reconfiguration during the Early Permian (Artinskian). Saudi Arabia (green) is placed well with the westerly (present day) wind belt (modified after Ziegler et al. 1997).

5.7 RESERVOIR IMPLICATIONS

Eolian sandstone deposits can form excellent reservoirs. Wind is a very effective agent for sorting grain size (sand, silt and clay), both vertically within the air column and horizontally in the downwind direction. Therefore, at any given eolian depositional site, the deposit will tend to be fairly well-sorted by grain size. Good sorting generally leads to good reservoir quality (Slatt 2006). Eolian dune deposits comprise thick, cross-bedded intervals of well-rounded, well-sorted sandstones. They are normally the most productive lithofacies in eolian reservoir systems and the interdune areas can provide permeability barriers and baffles within the eolian sediments (Shepherd 2009).

The borehole image log, or dipmeter, is an extremely useful tool for recognizing and interpreting eolian deposits in the subsurface. As has been shown, measuring the eolian dune deposit's cross-bedding is useful for interpreting dune bedforms and thus sandstone geometry. The dipmeter plots through the Unayzah-A member's eolian dune facies suggests a transverse dune type migrating to the east-northeast (present day).

Eolian dune cross-bed sets show strong lateral permeability anisotropy within the reservoir. Thus, the optimum permeability trends are typically perpendicular to the paleowind transport direction and parallel to the dune axis (Krystinik and Blakeney 1990). Reservoir fluids flowing across the wind-flow direction are impeded by pin-stripe lamination of fine-grained material along the dune cross sets (Shepherd 2009). On the other hand, the individual layers and

laminae are much more continuous along the depositional strike trend of the dune system, which is perpendicular to the winds flow direction (Weber 1987) (Figure 5.20).

This work revealed that the Unayzah-A member in the studied fields is dominated by transverse dune types migrating to the east-northeast (present day). Thus, the optimum permeability direction will be perpendicular to the migrating direction (paleowind direction).

The cross-bedding in the eolian reservoir sandstones consists of alternating layers of fine and coarse grains. In transverse dunes, that texture is more continuous perpendicular to the wind transport direction. This directionally dependent textural continuity causes permeability anisotropy within the rock. This reflects the importance of identifying the paleowind direction in eolian reservoirs.

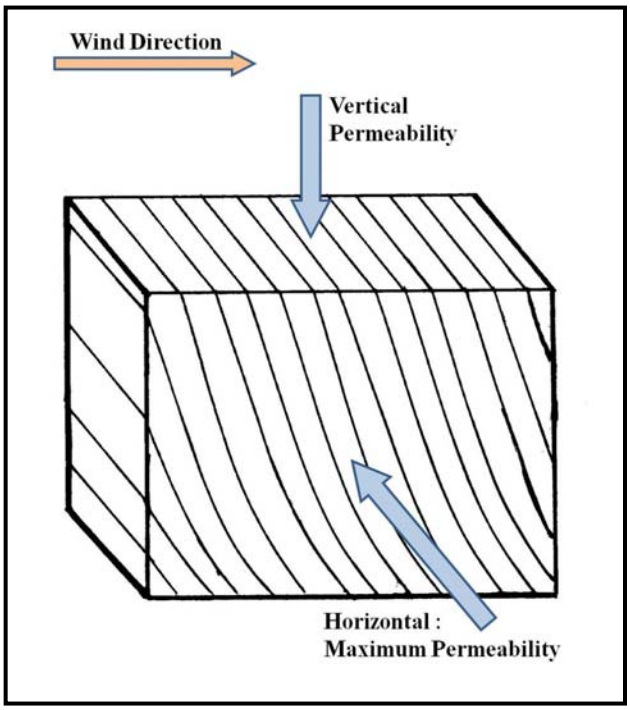

Figure 5.21. Three-dimensional schematic illustration showing the lateral (horizontal) permeability anisotropy in eolian sediments resulting from more continuous laminae perpendicular to the wind direction. In this diagram the wind is blowing from west to the east. The optimum permeability is perpendicular to the wind direction.

5.8 CONCLUSIONS

The detailed description and analysis of over 1096 ft of core from the Unayzah-A sandstone of eastern central Saudi Arabia has confirmed the continental deposition of the Unayzah-A member under arid to semi-arid conditions, very commonly in a wind-dominated, eolian setting. A number of distinctive depositional facies were recognized in the studied wells. These include: eolian dunes (representing 46% of the total facies in the studied wells), sand sheets, interdune (wet and damp) and paleosols. This mixed facies association is interpreted as an eolian erg-center system and erg-margin deposits.

Electrical borehole images and dipmeter data are very important and continue to add great value in geological interpretations. The oriented image data can be used for measuring paleocurrent directions in the absence of oriented cores, and the image logs also provide for a rapid facies interpretation, particularly for cross-bedded sands. Image logs provide a wealth geologic information previously obtained only from cores. Analysis based on image logs, calibrated with key core data, can improve geological interpretation and reduce or eliminate uncertainties.

Electrical borehole images from twenty-one wells were processed and interpreted using GeoLog software. The dip magnitude and dip azimuth were analyzed from the image logs. In addition, electrofacies analysis was performed using the image logs, through calibration with core data, to diagnose facies types.

Based on the image logs the following bedding facies were distinguished: igh-angle cross-bedding (20-34º), low-angle cross-bedding (0-20º) and horizontal lamination, which reflects dune, sand sheet and interdune facies, respectively.

The paleowind investigation was based mainly on dip data that were picked manually across all the dune facies in the studied wells. This required examining over 4000 ft of image log data, using a hierarchical approach starting from bed level through to field level.

From the spectrum of the dune bedding dip and azimuth data, the Unayzah-A member's wind direction was determined using the orientation of the prograding slipface deposits of the dunes facies as recognized on image logs. This analysis resulted in the conclusionthat the dominant wind direction was east-northeast (N72°E) present day. The analysis of the azimuthal data showed a narrow unimodal wind regime, which reflects a dominant transverse dune type with paleo-dune crests trending N-S.

The economic implication of understanding the permeability anisotropy in eolian depositsis crucial for optimized reservoir development and management. The dune facies are normally the most productive lithofacies in eolian reservoir systems, and the interdune areas can act as permeability barriers and baffles within the eolian deposits. The N-S trending transverse dunes suggest an optimum permeability direction perpendicular to the dominant paleowind direction, which is generally to the east-northeast (present day).

APPENDIX 1

CORE DESCRIPTION DATA

Well A1

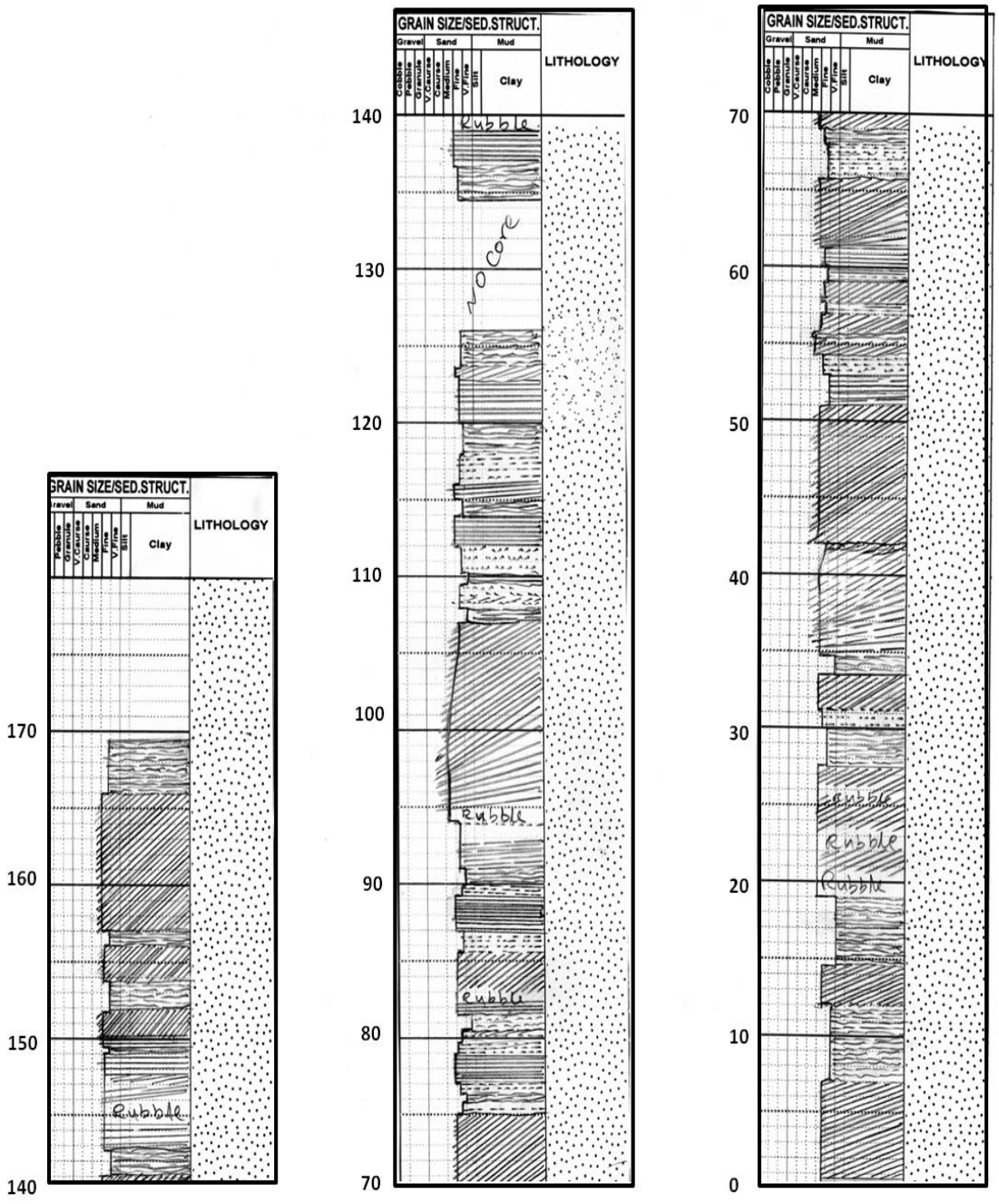
GRAIN SIZE/SED.STRUCT.
Gravel
Sand
Mud
Pebble
V.Caurse
Caurse
Medium
Fine
V.Fine
Silt
Clay
LITHOLOGY
170
160
150
140
Rubble
140
130
120
110
100
90
80
70
No Core
Rubble
Rubble
70
60
50
40
30
20
10
0
Rubble
Rubble
Rubble

Well A2

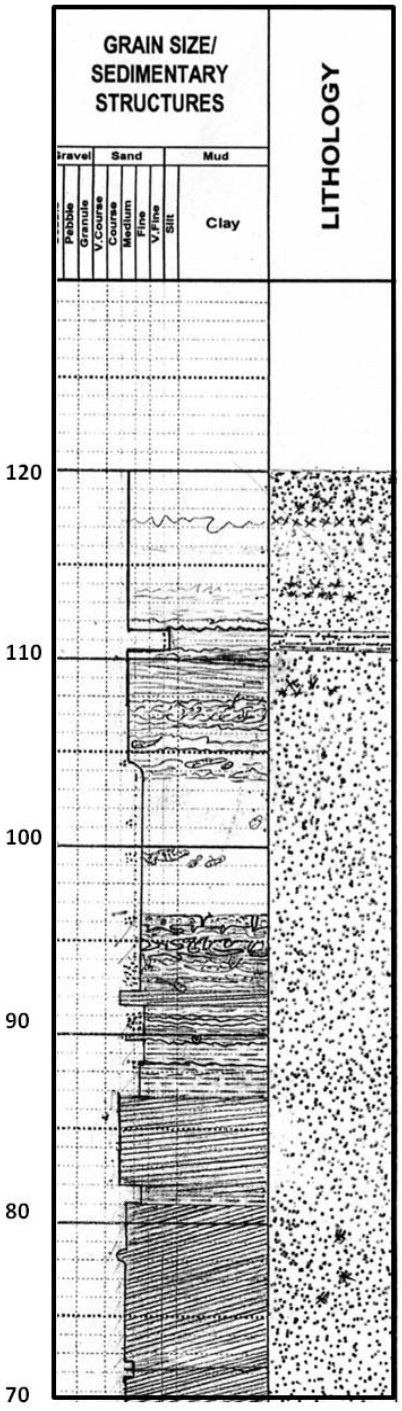
GRAIN SIZE/
SEDIMENTARY
STRUCTURES
LITHOLOGY
Sand
Mud
Pebble
Granule
V.Course
Course
Medium
Fine
V.Fine
Silt
Clay
120
110
100
90
80
70

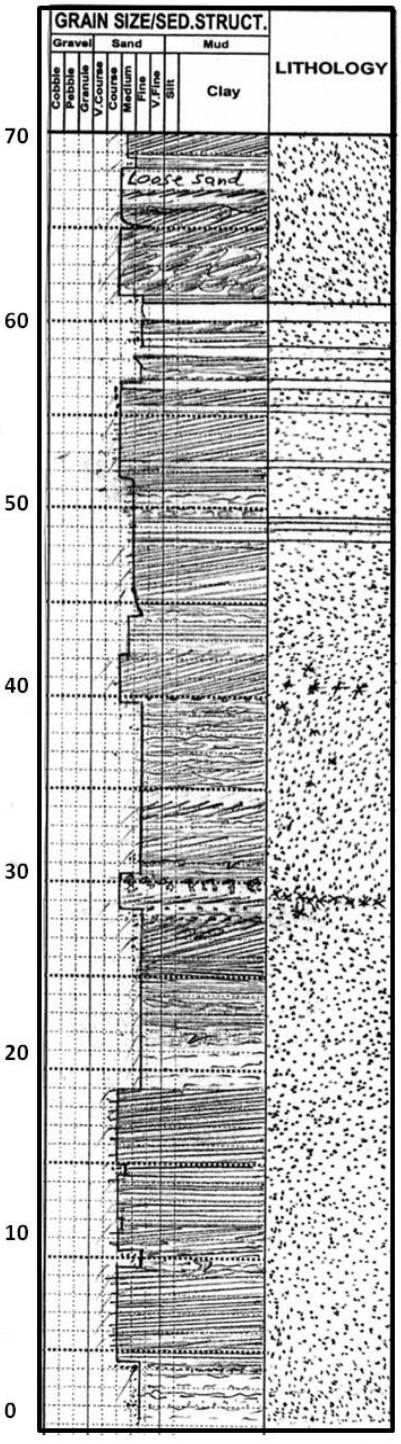
GRAIN SIZE/SED.STRUCT.
Gravel
Sand
Mud
LITHOLOGY
Cobble
Pebble
Granule
V.Course
Course
Medium
Fine
V.Fine
Silt
Clay
Loose Sand
70
60
50
40
30
20
10
0

Well B1

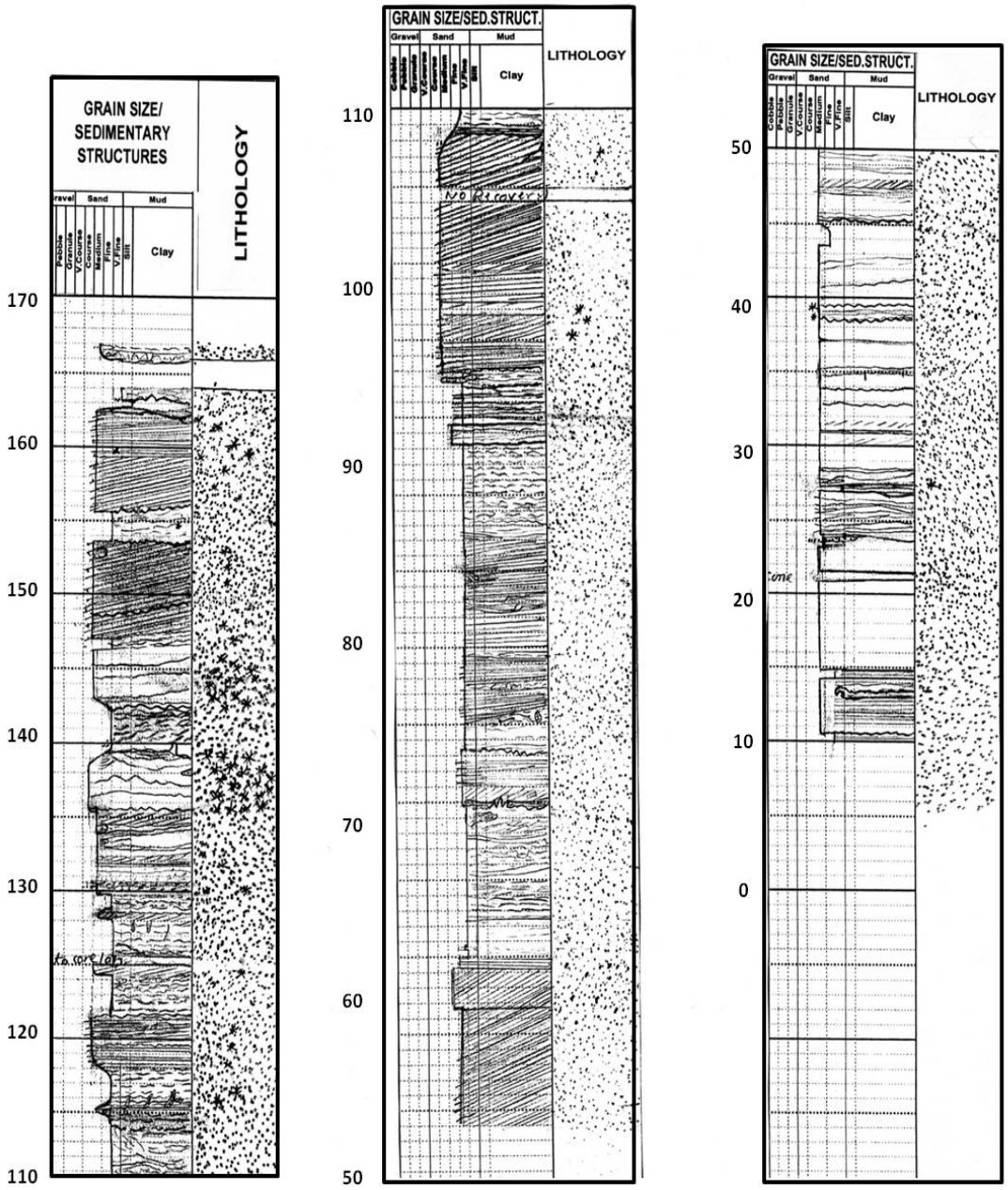
GRAIN SIZE/ SEDIMENTARY STRUCTURES
LITHOLOGY
Gravel
Sand
Mud
Clay
170
160
150
140
130
120
110
GRAIN SIZE/SED.STRUCT.
LITHOLOGY
110
100
90
80
70
60
50
GRAIN SIZE/SED.STRUCT.
LITHOLOGY
50
40
30
20
10
0

Well C1

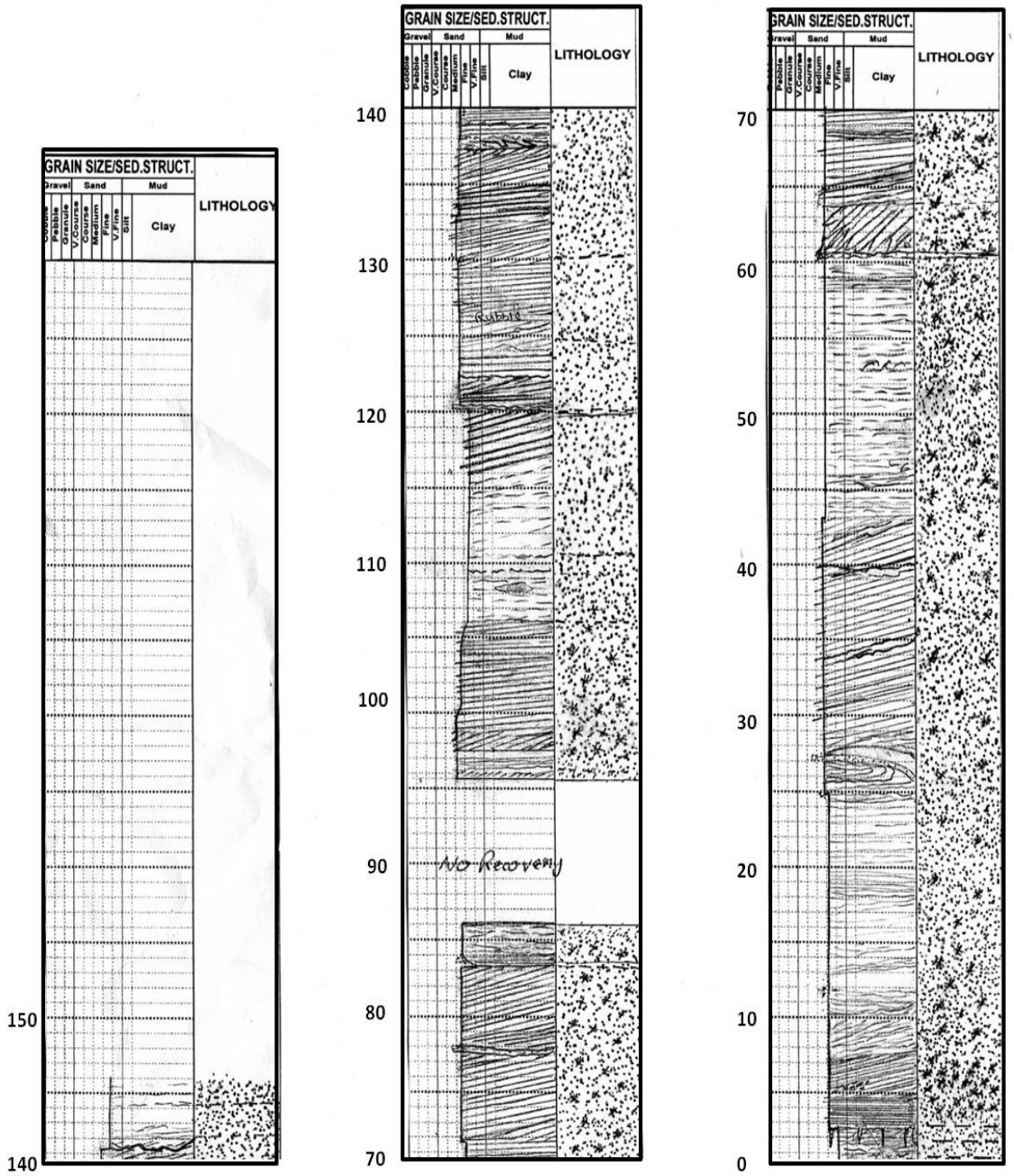
GRAIN SIZE/SED.STRUCT.
Gravel
Sand
Mud
Cobble
Pebble
Granule
V.Course
Course
Medium
Fine
V.Fine
Silt
Clay
LITHOLOGY
140
130
120
110
100
90
80
70
150
140
70
60
50
40
30
20
10
0
Rubble
No Recovery

Well D1

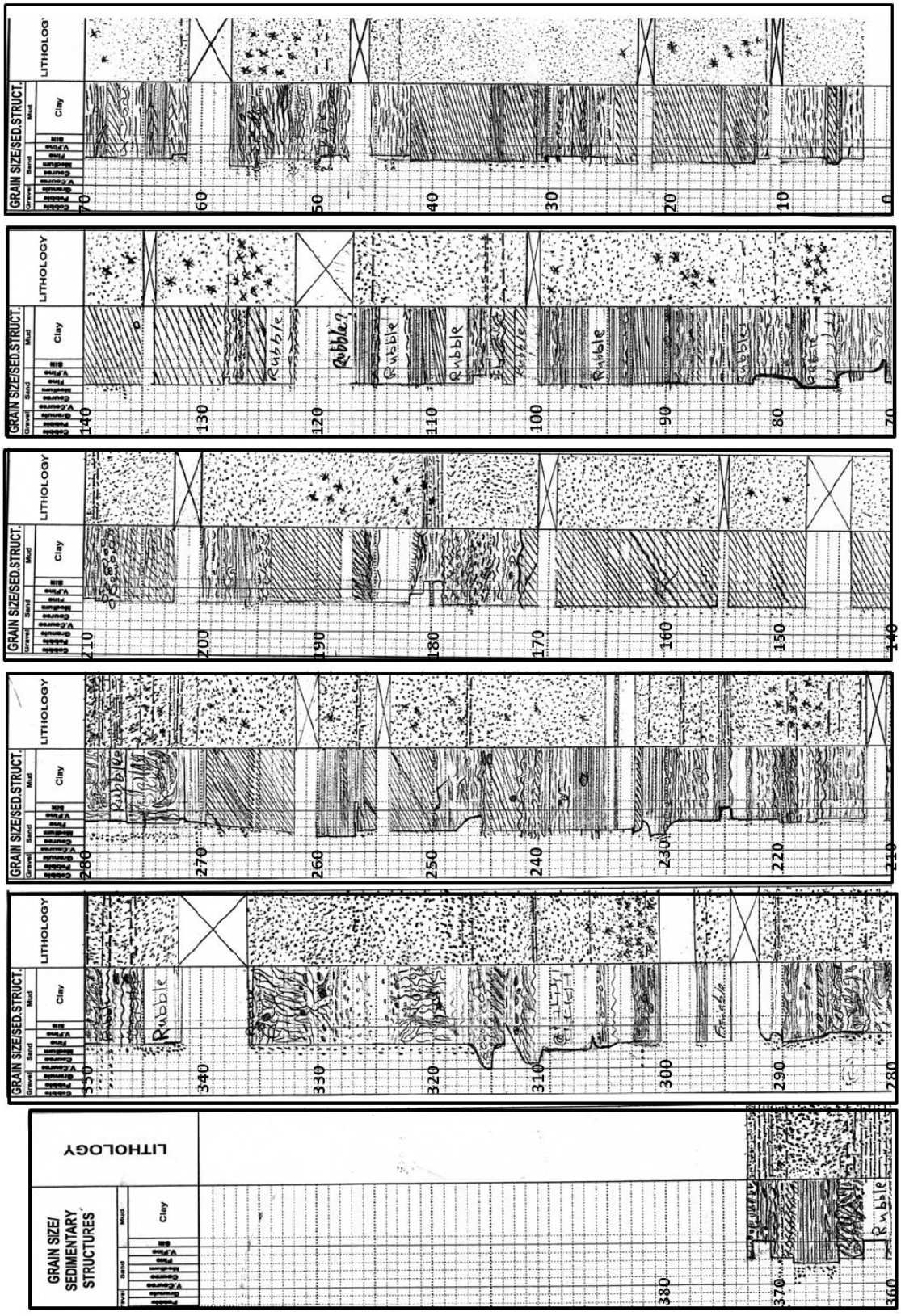
GRAIN SIZE/SED.STRUCT.
LITHOLOGY
Gravel
Sand
Mud
Clay
Rubble
70
60
50
40
30
20
10
0
140
130
120
110
100
90
80
70
210
200
190
180
170
160
150
140
280
270
260
250
240
230
220
210
350
340
330
320
310
300
290
280
380
370
360
GRAIN SIZE/ SEDIMENTARY STRUCTURES
LITHOLOGY

Sedimentological core log legend


Irregular Crinkly lamination

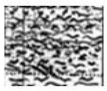
Disrupted Crinkly lamination


Over-steepened bedding (slump)


Crinkly lamination with desiccation cracks

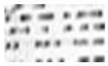
Coarse sand lamination

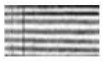
Flat lamination


Low-angle lamination

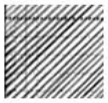
High-angle cross lamination


Grain size-segregated cross lamination

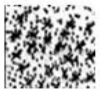
Spherical concretions


Rooted horizons


Slumps (dune toe)


Wispy lamination


Climbing ripples


Stylolites


Soft sediment deformation

APPENDIX 2

IMAGE LOG DATA

Representative Image log intervals from each well used in this study

Field A, Well A1

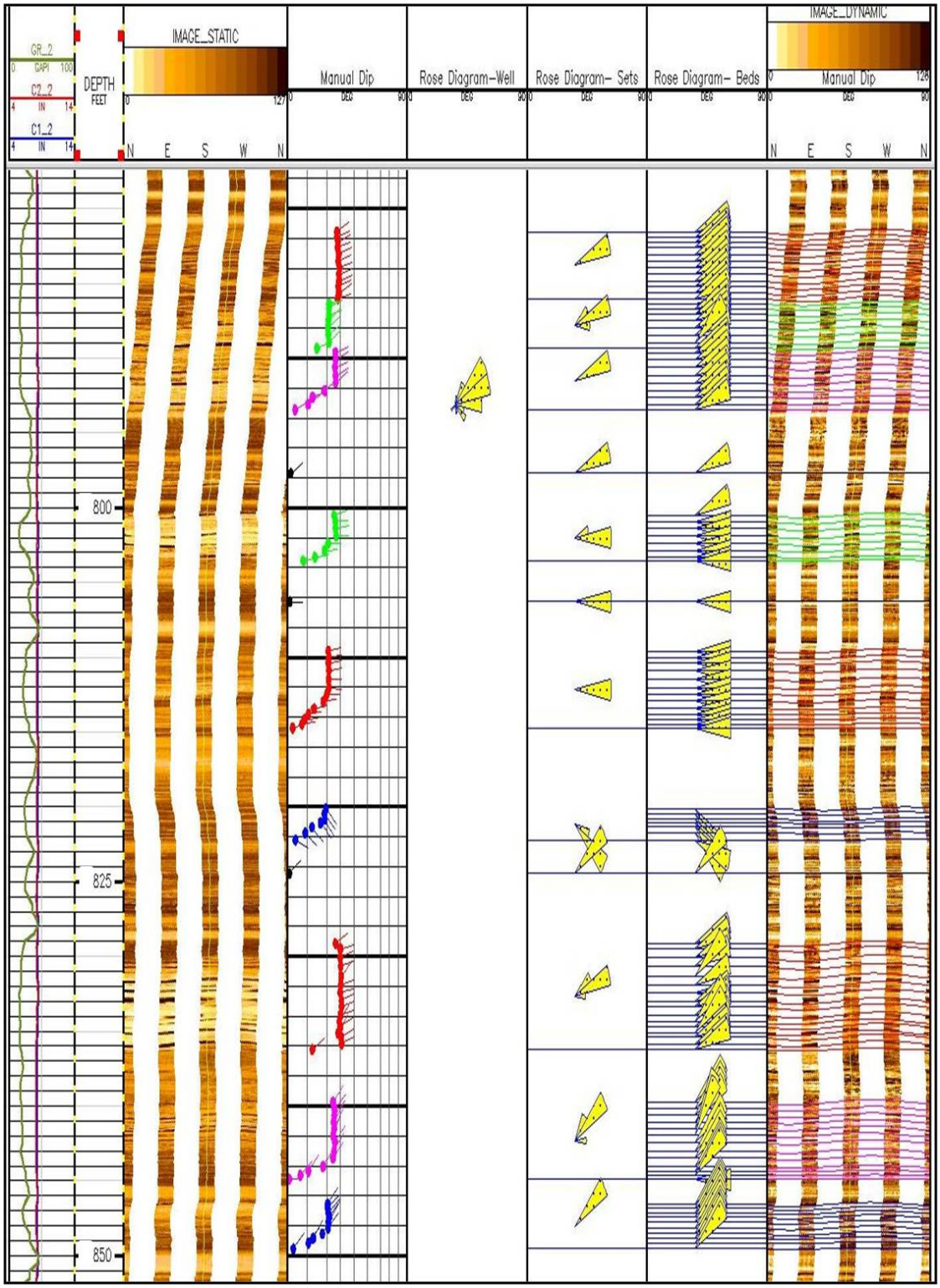

Field A, Well A2

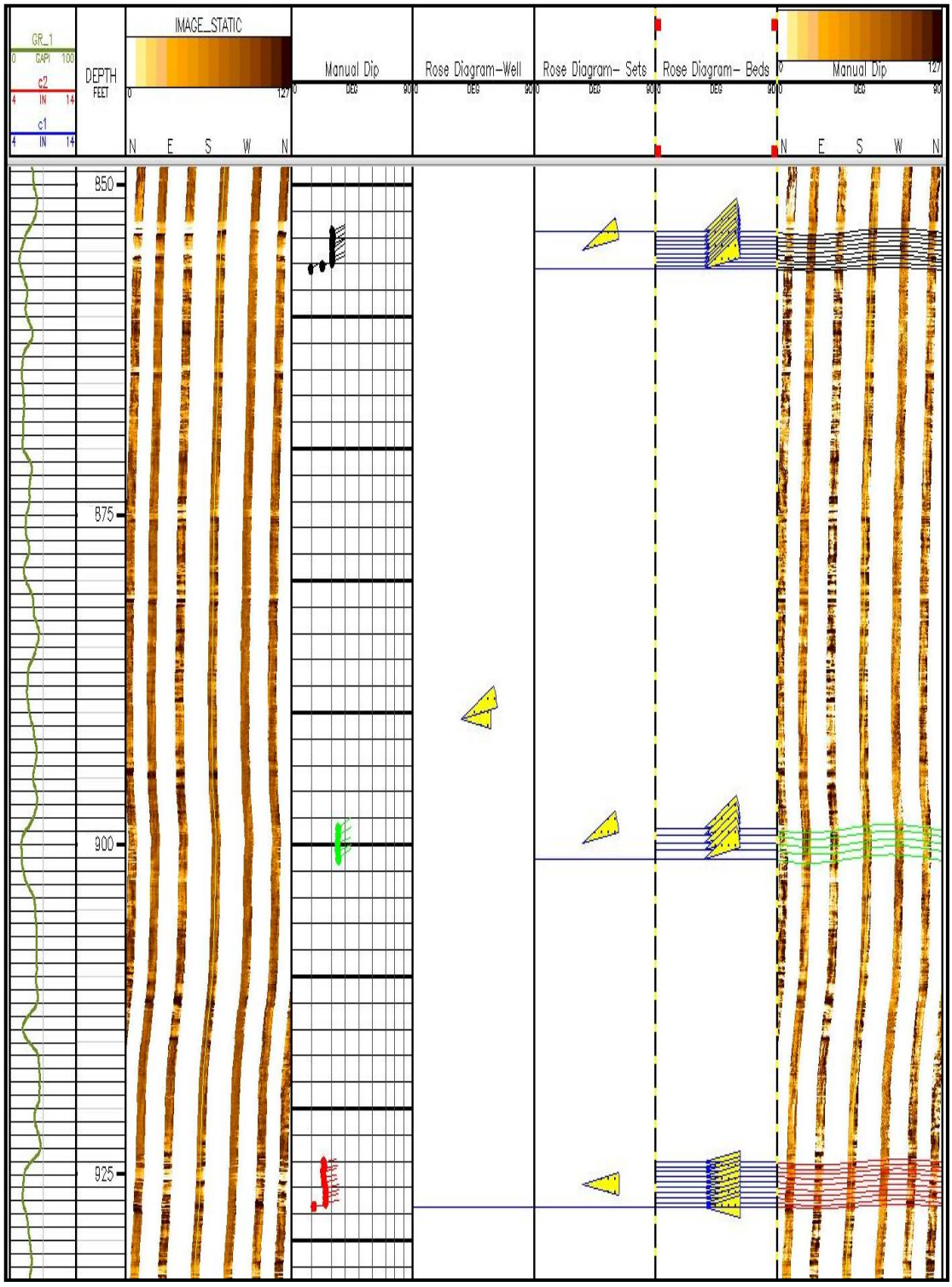

Field A, Well A3

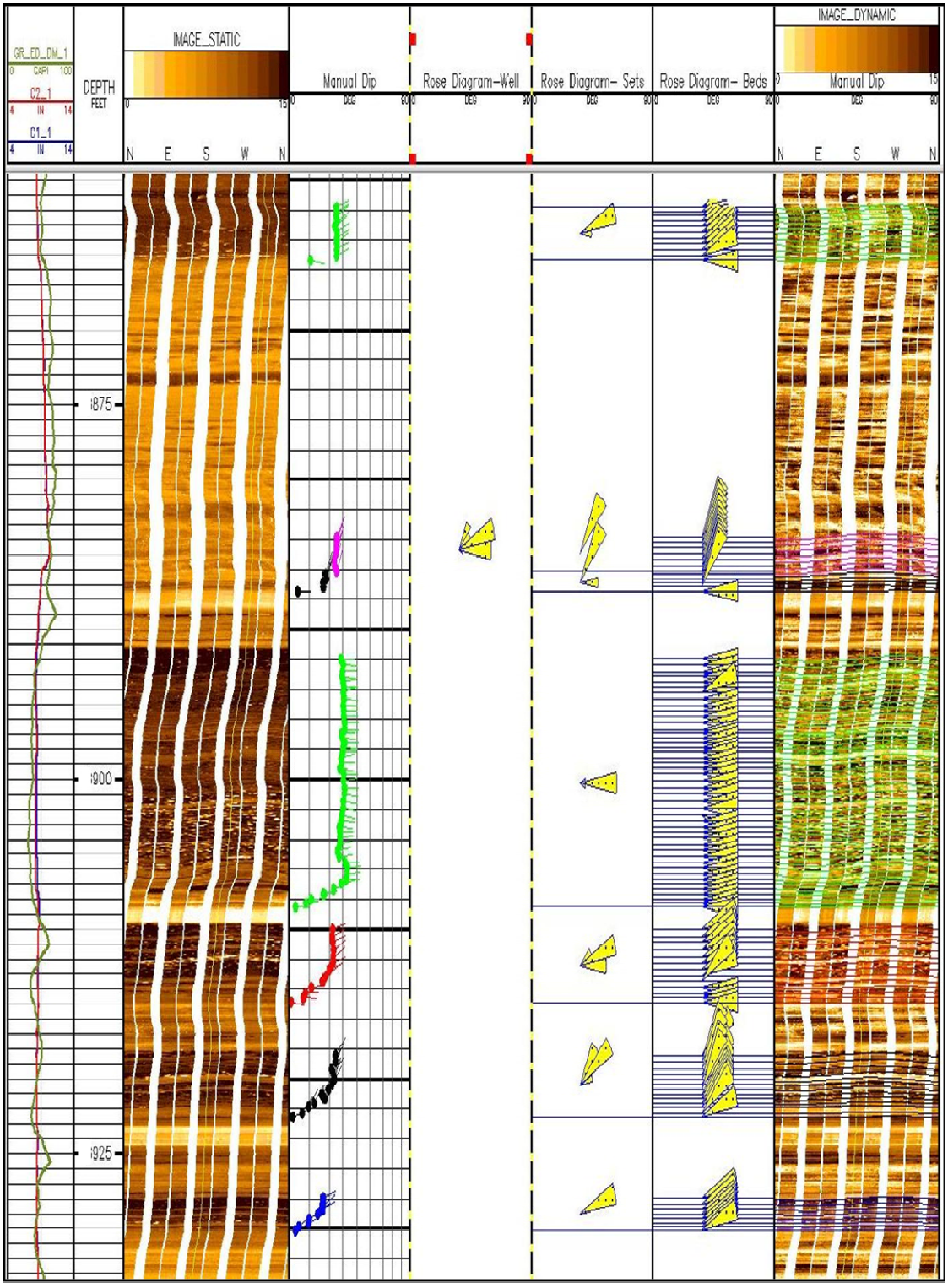

Field A, Well A4

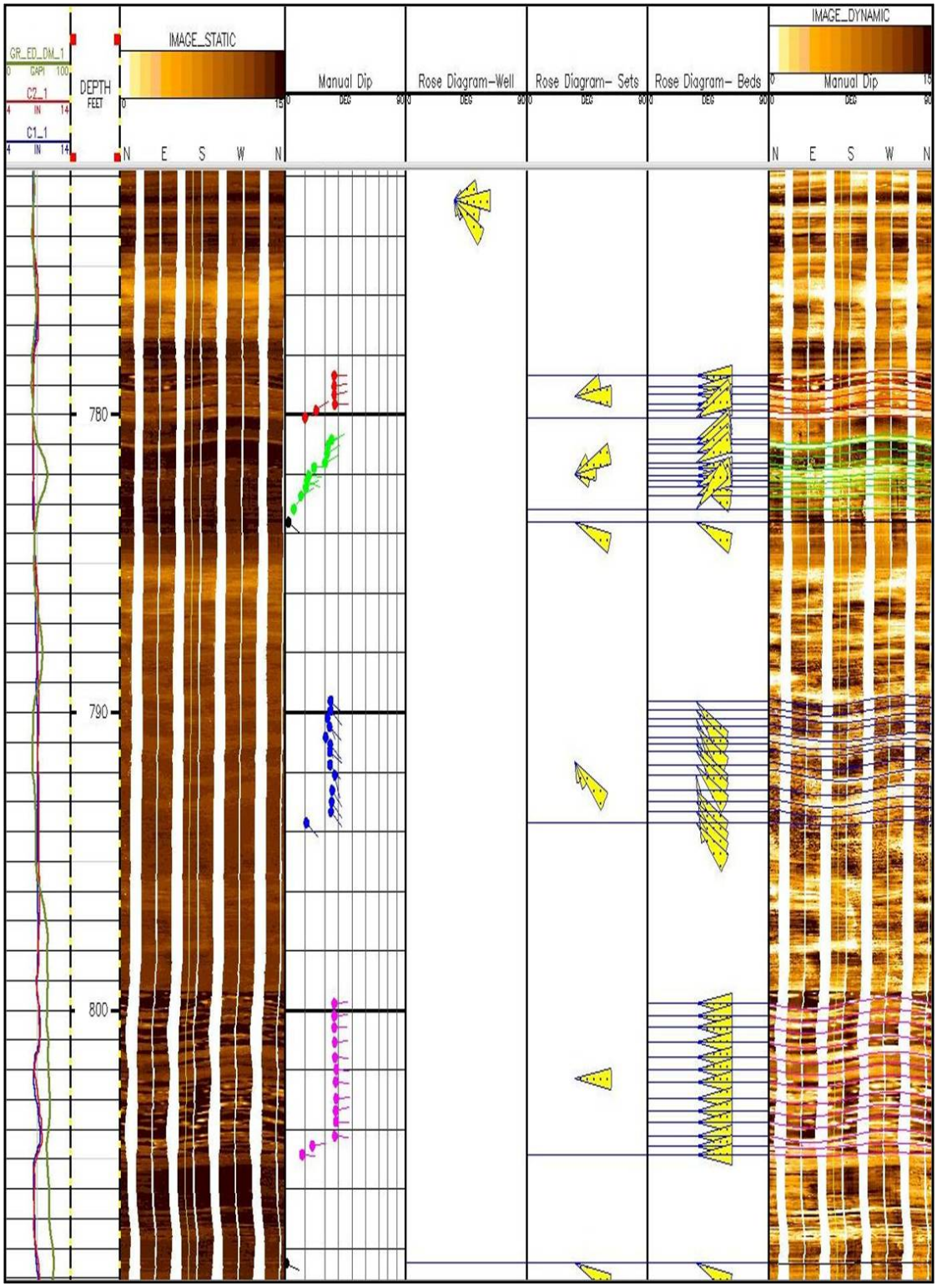

Field A, Well A5

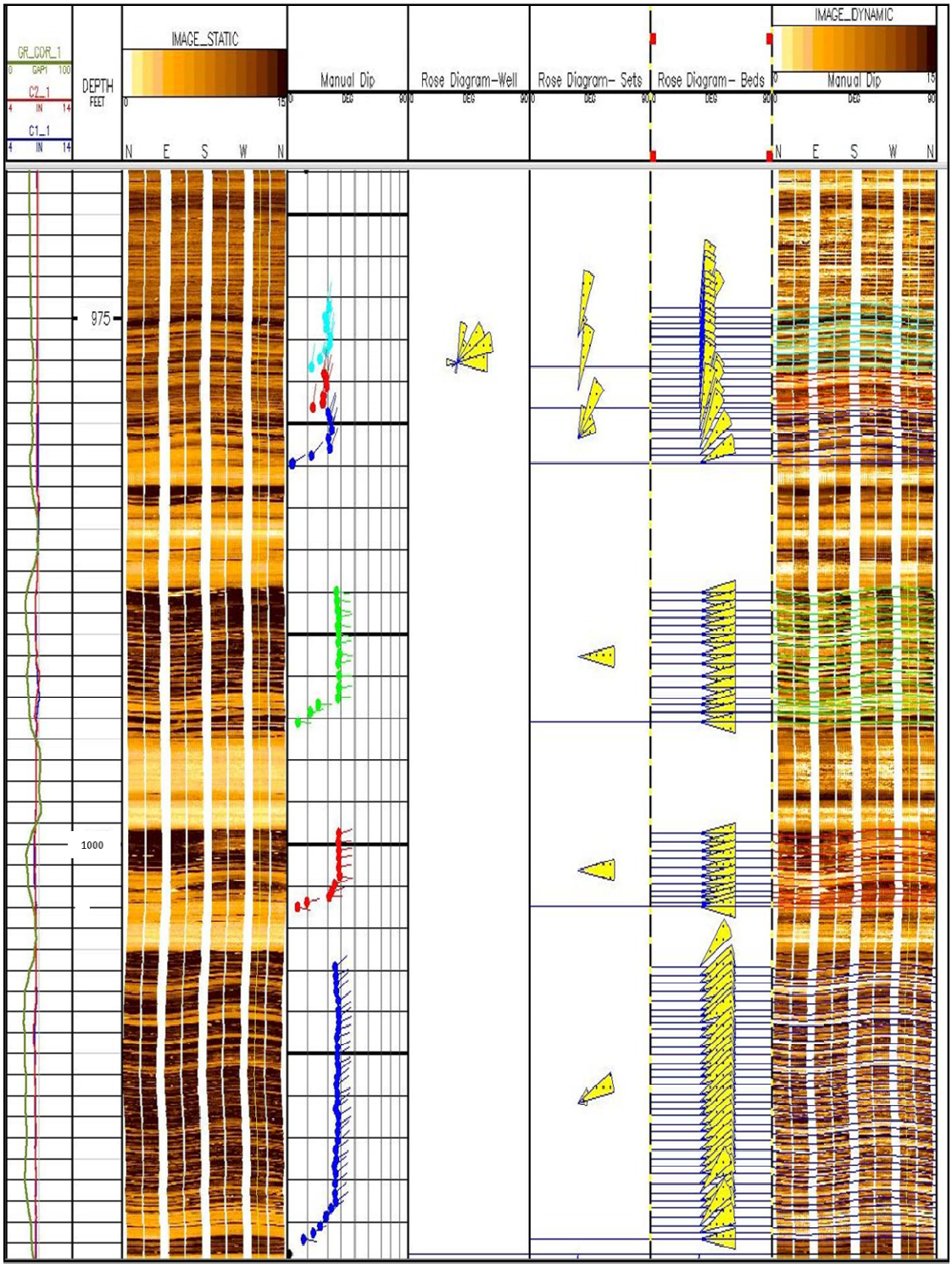

Field A, Well A6

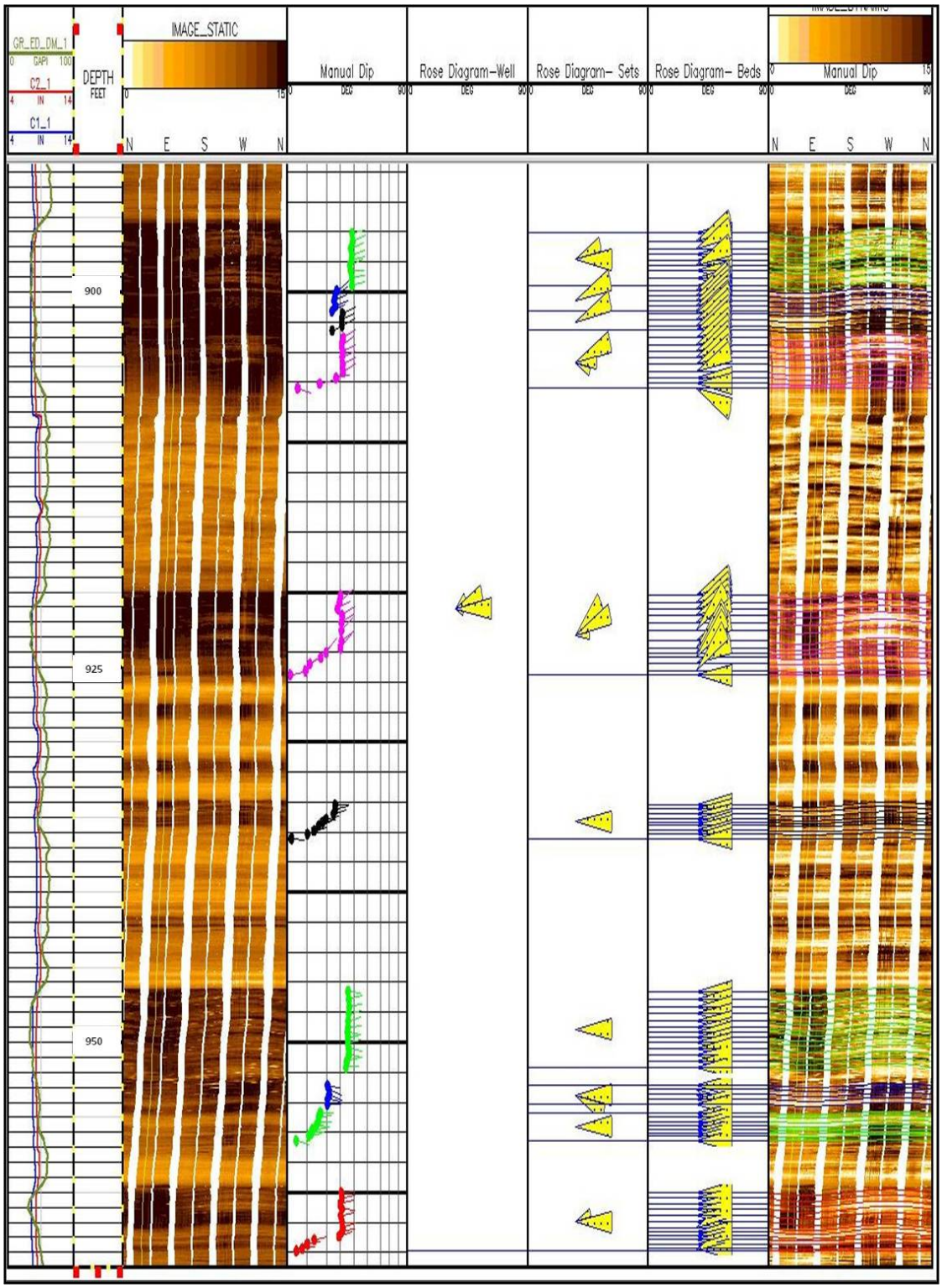

Field B, Well B1

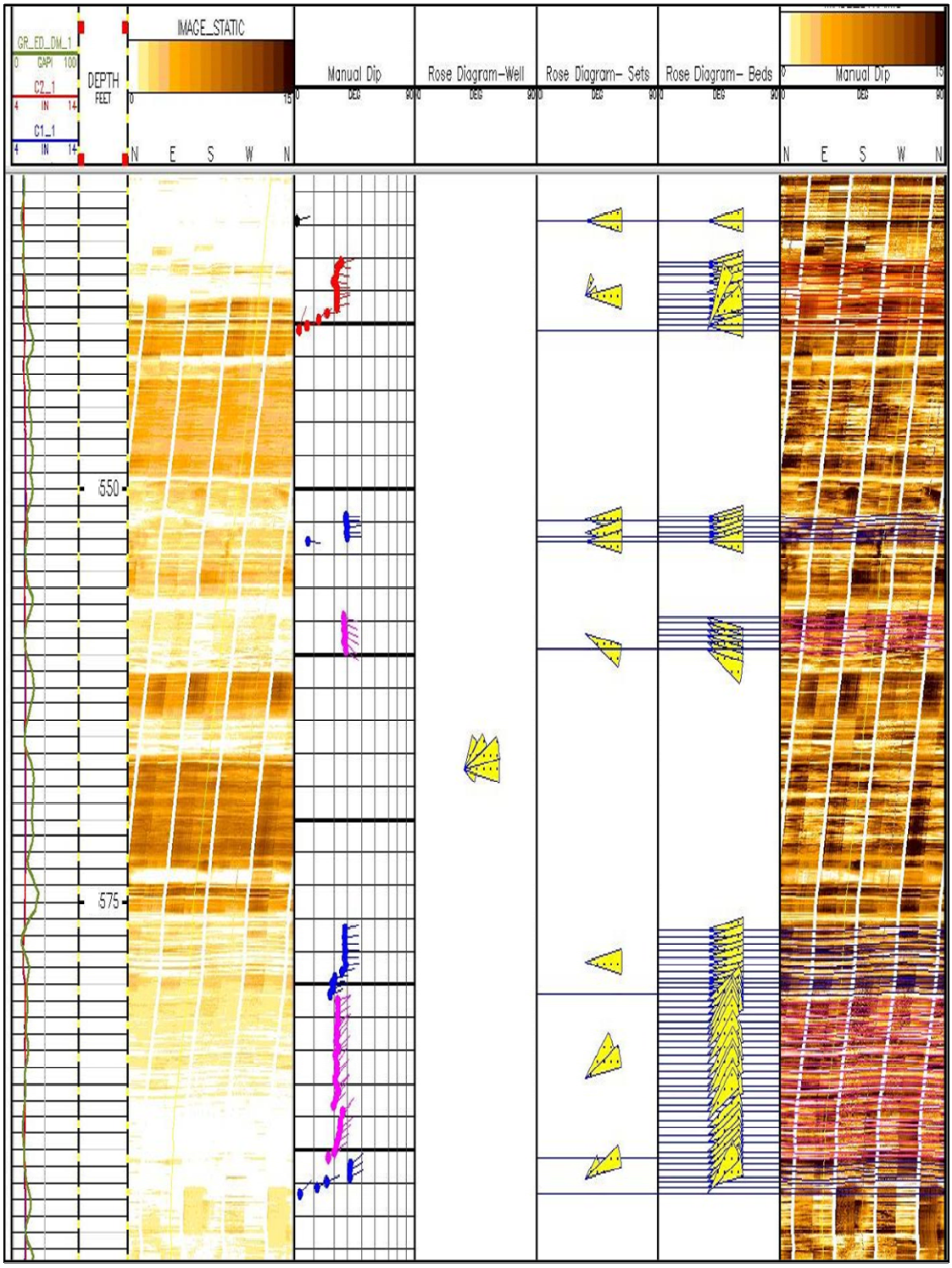

Field B, Well B2

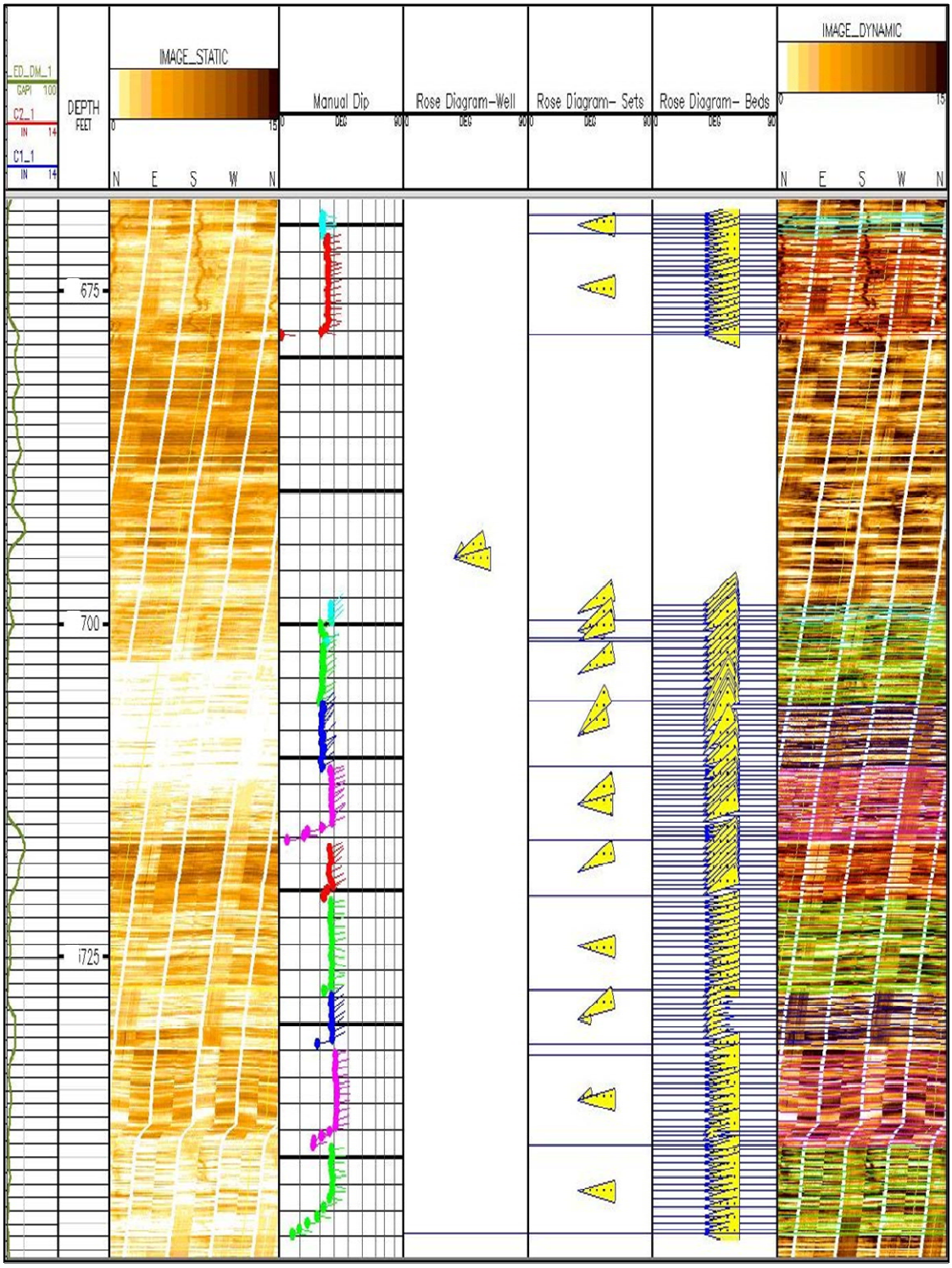

Field B, Well B3

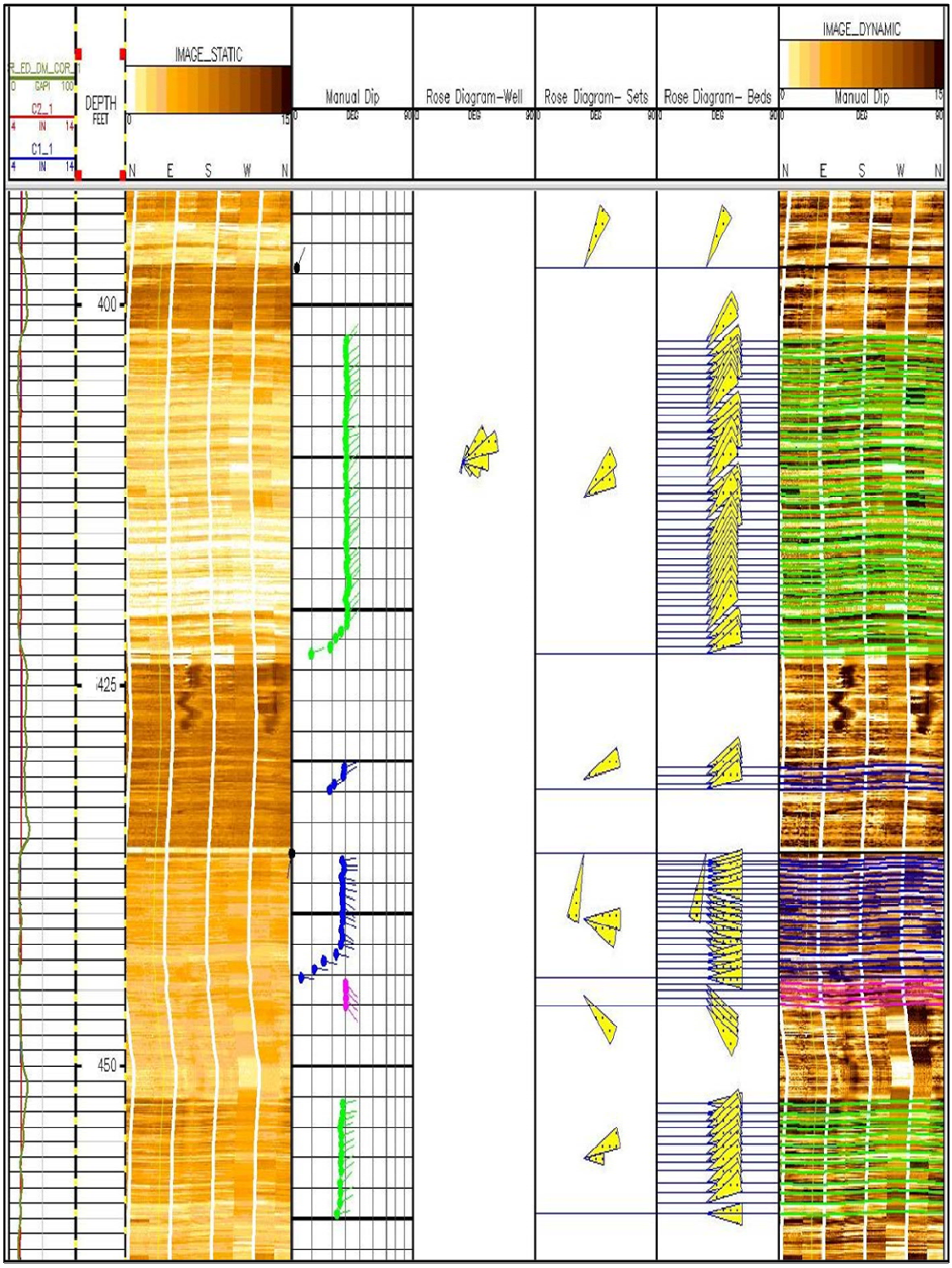

Field B, Well B4

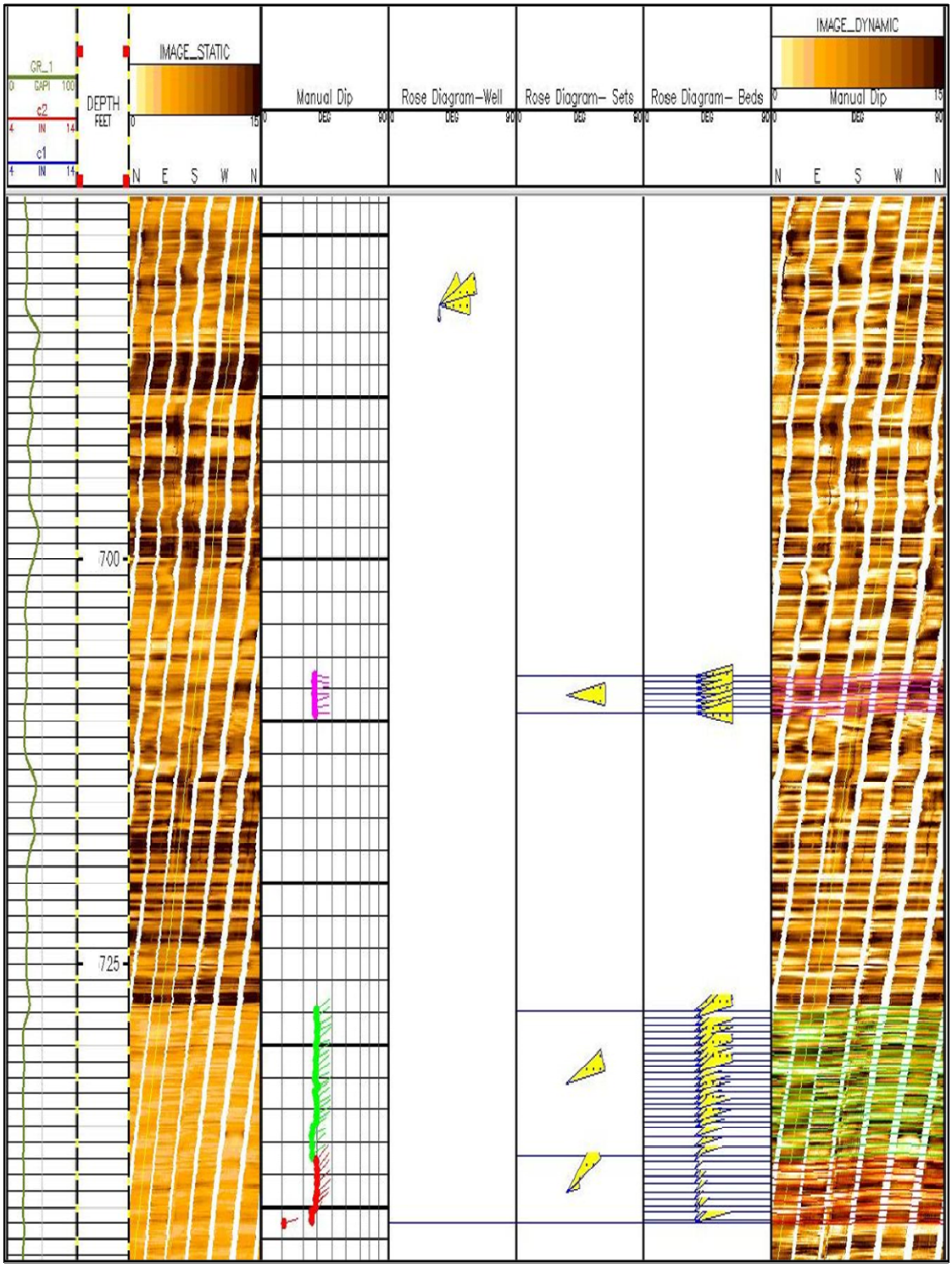

Field B, Well B5

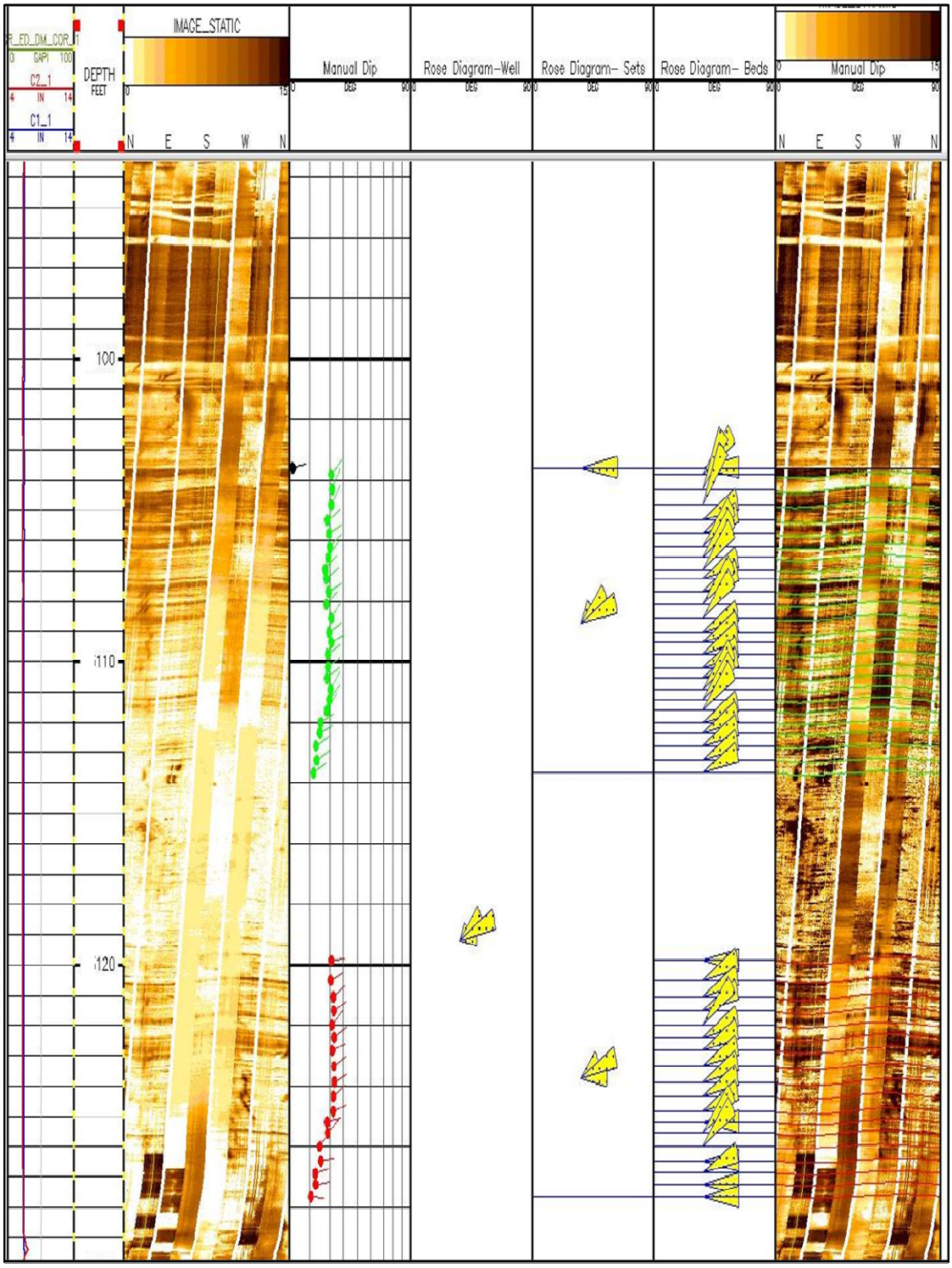

Field C, Well C1

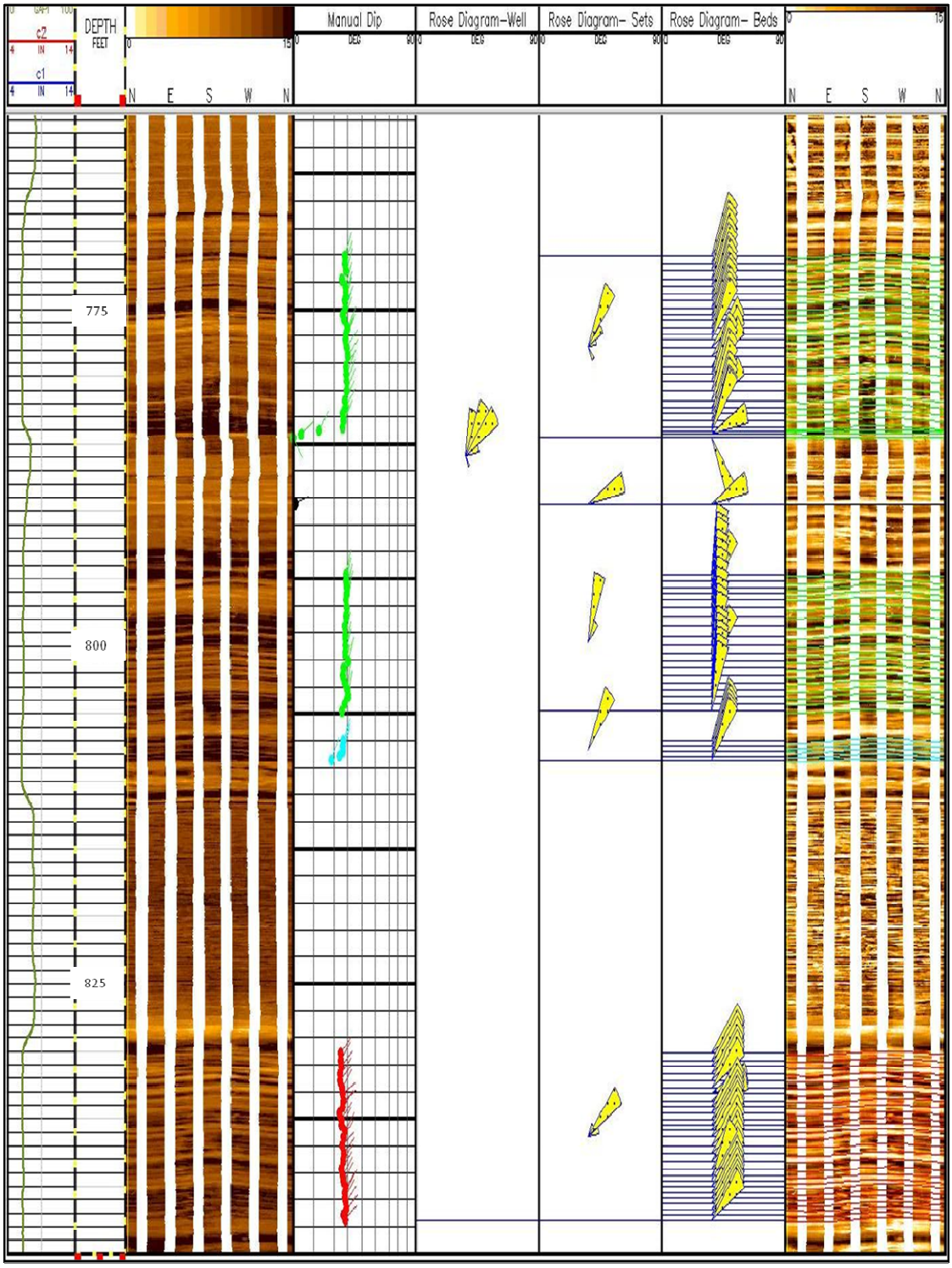

Field C, Well C2

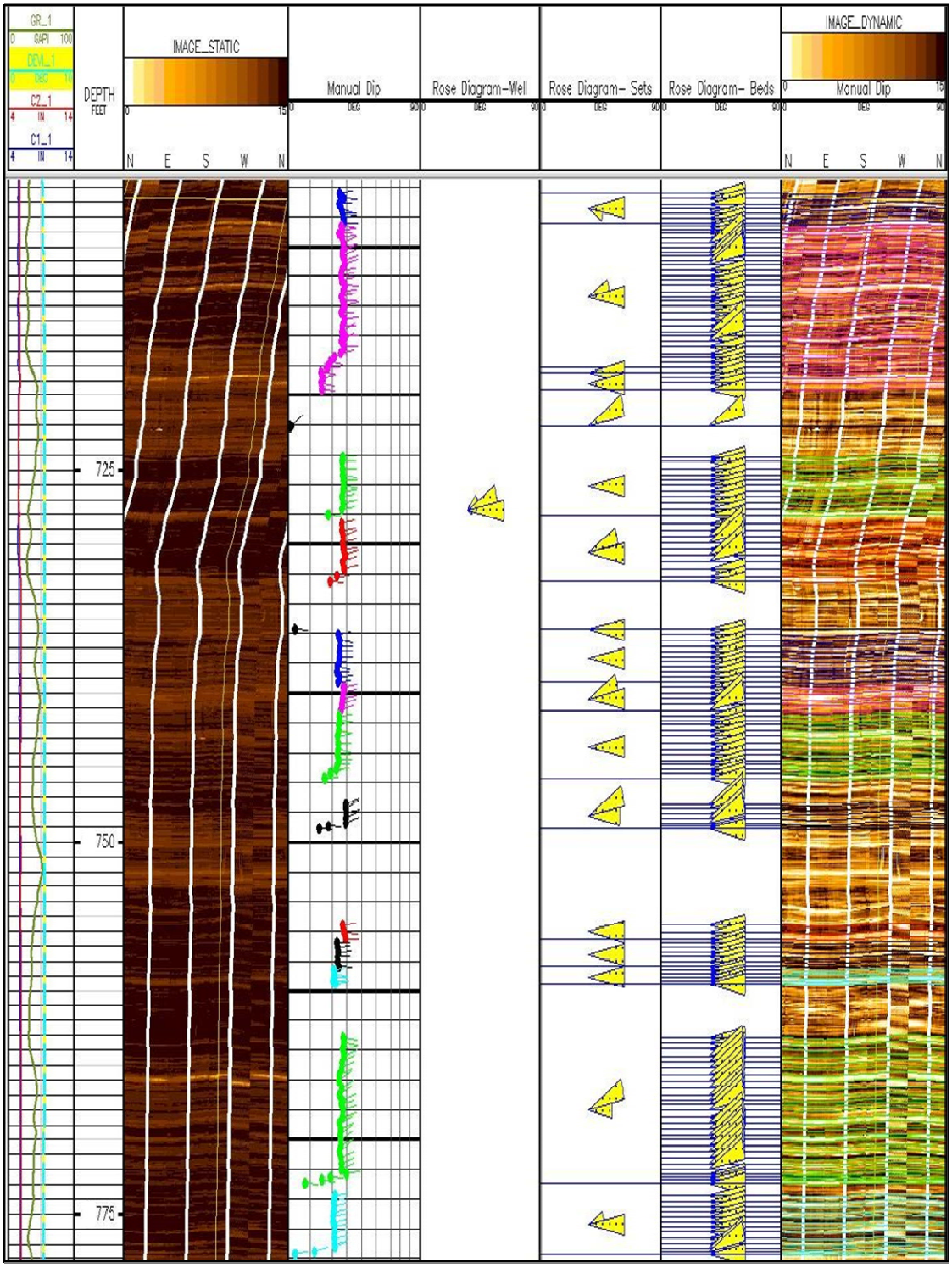

Field C, Well C3

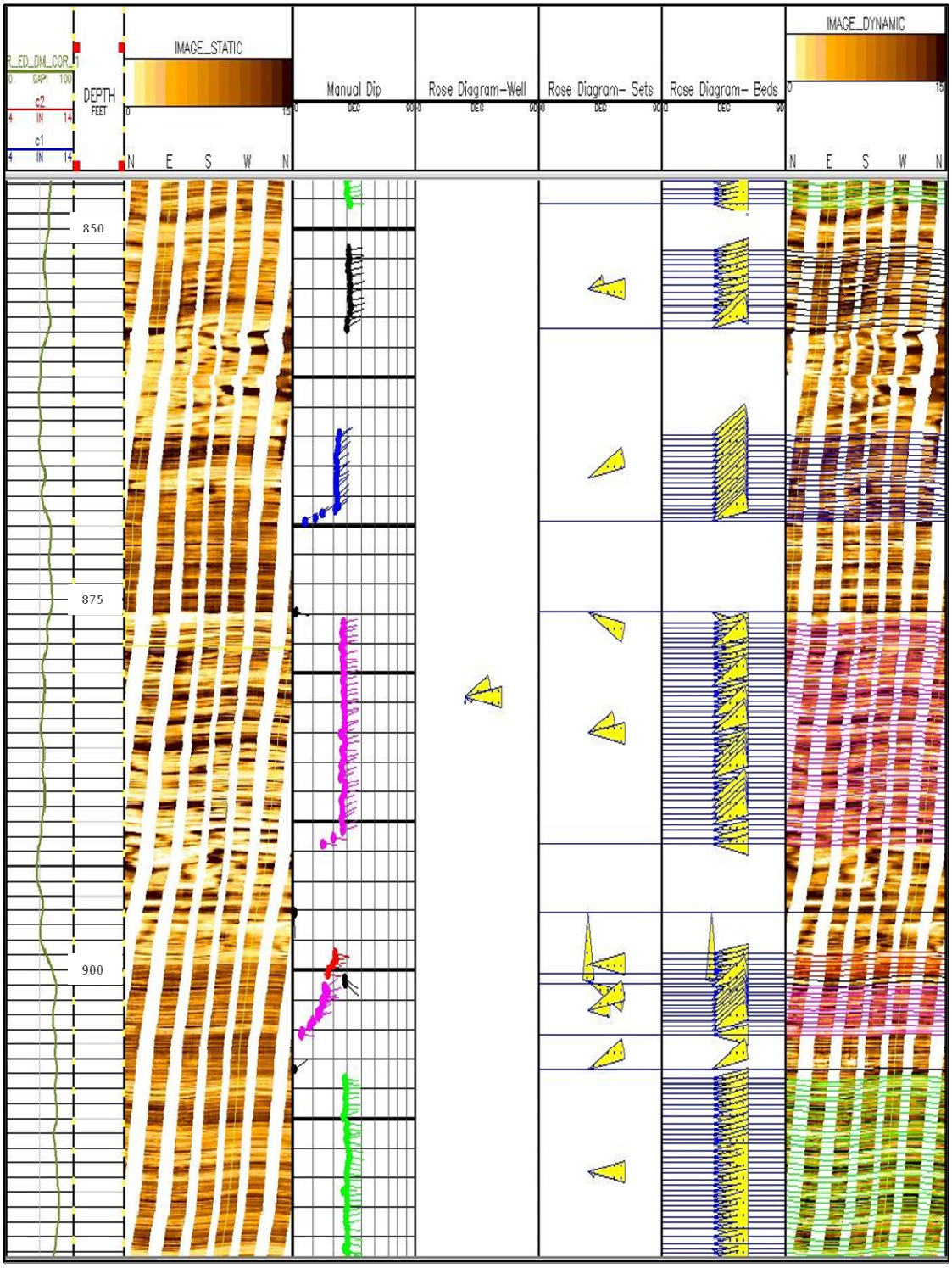

Field C, Well C4

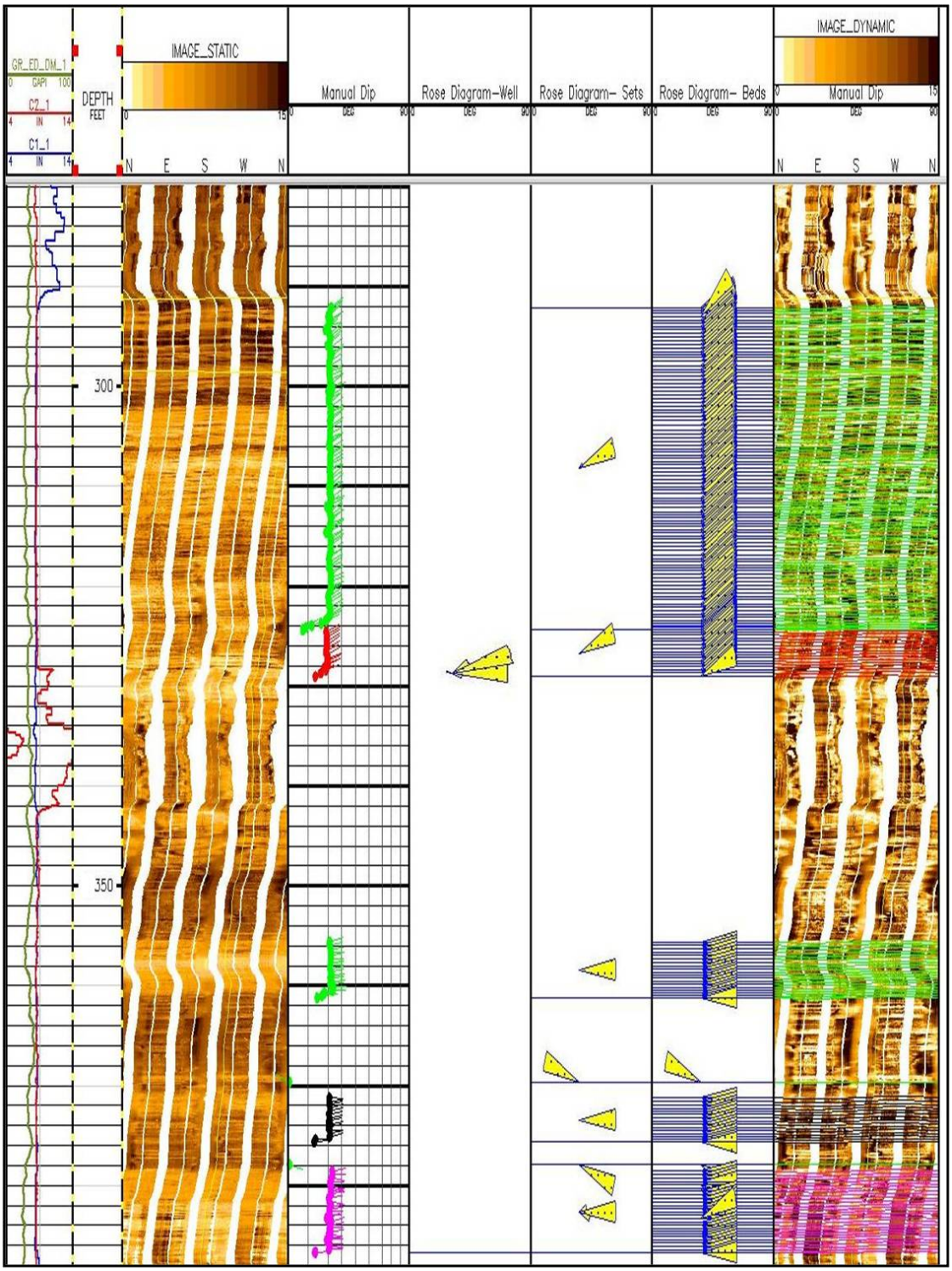

Field C, Well C5

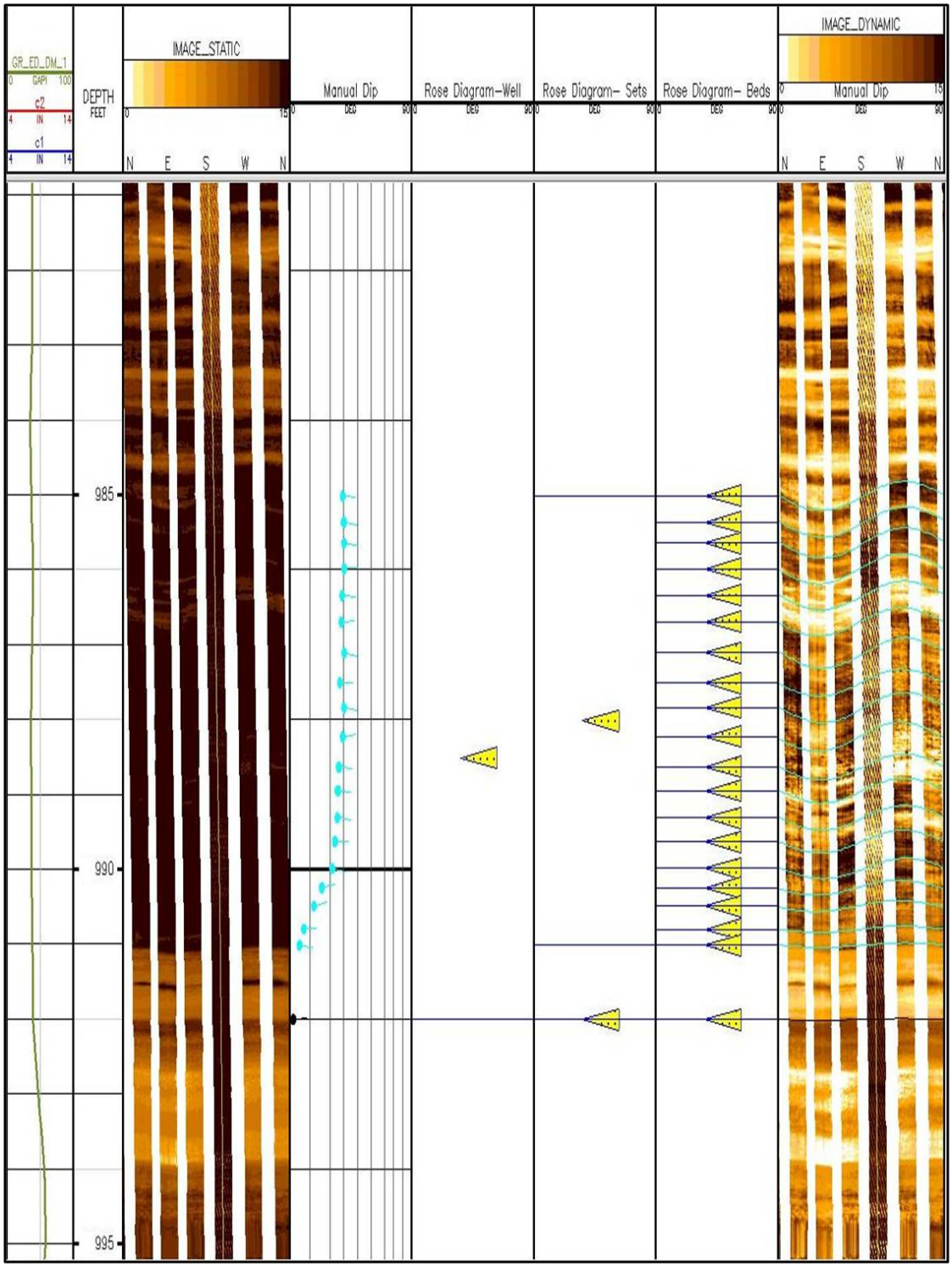

Field D, Well D1

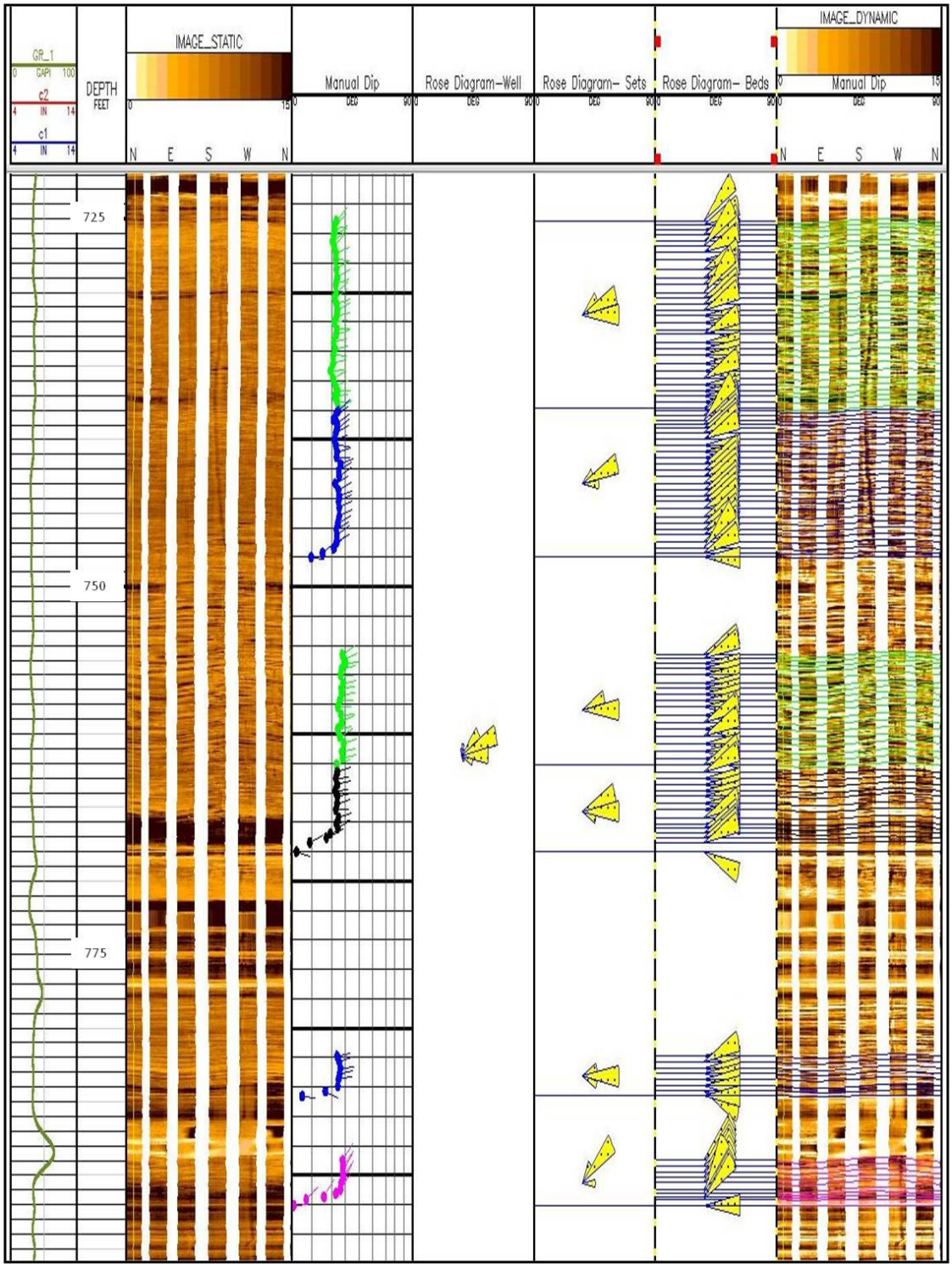

Field D, Well D2

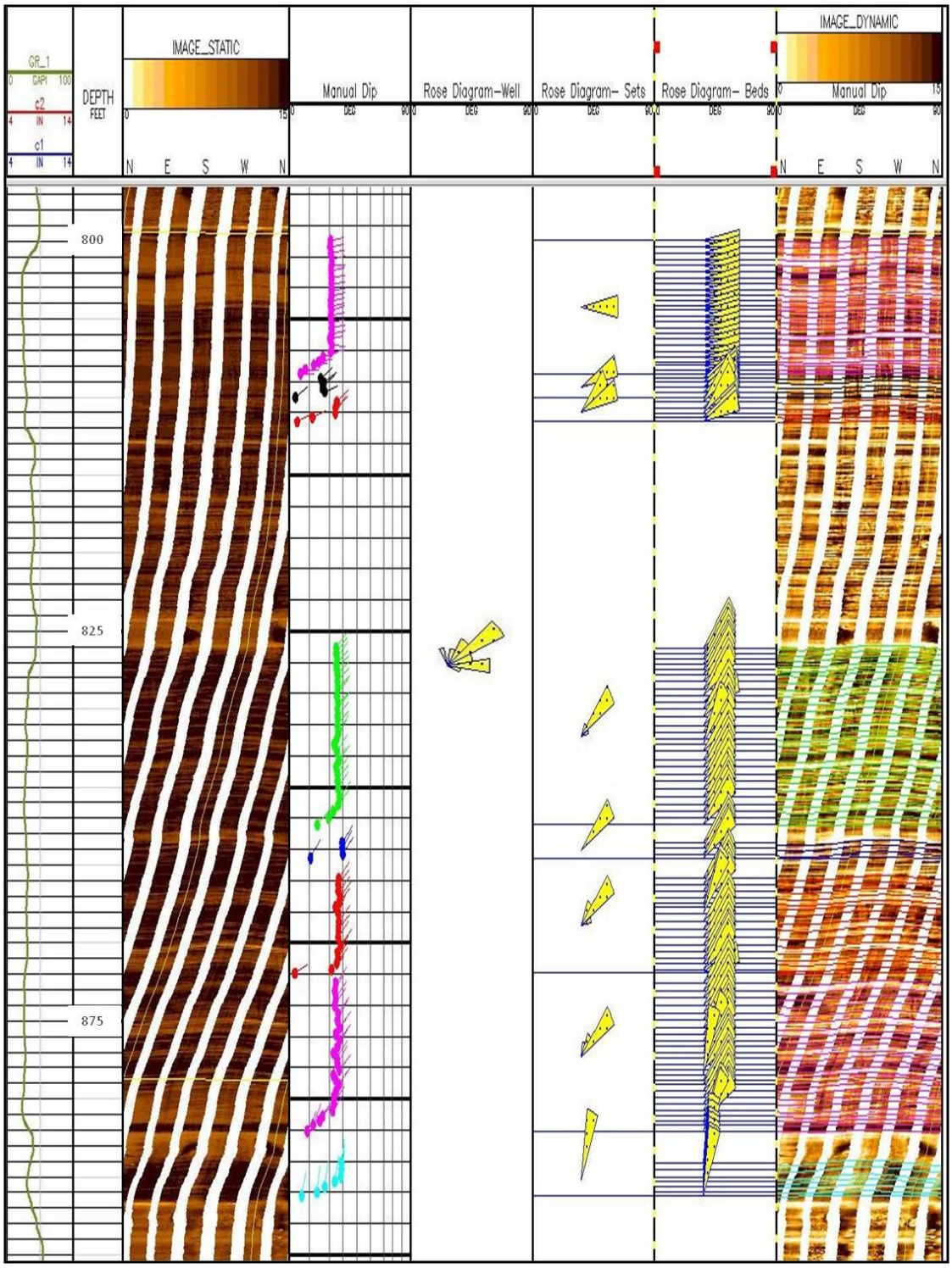

Field D, Well D3

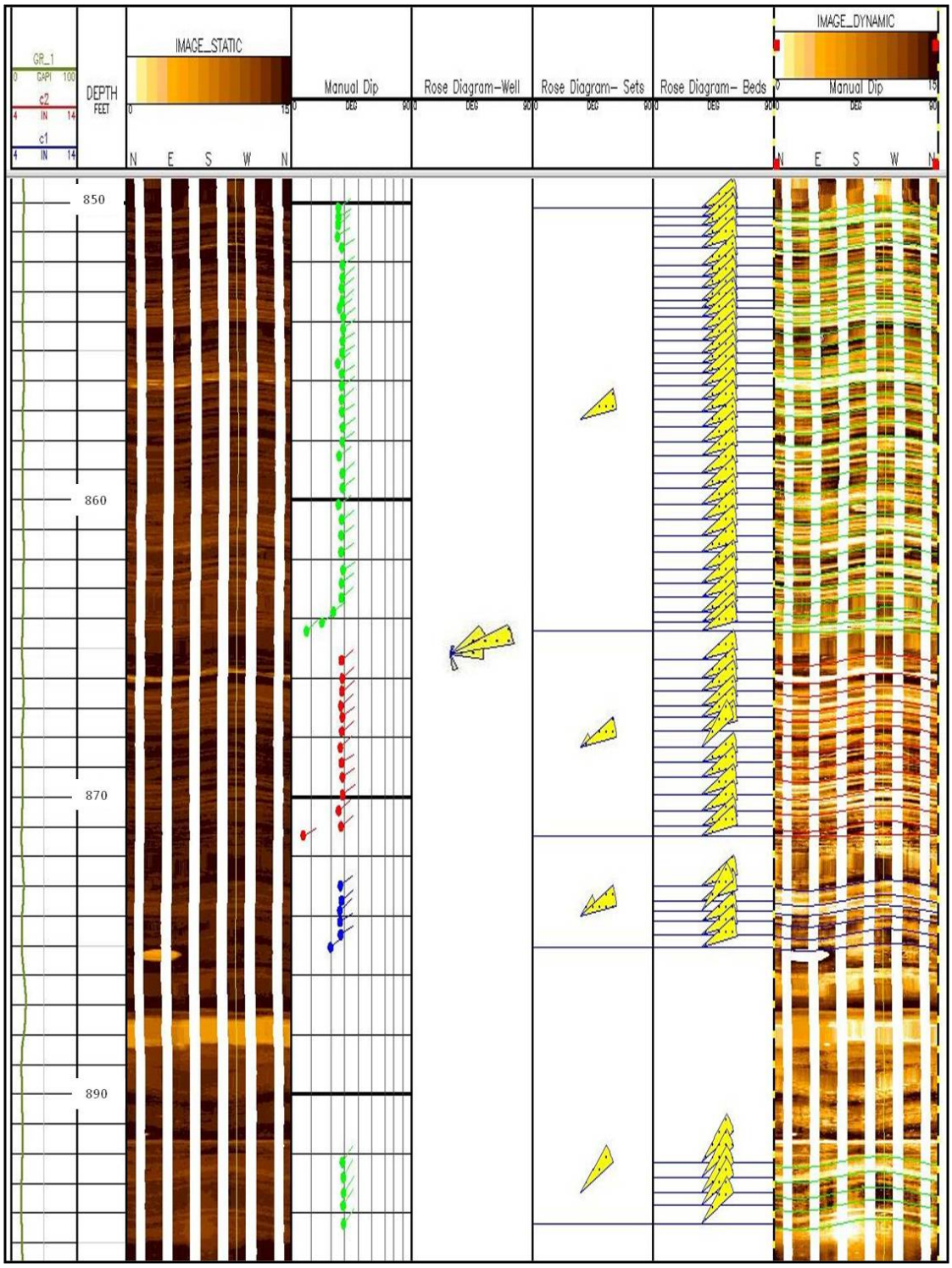

Field D, Well D4

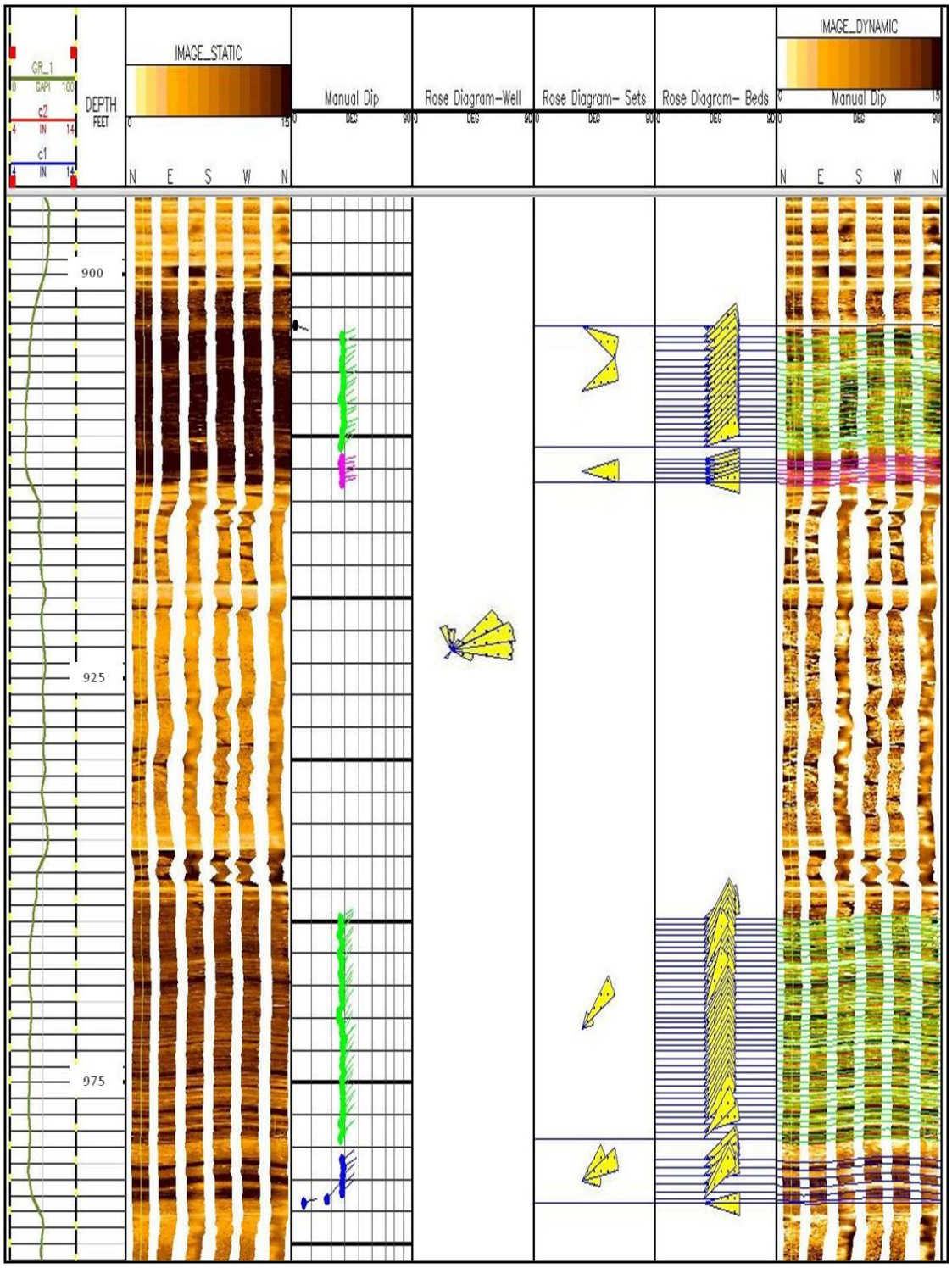

Field D, Well D5

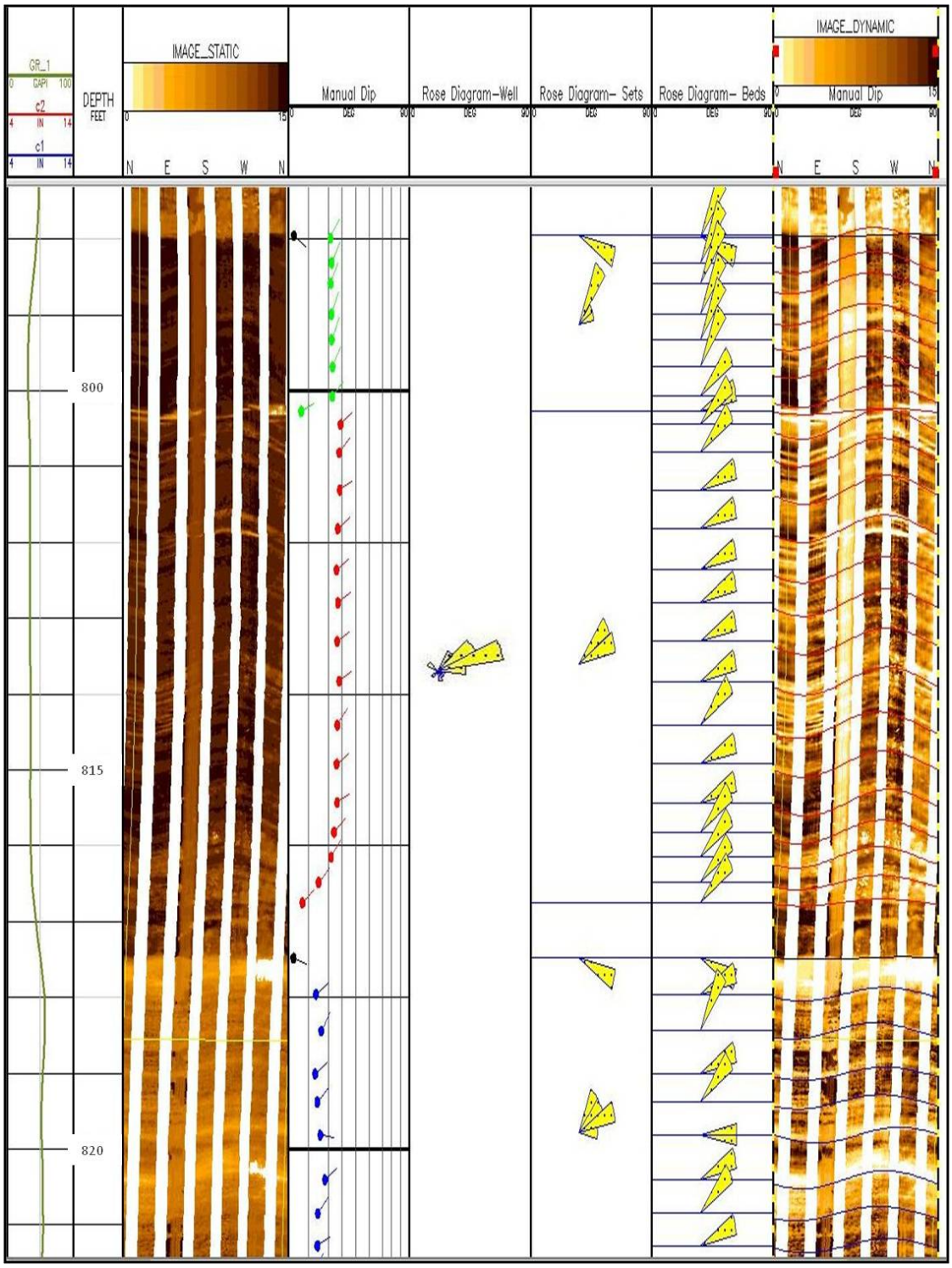

LIST OF REFERENCES

Adams, J., Bourke, L, and Buck, S., 1990, Integrating Formation MicroScanner images with core: Schlumberger, Oilfield Review, v. 2, no. 1, January, p. 52-65.

Adams, J., L. Bourke, and R. Frisinger, 1987, Strategies for dipmeter interpretation: Part 2: The Technical Review, v. 35, p. 20–31.

Adams, J., and Patron, J., 1979, S*ebkha-dune deposition in the Lyons Formation (Permian) northern Front Range, Colorado: Mountain*, Geol., v. 16, p. 45-57.

Al-Qassab, H.M., M.A. Al-Khalifa, G. Aktas, J. Fitzmaurice, Z.A. Al-Ali and P.W. Glover 2001. *Cross-discipline integration in reservoir modelling: the impact of fluid flow simulation and reservoir management.* The Saudi Aramco Journal of Technology, Summer Issue p. 44-57.

Al-Husseini, M.I. 2004. *Pre-Unayzah unconformity, Saudi Arabia.* GeoArabia Special Publication 3, Gulf PetroLink, Bahrain, p. 15-59.

Ahlbrandt, T.S, and S. G. Fryberger, 1981, *Sedimentary features and significance of interdune deposits, in F. g. Ethridge and R. O. Flores (ed.), Recent and ancient nonmarine depositional environments: Models for exploration*: Soc. Econ. Paleontologists and Mineralogists Spec. Pub. 31, p. 293-314.

Ahlbrandt, T.S, and S. G. Fryberger, 1982, *Introduction to eolian deposits, Sandstone depositional environments. In: (ed.) Peter A. and Darwin Sprearing, Sandstone Depositional Environments*. AAPG, Mem. 31,P.11-47.

Aktas, G., and J. D. Cocker, 1996, Diagenetic and depositional controls on reservoir quality in Khuff and Unayzah sandstones, Hawtah trend, central Saudi Arabia: Geo ’94: The Middle East Petroleum Geosciences, v. 1, p. 44–52. *Saudi Arabia.* GeoArabia, Abstract, v. 5, no. 1, p. 11.

Aktas, G., M. Al-Khalifa and H. Al-Qassab 2000. *Sequence stratigraphy and reservoir architecture of Unayzah continental deposits, Hawtah trend, Saudi Arabia.* GeoArabia, Abstract, v. 5, no. 1, p. 11.

Allen, J. R. L., 1963, *The classification of cross-stratified units with notes on their origin*: Sedimentology, V. 2, p. 93-114.

Allen, J. R. L., 1968, *Current ripples: Their relation to patterns of water and sediment motion*: North Holland Publishing, Amsterdam, 433 p.

Allen, J. R. L., 1970, *Physical processes of sedimentation*: Georg Allen & Unwin, London, 248 p.

Bagnold, R. A. 1941. *The Physics of Blown Sand and Desert Dunes. Methuen,* London, Chapman and Hall, 265 p.

Bagnold, R. A. 1954. *Experiments on gravity-free dispersion of large solid spheres in a Newtonian fluid under shear*. Proceeding of the Royal Society, 255 A, p. 49-63.

Beydoun, Z.R. 1991. *Arabian plate hydrocarbon geology and potential: A plate tectonic approach*. A. Studies in Geology 33, 77 p.

Bigarella, J. J., 1972. E*olian environments, their characteristics, recognition and importance: In recognition of ancient sedimentary environments. (Ed. J. K. Rigby and K. W. Hamblin)* Soc. Econ. Pal. Min. Sp. Publication no. 16, p. 12-62.

Bigelow, E. L., 1985a, *Making more intelligent use of log derived dip information. Part 1, Suggested guidelines*: The Log Analyst, v. 26, no. 1, p. 41–53.

Bigelow, E. L., 1985e, *Making more intelligent use of log derived dip information. Part 5, Stratigraphic interpretation*: The Log Analyst, v. 26, no. 5, p. 25–64.

Bourke, L. T., P. Delfiner, J. C. Trouiller, T. Fett, M. Grace, S. Luthi, O. Serra, and E. Standen, 1989, *Using Formation MicroScanner images*: The Technical Review, v. 37, no. 1, p. 16–40.

Breed. Carol S. and Grow, Teresa. 1979. *Morphology and distribution of dunes in sand seas observed by remote sensing*. In A Study of Global Sand Seas, E. McKee, ed., pp 253-304. Washington, U.S. Geological Survey Paper 1052.

Brinkman, R., 1933, *Ueber Kreuzschichlung ini deut-schen Buntsandsteinbecken: Nachr. von der Gessel-schatt der Wissensch. zu Gottingen, Math*. Phys. Kl. Fachtgruppe iv, no. 32.

Brookfield, Michael, 2011, *Aeolian processes and features in cool climates.* From: Martini, I. P., French, H.M. & Pe´rez Alberti, A. (eds) *Ice-Marginal and Periglacial Processes and Sediments.* Geological Society, London, Special Publications, 354, 241–258.

Carr-Crabaugh M., Hurley, N. F. and Carlson, J. 1996, *Interpreting eolian reservoir architecture using borehole images. In Pacht, J. A., Sheriff, R. E. and Perkins, B. F*. (eds) *Stratigraphic Analysis Utilizing Advanced Geophysical, Wireline, and Borehole Technology for Petroleum Exploration and Production*. (17th Annual Research Conference Proceedings). Society of Sedimentary Geology Foundation, Gulf Coast Section, p. 39-50.

Carr, D. L., R. A. Johns, R.Y. Elphick, and L. S. Foulk, 1997, *High-resolution reservoir characterization of midcontinent sandstones using wireline resistivity imaging, Boonsville (Bend Conglomerate) gas field, Fort Worth Basin, Texas*: The Log Analyst, v. 38, no. 6, p. 54–70.

Chan, M. A., Kocurek, G. 1988. *Complexities in eolian and marine interactions: processes and eustatic controls on erg development*. P. 283-300.

Clemmensen, L. B., 1988. *Aeolian morphology preserved by lava cover, the Precambrian Mussartut Member, Eriksfjord Formation, South Greenland*. Bulletin. Geol. Soc. Den. V. 37, p. 105-116.

Collinson, J.D., 1978, *Vertical sequence and sand body shape in alluvial sequences, in Miall, A.D., Fluvial Sedimentology*: Canadian Society of Petroleum Geologists Memoir 5, p. 577-586.

Collinson, J.D. (1986). *Deserts, In: H.G. Reading. (Eds.) Sedimentary Environments and Facies*, 2nd edition. Blackwell, Oxford, p. 95-112.

Cook, R. U., and A. Warren, 1973, *Geomorphology in deserts*: University California Press, Los Angeles, 393p.

Eschner, T. B. and Kocurek G. 1986. *Marine destruction of eolian sand seas: origin of mass flow*. Journal of Sedimentary Petrology, v. 56, p. 401-411.

Eschner, T. B. and Kocurek G. 1988. *Origins of relief along contacts between eolian sandstones and overlying marine strata*. American Association of Petroleum Geologists Bulletin, v. 72, p. 932-943.

Evans, D.S., Bahabri, B.H., and Al-Otaibi, A.M., 1997, *Stratigraphic trap in the Permian Unayzah Formation, central Saudi Arabia*: GeoArabia, v. 2, p. 259–278.

Ferguson, G.S. and T.M. Chambers 1991. *Subsurface stratigraphy, depositional history, and reservoir development of the Early-to-Late Permian Unayzah Formation in central Saudi Arabia*. Proceedings of the 7th Society of Petroleum Engineers Middle East Oil Show, Bahrain, SPE Paper 21394, p. 487-496.

Fryberger, Steven G. 1978. *Technique for the evaluation of surface wind data in term of eolian sand drift*: US Geological Survey, open-file report 78-405, 24 p.

Fryberger, Steven G. 1979, *Dune forms and wind regime, in E.d McKee, ed., A study of global sand seas*: U.S. Geological survey professional paper 1052, p. 137-169.

Fryberger, Steven G. 1986. S*tratigraphic traps for petroleum in wind-laid rocks*. Bulletin, American association of petroleum geologist, v. 70, p. 1765-76.

Fryberger, Steven and Ahlbrandt, Thomas. 1979. M*echanisms for the formation of eolian sand seas*. Zeitschrift fur Geomorphologie, v.. 23, no. 4, pp. 440-460.

Fryberger, S. G. and Schenk, C. J., 1988. *Pin-strip lamination: A distinctive feature of modern and ancient eolian sediments*, Sedimentary Gelogy, v. 55, p. 1-15.

Fryberger, S. G., C. J. Schenk, and L. F. Krystinik, 1988. S*tokes surface and the effects of near surface groundwater-table on aeolian deposition. Sedimentology*, v. 35, p. 21-41.

Fryberger, S. G., T. S. Ahlbrandt and S. Andrews 1979. *Origin, sedimentary features and significance of low-angle eolian "sand sheet" deposits, Great Sand Dunes National Monument and vicinity, Colorado*. Journal of Sedimentary Petrology, v. 49, p. 733-746.

Fryberger, Steven and Dean, Gary. 1979. *Dune forms and wind regime. In A Study of Global Sand Seas, E. McKee, ed., pp. 137-170*. Washington, U. S. Geological Survey Paper 1052.

Fryberger, S.G., 1990. *Eolian Stratification. Modern and Ancient Eolian Deposits*: Petroleum Exploration and Production. S.E.P.M. P. 4.1-12.

Gilbreath, J. A., 1987, *Strategies for dipmeter interpretation: Part I*: The Technical Review, v. 35, no. 3, p. 28–41.

Glennie, K. W. 1972, *Permian Rotliegendes of north-west Europe interpreted in light of modern desert sedimentation studies*: AAPG Bulletin, v. 56, p. 1048-1071.

Goodal T. M, Moller N. K. and Ronningsland T. M. 1998, *The inergration of electrical image logs with core data for improved sedimentology interpretation*. Geological Society, London, special publication 136, p. 237-248.

Grace, L. M., and B. Newberry, 1998, *Geological applications of electrical images and dipmeter: Short Course Notes*, Schlumberger Oilfield Services, v. 8.1.

Heine, C. J., K. W. Glennie and B.P.J. Williams 1998. *Peri-glacial dune sand reservoirs of the Permian Unayzah Formation, central Saudi Arabia* (Abstract). GeoArabia, v. 3, no. 1, p. 100.

Heine, C. J. Melvin, J. and Wilkins, J., 2004. *Impact of Image-Log-Derived Lithofacies on Eolian Reservoir Layering and Geocellular Modeling, Unayzah 'A' Reservoir, Hawtah Formation, Tinat Field, Saudi Arabia.* (Abstract). AAPG International Conference. Bulletin, v. 88, no. 13. (Supplement).

Hocker, C., K. M. Eastwood, J. C. Herweijer, and J. T. Adams, 1990, *Use of dipmeter data in clastic sedimentological studies*: AAPG, Bulletin, v. 74, p. 105–118.

Husseini, M.I. 1992. *Upper Palaeozoic tectono-sedimentary evolution of the Arabian and adjoining plates*. Journal of the Geological Society, London, v. 149, no. 5, p. 419-429.

Hurley, N. F., 1994, *Recognition of faults, unconformities, and sequence boundaries using cumulative dip plots*: AAPG, Bulletin, v. 78, p. 1173–1185.

Hurley, Neil, 2004, *Borehole images, in G. Asquith and D. Krygowski, Basic Well Log Analysis*: AAPG Methods in Exploration no. 16, p. 151-163.

Hunter, R. E., 1977. *Basic types of stratification in small eolian dunes*: Sedimentology, v. 24, p. 361-387.

Inman, D. L., Ewing, G. C. and Corliss, J. B. 1966. *Costal sand dunes of Guerrero Negro, Baja California, Mexico*. Geological Society of America Bulletin, 77, p. 787-802.

Jackson, Julia A. 1997, *Glossary of Geology*, American Geological Institute.

K. W. Glennie. 1970. *Desert sedimentary environments*. Elsevier, 222 P.

Kenneth W. Glennie. 2005, *The desert of Southeast Arabia.* GeoArabia Special Publication, Gulf PetroLink, Bahrain, 215 p.

Kocurek, Gary, 1981, Significance of interdune deposits and bounding surfaces in eolian dune sands: Sedimentology, v. 28, p. 753-780.

Kocurek, Gary, 1991, *Interpretation of ancient eolian sand dunes*. Annual. Review. Earth Planet, p. 43-75.

Kocurek, Gary, and K. G. Havholm, 1993, *Eolian sequence stratigraphy-A conceptual framework, in Weimer, P. and H. W. Posaamentier (eds.), Siliciclastic sequence stratigraphy: Recent developments and applications:* American Association of Petroleum Geologists Mem. 58, p. 393-400.

Kocurek, G., and Dott, R. H., 1981. *Distinctions and uses of stratification types in the interpretation of eolian sand.* Journal of Sedimentary Petrology, v. 51, p. 579-595.

Kocurek, G., and G. Fielder 1982. *Adhesion structure*. Journal of Sedimentary Petrology, v. 52, p.1229-1241.

Kocurek, G., and Nielson, J., 1986. *Conditions favorable for the formation of warm-climate aeolian sand sheets,* Sedimentology, v. 33, p. 795-816.

Konert, G., A.M. Al-Afifi, S.A. Al-Hajri and H.J. Droste 2001. *Paleozoic stratigraphy and hydrocarbon habitat of the Arabian Plate*. GeoArabia, v. 6, no. 3, p. 407-442.

Krystinik, L. F., and Blakeney, B. A., 1990, *Sedimentology of the upper Morrow Formation in eastern Colorado and western Kansas; in, Morrow Sandstones of Southeast Colorado and Adjacent Areas, S. A. Sonnenberg, L. T. Shannon, K. Rader, W. F. von Drehle, and G. W. Martin, eds.*: The Rocky Mountain Association of Geologists, Special Paper, p. 37-50.

Lancaster, N., 2009: *Dune morphology and dynamics,* In: Parsons, A.J. and Abrahams, A.D (eds.) *Geomorphology of Desert Environments,* 2nd edition, 557-595.

Lancaster, N., 1995. *Geomorphology of desert dunes.* Edited by Keith Richard, University of Cambridge. Routledge, London 290 p.

Luthi, S. M., and J. R. Banavar, 1988, A*pplication of borehole images to three-dimensional geometric modeling of eolian sandstone reservoirs, Permian Rotliegende, North Sea*. AAPG, Bulletin, v. 72, p. 1074–1089.

Loop, D. B., Maureen B. Steiner, Clinton M. Rowe and Nicholas Lancaster, 2004. *Tropical westerlies over Pangaean sand seas.* Sedimentology v.51, P. 315-322.

McGillivray, J. G. and M.I. Husseini 1992. *The Palaeozoic petroleum geology of central Arabia*. AAPG, Bulletin, v. 76, no. 10, p. 1473-1490.

McGillivray, J.G., 1994, *Late Carboniferous and Early Permian petroleum geology, Central Saudi Arabia, in Embry, A.F., Beauchamp, B., and Closs, D.J., eds., Pangea, global environments and resources*: Canadian Society of Petroleum Geologists Memoir 17, p. 383–396.

McKee, Edwin. 1979a, *Sedimentary structures in dunes*, in McKee, E. D. (ed.), *A Study of Global Sand Seas:* U. S. Geological Survey Paper 1052, p. 83-134.

McKee, Edwin. 1979b. *An introduction to the study of global sand seas*. in McKee, E. D.(ed.), *A Study of Global Sand Seas:* U. S. Geological Survey Paper 1052, p. 1-20.

McKee, Edwin. 1966. *Structure of dunes at White Sands National Moment,*

New Mexico (and a comparison with structures of dunes from other selected areas). Sedimentology, v. 7, p. 1-69.

Melvin, J. and C. J. Heine 2004. S*equence stratigraphy of an eolian gas sand: layering in the Permian Unayzah-A reservoir at south Ghawar, eastern Saudi Arabia* (Abstract). GeoArabia, v. 9, no. 1, p. 103.

Melvin, J., R. A. Sprague and C.J. Heine 2005a. *Diamictites to eolianites: Carboniferous-Permian climatic change seen in subsurface cores from the Unayzah Formation, east-central Saudi Arabia*. In, G.E. Reinson, D. Hills and L. Eliuk (Eds.), 2005 CSPG Core Conference Papers and Extended Abstracts CD. Calgary, Canadian Society of Petroleum Geologists, p. 237-282.

Melvin, J., and R.A. Sprague 2006. *Advances in Arabian stratigraphy: Origin and stratigraphic architecture of glaciogenic sediments, sediments in Permian-Carboniferous lower Unayzah sandstones, eastern central Saudi* Arabia. GeoArabia, v. 11, no. 4, p. 105-152.

Melvin et al. 2010a. *Advances in Arabian stratigraphy: Allostratigraphic layering related to paleo-water table fluctuation in eolian sandstone of the Permian Unayzah A reservoir, South Haradh, Saudi Arabia*. GeoArabia, v. 15, no. 2, p. 55-86.

Melvin et al. 2010b.From bergs to ergs: *The late Paleozoic Gondwanan glaciation and its aftermath in Saudi Arabia*. Geological Society of America, special paper 468, p. 37-80.

Mountney, N. P. and A. Jagger 2004. S*tratigraphic evolution of an aeolian erg margin system: the Permian Cedar Mesa Sandstone, SE Utah, USA.* Sedimentology, v. 51, p. 713-743.

Nicholas, Gary, 2009. *Sedimentology and stratigraphy.* Second edition, Wiley-Blackwell p. 419.

Nurmi, R. D. 1985. *Eolian sandstone reservoirs: Bedding facies and production geology modeling:* Society of Petroleum Engineers paper 14172, 8 p.

Nurmi, R. D. and Hepp, V. R. 1979. *Eolian Sedimentology interpreted from dipmeter results,* American Association of Petroleum Geologists Bulletin, v. 63, p. 504.

Reid, R. R., and M. B. Enderlin, 1998, *True pay thickness determination of laminated sand and shale sequences using borehole resistivity image logs:* Society of Professional Well Log Analysts, 39th Annual Logging Symposium, Transactions, Paper GGG, 9 p.

Reineck, H. E. and Singh, I.B. 1975. *Depositional sedimentary environments,* Sprenger-Verlag, New York, 439 p.

Robinson P. (1973) *Palaeoclimatology and continental drift. In: Implications of continental drift to the earth science, v. 1 (ed. By D. H. Tarling and S. K. Runcorn), P. 451-476.* Academic Press, London.

Pollastro, R. M. 2003. *Total Petroleum Systems of the Paleozoic and Jurassic, Greater Ghawar Uplift and Adjoining Provinces of Central Saudi Arabia and Northern Arabian-Persian Gulf. U.S.* Geological Survey Bulletin 2202-H.

Pye and Tsoar, 2009. *Aeolian and Sand Dunes*. Springer, 458p.

Pye, K. 1987. *Aeolian Dust Deposits,* Academic Press, London, 334p.

Rubin, D.M., and R.E.Hunter,1982, *Bedform climbing in theory and nature:* Sedimentology, v. 29, p. 121-138.

Rubin, D.M., 1987 *Cross-bedding, Bedforms and Paleocurrents: Society of Economic Paleontologists and Minerallogist,* Concepts in Geology, v.1, 187p.

Sam Boggs, JR. 2001, *Principles of Sedimentology and Stratigraphy*. Third edition. Prentice Hall. 726p.

Schenk, C. J. 1990. *Eolian dune morphology and wind regime*: in Steven G. Fryberger, Lee F. Krystinik, Chistopher J. Schenk, *Modern and Ancient Eolian Deposits*: Petroleum Exploration and Production, (SEPM), P. 3.1-3.8.

Schlumberger, 1983, *Stratigraphic high resolution dipmeter tool*: Paris, Schlumberger Limited, Document no. M-08630, 23 p.

Schwan, J., 1988. *The structure and genesis of Weichselian to Early Holocene aeolian sheets in western Europe*: Sedimentary Geology, v. 55, p. 197-232.

Selley, R. C.**,** 1978**,** *Ancient sedimentary environments* (2nd edition): Ithaca, New York, Cornell University Press, 287 p.

Senalp, M. and A. Al-Duaiji 1995. *Stratigraphy and sedimentation of the Unayzah reservoir, central Saudi Arabia. In, M.I. Husseini (Ed.),* Middle East Petroleum Geosciences Conference, GEO'94. Gulf PetroLink, Bahrain, v. 2, p. 837-847.

Serra, O., 1989, *Formation MicroScanner image interpretation:* Houston, Texas, Schlumberger Educational Services, 117 p.

Shepherd, M., 2009, *Eolian reservoir, in M. Shepherd, oil field production geology,* American Association of Petroleum Geologists, Memoir 91, p. 255-259.

Sharland, P.R., R, Archer, D.M. Casey, R.B. Davies, S.H. Hall, A.P. Heward ,A.D. Horbury and M.D. Simmons 2001. *Arabian Plate Sequence Stratigraphy*. GeoArabia Special Publication 2, Gulf PetroLink, Bahrain, 371 p., with 3 charts.

Shotton, F. W., 1937, *Lower Bunter Sandstones of north Worcestershire and east Shropshire*: Geol. Mag., V. 74, p. 534-553

Slatt, Roger, 2006. *Stratigraphic reservoir characterization for petroleum geologist, geophysicist and engineers*. Elsevier, 478 p.

Sovich, J., J. Klein, and N. Gaynor, 1996, *A thin bed model for the Kuparuk A sand, Kuparuk River field, North Slope, Alaska*: Society of Professional Well Log Analysts, 37th Annual Logging Symposium, Transactions, Paper D, 13 p.

Stephen E. Prensky, 1999. *Advances in borehole imaging technology and applications*, Geological Society, London, Special Publications 1999; v. 159; p. 1-43.

Stephenson, M.H. and J. Filatoff 2000a. *Correlation of Carboniferous-Permian palynological assemblages from Oman and Saudi Arabia. In, S. Al-Hajri and B. Owens (Eds.), Stratigraphic palynology of the Palaeozoic of Saudi Arabia.* GeoArabia Special Publication 1, Gulf PetroLink, Bahrain, p. 168-191.

Stephenson, M. H. and J. Filatoff 2000b. *Description and correlation of Late Permian palynological assemblages from the Khuff Formation, Saudi Arabia and evidence for the duration of the pre-Khuff hiatus. In, S. Al-Hajri and B. Owens (Eds.), Stratigraphic palynology of the Palaeozoic of Saudi Arabia.* GeoArabia Special Publication 1, Gulf PetroLink, Bahrain, p. 192-215.

Stephenson, M. H. et al., 2003. *Palynological biozonation of Permian of Oman and Saudi Arabia: progress and challenges*. GeoArabia, v. 8, no. 3, p. 467.

Sorby, H. C. (1859), *On the structures produced by the currents during the deposition of stratified rocks,* Geologist, II, 137–147. (Reprinted in *Sorby on Sedimentology, 1976: A Collection of Papers From 1851 to 1908 by Henry Clifton Sorby*, edited by C. H. Summerson, pp. 26–33, Compar. Sediment. Lab., Univ. of Miami, Miami, Fla.).

Stokes, W. L., 1968. *Multiple parallel-truncation bedding plains- a feature of wind-deposited sandstone formation*, *Journal of Sedimentary Petrology, v. 38, p. 510-515.*

Sharp, Robert P. 1963. *Wind ripples*. Journal of Geology, Vol. 71, No. 5, pp. 617-36.

Sharp, Robert P. 1966. *Kelso dunes, Mojave desert, California*. *Geological Society of America Bulletin*, Vol. 77, No. 10, pp. 1045-1073.

Sharp, Robert P. 1978. The Kelso dune complex. In *Aeolian Features of Southern California: A Comparative Planetary Geology*, R. Greeley, M. Womer, R. Papson and P. Spudis, eds., pp. 54-63. Washington, NASA.

Sharp, Robert P. and Saunders, R. S. 1978. *Eolian activity in westernmost Coachella Valley and at Garnet Hill*. In *Aeolian Features of Southern California: A Comparative Planetary Geology*, R. Greeley, M. Womer, R. Papson and P. Spudis, eds., pp. 9-22. Washington, NASA.

Smith, H. T. U. 1968. *Eolian Geomorphology, Wind Direction, and Climatic Change in North Africa*. Bedford, MA, U. S. Air Force Geophysics Research Directorate.

Wender, L. E., Bryant, J. W., Dickens M. F., Neville A. S. and Al-Moqbel, A. M. 1998. *Paleozoic (Pre-Khuff) Hydrocarbon Geology of the Ghawar Area, Eastern Saudi Arabi.* GeoArabia, Vol. 3, No.2, 1998, P. 273-302.

Weber, K. J., 1987. *Computation of intial well productivities in aeolian sandstone on the basis of a geological model. Leman gas field, UK. In: R.W. Tillman, K.J. Weber (eds.) Reservoir Sedimentology, Soc. Econ. Paleon. And Mineral.* (SEPM) Special Publication no. 40, p. 333-354.

Wilson, I. G., 1972, A*eolian bedforms –Their development and origins*: Sedimentology, v. 19, p. 173-210.

Witton, E.M., 1999, *Outcrop and subsurface characterization of the Lewis Shale, Carbon County*, Wyoming, Colorado School of Mines, Golden, Colo., 214 p.

Zemanek, Joseph, and others, 1969. T*he borehole televiewer-A new logging concept for fracture location and other types of borehole inspection*: Journal. Pet. Tech., v. 21, no. 6, p. 762-774.

Ziegler, A.M., Hulver, M.L., and Rowley, D.B., 1997 *Permian World Topography and Climate. In: Late glacial and Postglacial Environmental Changes*. Oxford University Press, New, York, Pages 111-142, I.P. Martini (editor).

http://www.nps.gov/archive/whsa/sand%20dune%20geology.htm
http://www.merriam-webster.com/dictionary
http://hsb.iitm.ac.in/~jm/ARCHIVES/Mar-April04/articles_files/sanddunes.html

CURRICULUM VITA

Mohammed Al-Masrahy was born in Khamiss Mushait, Saudi Arabia. He graduated from King Abdul Aziz University, Jeddah, Saudi Arabia in 2000 with a Bachelor of Science Degree in Petroleum Geology. After graduation, he was hired by the Ministry of Education as a geology subject teacher and then as an administrator of scientific activities in the directorate of education. He joined Saudi Aramco in 2002 and started working with the Area Exploration Department (Wellsite Geology) where he followed up on drilling operations, In 2005, Mohammed moved to the Gas Field Characterization Division and worked as an operations and development geologist for pre-Khuff reservoirs. In October 2009, he moved to the gas fields special studies team within the Gas Fields Characterization Division. Currently he is working with the Reservoir Characterization Department's (RCD) Integration Team.

Please address correspondence to:

Name: Mohammed Ali Al-Masrahy

Company: Saudi Arabia Oil Company (Saudi Aramco)

Address: P. O. Box 12977, Dhahran 31311, Saudi Arabia

Tel.: +96638731605

E-mail: mohammed.masrahy@aramco.com